universität wien

MASTERARBEIT / MASTER'S THESIS

Titel der Masterarbeit / Title of the Master's Thesis

„*In vivo* and *in vitro* characterization of gp44, a putative toxin of φCh1"

verfasst von / submitted by

Alexandros Vaios Athanasiou, BSc

angestrebter akademischer Grad / in partial fulfilment of the requirements for the degree of

Master of Science (MSc)

Wien, 2020 / Vienna, 2020

Studienkennzahl lt. Studienblatt / degree programme code as it appears on the student record sheet:	UA 066 830
Studienrichtung lt. Studienblatt / degree programme as it appears on the student record sheet:	Masterstudium Molekulare Mikrobiologie, Mikrobielle Ökologie und Immunbiologie
Betreut von / Supervisor:	Ao. Univ.-Prof. Dipl.-Biol. Dr. Angela Witte

Acknowledgements

I would like to express my gratitude towards my supervisor, mentor and friend, Ao. Univ.-Prof. Dipl.-Biol. Dr. Angela Witte for her assistance and patience throughout this past year. I was able to learn many things under her guidance, which resulted in me becoming both a better scientist and person. Thank you for providing me with the opportunity to work with you!

Furthermore, I want to thank my lab colleagues Dina Sabic, Seyda Kigili, Laxmikant Wali and Julian Szalay for all the laughs, memories, and inside jokes. Thank you for being honest and your continuous support and help. I am also grateful for the members of Blaesi and Moll groups, especially Branislav Lilic, Anastasia Cianciulli, and Flavia Bassani for providing feedback and giving important hints whenever needed.

Finally yet importantly, I would like to thank my family for supporting me all these years, throughout my bachelor and master studies, especially my brother Angelos for critical reading of this thesis.

Table of Contents

Abbreviations 10
1. Introduction 11
1.1. *Archaea* 11
1.1.1. Halophilic *Archaea* 12
1.1.1.1. Haloferax volcanii 13
1.1.1.2. H. volcanii as a model system for archaeal studies 13
1.1.2. Haloalkalophilic *Archaea* 14
1.1.2.1. Natrialba magadii 14
1.1.2.2. Laboratory N. magadii strains: L11 and L13 15
1.1.2.3. Genetic tools and manipulations in halophilic archaea 16
1.1.2.3.1. Transformation 16
1.1.2.3.2. Shuttle vectors and selection markers 17
1.2. Viruses of *archaea* 17
1.2.1. Viruses of haloarchaea 18
1.2.2. The haloalkalophilic virus φCh1 19
1.3. Toxin Antitoxin (TA) systems 22
1.3.1. VapBC toxin-antitoxin system 22
1.3.2. φCh1 ORF43/44 as a putative VapBC toxin-antitoxin system 24
2. Materials and Methods 27
2.1. Materials 27
2.1.1. Strains 27
2.1.2. Growth media 27
2.1.2.1. Lysogeny broth medium (LB) for E. coli 27
2.1.2.2. N. magadii rich medium – NVM$^+$ / NVM-CA$^+$ 28
2.1.2.3. Growth media for Haloarchaea – H. volcanii 29
2.1.2.3.1. Concentrated Salt Water (SW) solution - 30% (w/v) 29
2.1.2.3.2. Modified growth medium – 18 % MGM$^+$ 29
2.1.2.3.3. Hv – YPC complete medium 30
2.1.3. Antibiotics and further additives 30
2.1.4. Plasmids 31
2.1.5. Primers 33
2.1.6. DNA and protein ladders 34
2.1.7. Enzymes 34

2.1.8. Kits ... 35
2.1.9. Antibodies ... 35
2.1.9.1. Primary antibodies ... 35
2.1.9.2. Secondary antibodies ... 35
2.1.10. Oligo RNAs ... 36
2.1.11. Buffers and solutions ... 36
2.1.11.1. Gel electrophoresis ... 36
2.1.11.1.1. DNA gels ... 36
2.1.11.1.2. RNA gels ... 37
2.1.11.1.3. Protein gels ... 37
2.1.11.2. Gibson assembly ... 38
2.1.11.3. Western Blot ... 39
2.1.11.4. Preparation of competent cells and transformation ... 39
2.1.11.4.1. *E. coli* ... 39
2.1.11.4.2. *N. magadii* ... 40
2.1.11.4.3. *H. volcanii* ... 41
2.1.11.5. Protein isolation and purification ... 41
2.1.11.5.1. Purification from *E. coli* under denaturing conditions ... 41
2.1.11.5.2. Purification from *H. volcanii* under native conditions ... 43
2.2. Methods ... 43
2.2.1. DNA methods ... 43
2.2.1.1. Preparation of DNA templates and primers ... 43
2.2.1.2. Preparative and analytical PCR ... 44
2.2.1.3. Quality control of PCR products and purification ... 44
2.2.1.4. DNA restriction, dephosphorylation and ligation ... 44
2.2.1.5. Gibson assembly ... 45
2.2.2. Transformation procedures ... 45
2.2.2.1. Transformation in E. coli ... 45
2.2.2.1.1. Generation of *E. coli* competent cells ... 45
2.2.2.1.2. Transformation of *E. coli* competent cells and screening ... 46
2.2.2.2. Transformation in N. magadii ... 46
2.2.2.2.1. Generation of *N. magadii* competent cells ... 46
2.2.2.2.2. Transformation of *N. magadii* competent cells and screening ... 46
2.2.2.3. Transformation in H. volcanii ... 47
2.2.2.3.1. Generation of *H. volcanii* competent cells ... 47
2.2.2.3.2. Transformation of *H. volcanii* competent cells and screening ... 47

2.2.2.3.3. Preparation of *H. volcanii* acetone powder 47
2.2.3. Protein methods 48
2.2.3.1. Preparation of crude protein extracts 48
2.2.3.2. SDS-PAGE and Coomassie staining 48
2.2.3.3. Western Blot 49
2.2.4. Protein expression and purification 50
2.2.4.1. Gp44 purification from E. coli under denaturing conditions 50
2.2.4.2. Protein dialysis 50
2.2.4.3. Gp44 purification from H. volcanii under native conditions 51
2.2.5. Cell culture passaging 51
2.2.5.1. Stability of N. magadii L11-ΔORF44 deletion mutant 51
2.2.5.2. CFU meassurements and provirus detection 52
2.2.5.3. Virus titer analysis 52
2.2.6. In vitro endoribonuclease assay 52
2.2.7. Cloning strategies 53
2.2.7.1. pRV1-ptna-ORF44 53
2.2.7.2. pRo-5-Mev-p43-ORF43 and –p43-ORF43/44 53
2.2.7.3. pRo-5-Mev-tnaN-ORF44 54
2.2.7.4. pNB102-p43-ORF43 54
2.2.7.5. pMDS24-ORF34$_{52}$ 54
2.2.7.6. pMDS24-34$_1$ and -34$_{52}$ constructs via Gibson assembly 54
3. Results 56
3.1. Stability of the provirus in *N. magadii* L11-ΔORF44 deletion mutant 56
3.2. Further characterization of *N. magadii* L11-Δ44 61
3.3. Complementation of *N. magadii* L11-ΔORF44 63
3.4. Overexpression of ORF43 65
3.5. Overexpression of ORF44 72
3.6. Effect of ORF43 and ORF44 on the tail fiber protein gp34 in *H.volcanii* 74
3.7. Expression and purification of gp44 under denaturing conditions 78
4. Discussion 80
Abstract 85
Zusammenfassung 87

Abbreviations

LB: Liquid broth

NVM: Natrialba rich medium

Hv-YPC: *H.volcanii* – Yeast, Peptone, Casamino acids complete medium

CA: Casamino acids

RT: Room temperature

LD: Loading dye

min: minutes

sec: seconds

h: hours

GA: Gibson assembly

OD: optical density

CFU: Colony Forming Units

PFU: Plaque Forming Units

bp: base pairs

SEM: standard error of mean

Mtase: Methyltransferase

Tna: tryptophan inducible promoter

TA: Toxin-Antitoxin system

1. Introduction

1.1. *Archaea*

The *archaea* are prokaryotic organisms that thrive in extreme environments, defining the limits of life on earth. *Archaea* were initially classified as bacteria, but phylogenic analyses of the 16S rRNA sequence pointed out that *archaea* are evolutionarily distinct from the bacteria, resulting in their classification as the third domain of life (Woese and Fox, 1977). They were originally discovered and described in extreme environments, such as terrestrial hot springs and hydrothermal vents (Valentine, 2007), but could also be found in highly saline, acidic and anaerobic habitats (Pikuta, Hoover and Tang, 2007). Culture-independent studies, e.g. the isolation and analysis of nucleic acids from the environment, have shown that *archaea* can grow as mesophiles in both marine and terrestrial ecosystems (DeLong, 1992).

The current classification of *archaea* consists of three main phyla: the Euryarchaeota, the Crenarchaeota (Woese, Kandler and Wheelis, 1990) and the Thaumarchaeota. The Euryarchaeota is a rather diverse phylum containing mostly anoxically growing methanogens and halophiles. Haloarchaea comprises 213 species in 50 genera (Gupta, Naushad and Baker, 2015; Gupta *et al.*, 2016) which can be found in salt saturated (about 37 % salts) or nearly saturated marine environments (Yadav *et al.*, 2015). The phylum Chrenarchaeota consists of mostly sulfur-dependent thermophilic as well as hyperthermophilic *archaea*, which can survive at temperatures above 100 °C. Thaumarchaeota is a relative new phylum that was seperated from Crenarchaeota after sequencing of the genome of *Cenarchaeum symbiosum* and consists mostly of mesophiles (Brochier-Armanet *et al.*, 2008).

Further studies revealed that *archaea* share traits with both bacteria and eukaryotes. *Archaea* and bacteria have generally similar cell structure and are structurally most similar to gram-positive bacteria. Like bacteria, *archaea* consist of a single plasma membrane and cell wall and lack interior membranes and organelles (Woese, 1994). On the other hand, their transcriptional and translational machinery resembles the one from the eukaryotes (Brown and Doolittle, 1997; Olsen and Woese, 1997; Bernander, 2000). Despite their similarities with the other two domains of life,

archaeal membrane lipids are composed of branched isoprenoid acyl chains, which are ether-linked to their glycerol backbone in contrast to bacterial and eukaryotic membrane lipids that consist of ester-linked unbranched fatty acids (Jarrell, Jones and Nair, 2010; Albers and Meyer, 2011). Ether linkages confer an evolutionary advantage for *archaea* in order to be able to tolerate high temperatures and salinity, resulting in an increased membrane stability and resilience to hydrolysis (Van De Vossenberg *et al.*, 1999). Furthermore, unlike bacteria, the archaeal cell wall lack murein (Howland, 2000) except some methanogens whose cell wall is composed of pseudo-peptidoglycan (Albers and Meyer, 2011). Another cell wall feature is the pseudo-crystalline proteinaceous surface layer, namely S-layer, which is attached to the cytoplasmic membrane. The S-layer is composed of one or two different glycoproteins (Sleytr and Beveridge, 1999; Rodrigues-Oliveira *et al.*, 2017) which, when glycosylated, lead to an increased thermal stability (Yurist-Doutsch *et al.*, 2008; Albers and Meyer, 2011; König, Rachel and Claus, 2014).

1.1.1. Halophilic *Archaea*

Halophilic *archaea*, namely Haloarchaea, are a class of the Euryarchaeota and are commonly found in water-saturated environments, which are characterized by high evaporation rates that lead to hypersalinity (Oren, 2002). These microorganisms require high concentrations of salt for growth and survival. They can be divided in two subcategories, based on the amount of the salt they need. The moderate halophiles grow optimally at 0.5 - 2.5 M NaCl in contrast to the extreme halophiles that grow at 2.5 - 5 M NaCl (Andrei, Banciu and Oren, 2012). The metabolism of Haloarchaea is very diverse˙ they can grow both aerobically and anaerobically using amino acids as energy and carbon source (Wais *et al.*, 1975) and are unable to fix carbon from carbon dioxide (Bryant and Frigaard, 2006).

In order to withstand the high osmotic pressure and be able to survive in hypersaline environments, Haloarchaea developed an evolutionary strategy, the so-called “salt-in” approach. By effectively using Na^+/H^+ antiporter membrane proteins, potassium chloride accumulates in the cell cytoplasm while sodium ions are pumped out of the cell (Oren, 1999; Fendrihan *et al.*, 2007). In extremophiles, the internal K^+ levels can reach up to 5 M (Christian and Waltho, 1962; Lai and Gunsalus, 1992).

Normally, proteins precipitate at such high intracellular potassium chloride concentrations, but the halophilic enzymes contain high amount of negatively charged acidic amino acids, leading to a low isoelectric point, and a small number of hydrophobic amino acids (Oren, 1999). Another approach to counterbalance high osmolality is through accumulation of organic solutes, e.g. glycerol, by *de novo* synthesis, which is achieved only by methanogens (Lai *et al.*, 1991), or uptake from the environment.

1.1.1.1. *Haloferax volcanii*

Haloferax volcanii is a mesophilic archaeon that was isolated from hypersaline marine environments. It is a facultative anaerobic and chemoorganotrophic microorganism that metabolizes sugars or amino acids as a carbon source (Oren, 2006). Due to the high internal K^+ ion gradient, *H. volcanii* possesses enzymes specifically adapted to function in high salt concentrations (Ortega *et al.*, 2011). Like many *archaea*, *H. volcanii* possesses an S-layer composed of glycoproteins. In addition, the cell membrane contains large amounts of carotenoids, e.g. lycopene, which, when present in sufficient concentrations, grant a distinctive red color (Ronnekleiv, 1995).

1.1.1.2. *H. volcanii* as a model system for archaeal studies

H. volcanii is often used as a key model organism in studies of archaeal genetics because it can be easily cultured in a laboratory (Hartman *et al.*, 2010). Optimal growth occurs at salt and Mg^{2+} concentrations of 1.5 - 2.5 M and up to 1.5 M respectively, at a pH slightly below 7 and a temperature of 45 °C. Under the above mentioned conditions, doubling time is approximately 4 hours (Oren, 2006). Furthermore, *H. volcanii* can proliferate in different media: a high salt- and a low salt-rich medium containing yeast extract and peptone, as well as in minimal medium containing glycerol and sodium succinate or glycose as the solo energy source (Robb, DasSarma and Fleischmann, 1995).

Haloferax volcanii DS2 genome consists of a large (4 Mb), multicopy chromosome and four extrachromosomal replicons pHV4 (690 kb), pHV3 (440 kb),

pHV1 (86 kb) and pHV2 (6kb) (Charlebois *et al.*, 1987). The genome has been completely sequenced and consists of approximately 4130 genes (Hartman *et al.*, 2010).

The molecular biology of *H. volcanii* has been extensively investigated, in order to study archaeal genomics and even the function of eukaryotic proteins. Many protein functions have been verified, e.g. RadB protein, which is a member of the RecA family and is involved in recombination processes (Haldenby, White and Allers, 2009). In addition, several pHV2 derivatives are widely used for cloning and shuttle vectors. Another DS2 derivative, namely WR479, which contains deletions of both the *pyrE1* and *pyrE2* genes (Bitan-Banin, Ortenberg and Mevarech, 2003), is utilized as a host to knockout genes. So far, many tools for the genetic manipulation of *H. volcanii* are well developed. Strains and vectors have been constructed to facilitate different tasks from construction of gene knockouts, such as strain H26 (Allers and Ngo, 2003), to identification of promoters, e.g. tryptophan inducible promoter ptna (Large *et al.*, 2007) and conditional overexpression of proteins (Allers, 2010).

1.1.2. Haloalkalophilic *Archaea*

The term haloalkaliphilic was used to describe a newly isolated archaeon that was both halophilic and alkaliphilic (Soliman and Trueper, 1982). Haloalkaliphilic *archaea* grow optimally at high pH (pH 8 – 11) and high salinity conditions (Tindall, Ross and Grant, 1984; Xue *et al.*, 2005; Sorokin *et al.*, 2018) and can be found in hypersaline alkaline environments (Grant and Larsen, 1989). An example of such an extreme habitat is Lake Magadi in Kenya, Africa, which contains high salt concentrations, up to 300 g/L, high levels of carbonate ions and a pH above 11 (Oren, 2002; Ma *et al.*, 2010).

1.1.2.1. *Natrialba magadii*

Natrialba magadii is a haloalkaliphilic archaeon that was isolated from Lake Magadi in Kenya (Tindall, Ross and Grant, 1984) and belongs to the family of *Halobacteriaceae* of the phylum Euryarchaeota. It was initially classified within the genus *Natronobacterium*, but phylogenetic analysis of the 16S rRNA led to

reclassification in the genus *Natrialba* (Kamekura *et al.*, 1997). As mentioned above, *N. magadii* is both a halophilic and alkaliphilic archaeon and hence needs 4 to 5 M NaCl concentration and a pH value between 8.5 and 11. Due to the high levels of carbonate minerals in the surrounding environment, a low Mg^{2+} concentration (below 10 mM) is required and the optimal growth temperature ranges from 37 to 42 °C (Kamekura *et al.*, 1997).

Regarding the metabolism, *N. magadii* is obligately anaerobic, proteolytic and chemoorganotrophic. It utilizes therefore amino acids and peptides as sole carbon sources, and it is unable to process carbohydrates (Tindall, Ross and Grant, 1984). *N. magadii* cells are morphologically rod-shaped and contain flagella for locomotion. Caretenoids are incorporated in the cell membrane resulting in an orange/red color upon growth that is especially visible under stress conditions (e.g. proliferation in minimal medium).

In regards to the genomic composition, *N. magadii* is a polyploid microorganism, i.e. it contains up to 50 copies of chromosomal DNA per cell (Breuert *et al.*, 2006). The generation time is approximately 9 hours in comparison to the fast proliferating *E. coli*, whose generation time is about 20 minutes.

1.1.2.2. Laboratory *N. magadii* strains: L11 and L13

There are two different strains, which are being used in the laboratory: L11 and L13 (see Figure 1). *N. magadii* L11 is the wild type strain containing the virus φCh1, which leads to lysis of the host cell and is immune to superinfection. On the other hand, *N. magadii* L13 was cured of the provirus by continuous passaging of the wild type strain and is therefore non-lysogenic (Witte *et al.*, 1997). However, the L13 cured strain can be re-infected by φCh1 and hence was used as an indicator strain. *N. magadii* is the only known host of φCh1.

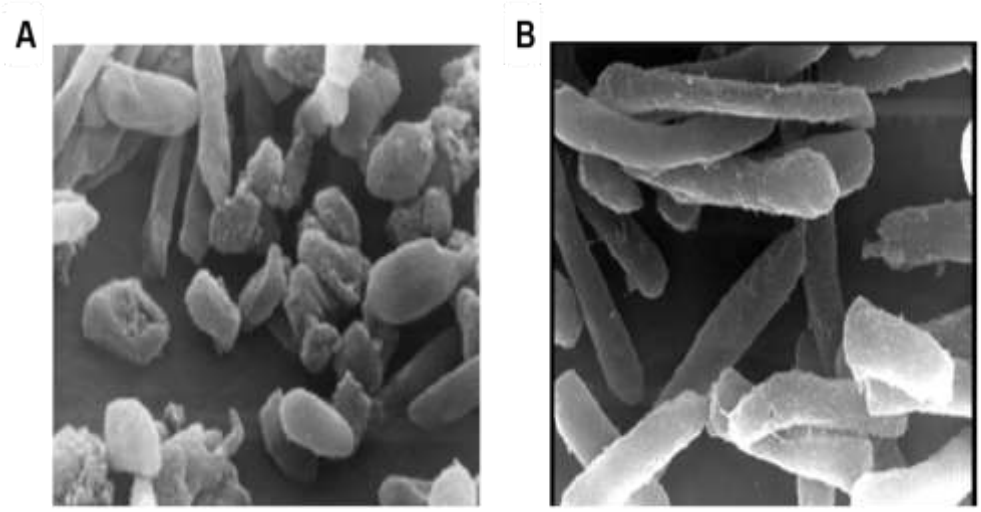

Figure 1. Cell morphology of *N. magadii* L11 and *N. magadii* L13. (A) Electron micrographs of the wild type *N. magadii* L11 strain after lysis and (B) non lysogenic L13 strain (Adapted from Iro, 2007).

1.1.2.3. Genetic tools and manipulations in halophilic *archaea*

Genetic engineering plays a major role in understanding gene functions and is widely used in medicine, research, industry and agriculture. Genetic manipulations in *N. magadii* can be quite challenging due to the polyploidy, the long generation times and the limited genetic tools. In order to overcome this problem, genetic manipulations are mostly performed in *E. coli*.

1.1.2.3.1. Transformation

The first transformation method in halophilic *Archaea* was developed by transfecting *Halobacterium salinarum* with isolated DNA from the φH virus (Cline and Ford Doolittle, 1987). For this purpose, a polyethylene glycol 600-based transformation was employed that generates spheroplasts through the addition of EDTA, resulting in the abolishment of the S-layer. The transformation procedure was further adapted for *Haloferax volcanii* (Charlebois *et al.,* 1987), but remained inefficient for *N. magadii*, due to the differences in glycosylation of related S-layer glycoproteins compared to moderate halophiles (Mengele and Sumper, 1992). However, incubation with bacitracin and treatment with proteinase K resulted in the successful removal of the glycoprotein

surface layer and thus the formation of spheroplasts. This led to the generation of viable cells capable of taking up DNA via PEG-mediated method (Mayrhofer-Iro *et al.*, 2013a).

1.1.2.3.2. Shuttle vectors and selection markers

Up to date, two shuttle vectors are available for *N. magadii*, namely pNB102 and pRo5. The plasmid pRo-5 is based upon the *E. coli* vector pKSII^{+} containing a mutated version of the DNA gyrase gene, which carries point mutations in the GyrB subunit, conferring resistance to novobiocin. Novobiocin binds to the B subunit of DNA gyrase and blocks the ATP-binding site (Drlica and Franco, 1988). In addition, pRo-5 contains the *bla* gene that encodes the enzyme beta-lactamase, conferring an additional ampicillin resistance for selection in *E. coli*. For autonomous replication in *N. magadii*, the minimal replicon of φCh1, namely ORF53 and ORF54, were cloned into the vector (Mayrhofer-Iro *et al.*, 2013b). These two ORFs are flanked by AT-rich regions and show homology to the plasmid replication protein RepH, which is essential for the replication in halophilic *archaea* (Ng and DasSarma, 1993).

The second shuttle vector pNB102 has been constructed from the plasmid pNB101, which was isolated from the *Natronobacterium sp.* AS7091 strain (Zhou, Xiang, Sun, Li, *et al.*, 2004), by inserting the *ColE1* origin of replication that allows autonomous replication in *E. coli*. For selection in *E. coli* and haloarchaea, the ampicillin and mevinolin resistance cassette were used respectively (Zhou, Xiang, Sun and Tan, 2004). Mevinolin inhibits the 3-hydroxy-3-methylglutaryl coenzyme A (HMG-CoA) reductase and prevents therefore the synthesis of archaeal isoprenoid lipids (Lam and Doolittle, 1992).

1.2. Viruses of *archaea*

Archaeal viruses display unique physiological and morphological characteristics compared to viruses infecting bacteria and eukaryotes, with genomes that show little to no similarity to genes of known function (Krupovic *et al.*, 2018). The first archaeal viruses were discovered in *Halobacterium cutirubrum* and *Halobacterium*

salinarium and were wistaken as bacteriophages due to their characteristic head-tail morphology (Torsvik and Dundas, 1974; Wais *et al.*, 1975). Even though the first archaeal virus was described over 40 years ago, less than 150 archaeal viruses have been discovered until now (Dellas *et al.*, 2014). These viruses are able to populate every ecosystem on the planet, including the extreme acidic, thermal, and saline environments where archaeal organisms thrive, and their hosts can range from halophilic microorganisms to thermophiles (Torsvik and Dundas, 1980; Janekovic *et al.*, 1983; Martin *et al.*, 1984).

The archaeal viruses are classified into *archaea*-specific viruses and cosmopolitan archaeal viruses (Iranzo, Krupovic and Koonin, 2016). *Archaea*-specific viruses show huge diversity with distinct morphological features (Arnold *et al.*, 2000; Haring *et al.*, 2005; Krupovic *et al.*, 2014) and are classified in 12 families. In contrast, cosmopolitan archaeal viruses are dsDNA viruses and classified into the order of Caudovirales. They consist of the icosahedral head and long contractile (*Myoviridae*) or noncontractile (*Siphoviridae*) tails (Senčilo and Roine, 2014). The majority of described viruses belong to the phyla of Euryarchaeota and Crenarchaeota.

1.2.1. Viruses of haloarchaea

The best-studied viruses of Halobacteriaceae are φH and φCh1 infecting *Halobacterium salinarum* and *Natrialba magadii* respectively. Both are latent viruses, i.e. can remain dormant or integrate into the genome of the host cell, and exhibit head-tail morphology. Despite the fact that their hosts are phylogenetically distant, the viruses show a high sequence similarity (Klein *et al.*, 2002). One of the main differences is that the genome of φH persists as a plasmid in the cytoplasm of *H. salinarum* (Schnabel *et al.*, 1984), whereas φCh1 integrates into the host chromosome (Witte *et al.*, 1997). The mechanism of action of both viruses resembles the well-studied temperate bacteriophages (Porter, Russ and Dyall-Smith, 2007).

Additional representatives of haloarchaeal viruses are HF1 and HF2, which were isolated from hypersaline environments and are the first reported lytic viruses (Dyall-Smith, Tang and Bath, 2003). HF1 and HF2 can infect a variety of hosts, for example *Haloferax*, *Halobacterium*, *Haloarcula* and *Natrialba* (Ventosa and Ventosa,

2004) . Despite the broad host range, their genomes show more than 80 % similarity. Many regions of the HF2 genome are identical to different haloarchaea, indicating a horizontal gene transfer during archaeal evolution (Dyall-Smith, Tang and Bath, 2003). Furthermore, lytic viruses infecting halophilic *archaea*, like Ja.1 or B10, have been discovered, but little is known so far (Porter, Russ and Dyall-Smith, 2007).

1.2.2. The haloalkalophilic virus φCh1

The virus φCh1 belongs to the family of *Myoviridae* and infects the haloalkaliphilic archaeon *N. magadii*, its only known host (Witte *et al.*, 1997). As depicted in Figure 2, the virus consists of an icosahedral head and a long contractile tail and has a length of approximately 200 nm. φCh1 is a temperate virus with a switch between lysogenic and lytic state. Wild type *N. magadii* cultures spontaneously lyse upon entry in the stationary phase, indicating that the lysis is growth dependent. As mentioned above, φCh1 is able to infect the cured *N. magadii* L13 strain, but display immunity to the superinfection (Witte *et al.*, 1997).

Due to the extreme conditions the host thrive in, the virus had to adapt to the physiological needs of its host. φCh1 requires salt concentrations higher than 2 M in order to maintain its infectivity and stability. Decreasing salt concentration below 2 M may result in dissociation of the virus particles or conformational changes of the capsid proteins (Witte *et al.*, 1997). Further analysis of whole protein extracts revealed that φCh1 contains four major (A, E, H and I) and five minor proteins (B, C, D, F and G), ranging in size from 15 to 80 kDa. These proteins contain many acidic residues, resulting therefore in low isoelectric points between pH 3.3 and 5.2. Similar pH values are observed for various proteins of other halophilic *archaea* (Lanyi, 1974). Further studies revealed that the genome of φCh1 is methylated in parts of the population at the adenine residues in the sequence GATC, leading to the assumption that φCh1 encodes its own methyltransferase (Witte *et al.*, 1997). Later on, the methyltransferase *M. NmaφCh1I* was discovered (Baranyi *et al.*, 2000). *M. NmaφCh1-I* is a Dam-like methyltransferase and a late gene, i.e. is produced during the late phase of the virus development. Furthermore, it was published that φCh1 produces two types of tail fiber proteins gp34 and gp36, but only the one encoded by ORF34 is able to bind to host in vitro (Klein *et al.*, 2012).

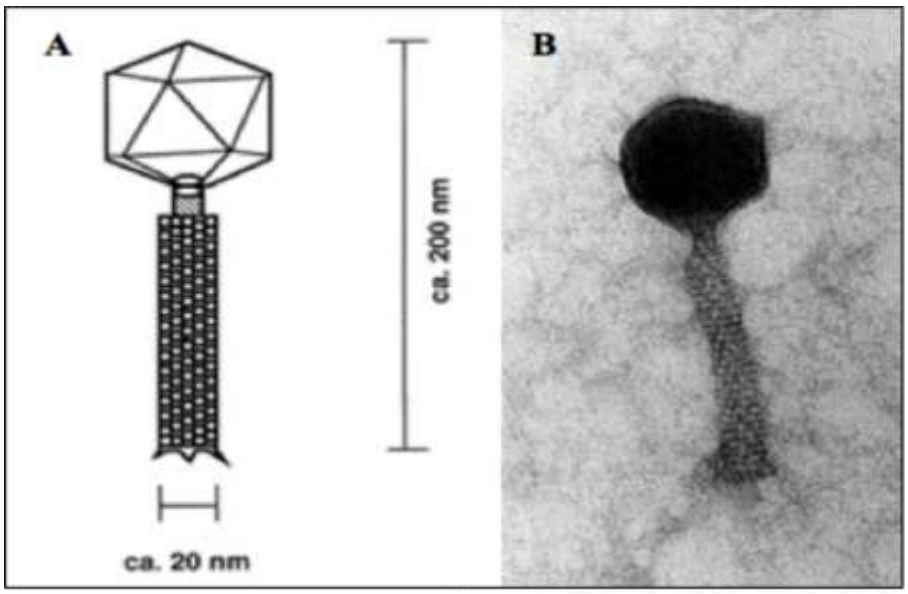

Figure 2. Morphology of the head-tail virus φCh1. (A) Schematic representation of the φCh1 consisting of an icosahedral head and a contractible tail. (B) Electron micrograph of φCh1 (Adapted from Witte *et al*, 1997).

φCh1 is the first virus of extreme haloalkaliphilic *archaea* whose genome has been completely sequenced. The genome size is 58.498 bp and contains 98 different open reading frames (Klein *et al.*, 2002). It is terminally redundant as well as circularly permuted, with a GC content of 61.9 %.

Based on the sequence similarities, the function of 48 out of 98 ORFs was assessed, while many proteins share up to 80 % sequence similarities with the φH virus (Klein *et al.*, 2002). The already verified and annotated functions of the gene products are shown in Figure 3. The genomic organization of φCh1 consists of three functional genetic modules and resembles that of bacteriophage λ. The left part of the genome contains genes that encode structural proteins and proteins involved in virion morphogenesis; genes in the central part are involved in DNA replication, plasmid partitioning and regulation of gene expression; the right part consists of genes whose functions remain unclear, as well as genes involved in DNA modifications, like methylation and restriction (Klein *et al.*, 2002). Some genes have overlapping start and stop codons and are therefore organized in operons (Klein *et al.*, 2002).

In addition, the mature viral particle contains several different RNA species, which range between 80 and 700 nucleotides. It has been shown that the virion-associated RNA is host-encoded and it is assumed to be involved in the packaging of the viral DNA (Witte *et al.*, 1997).

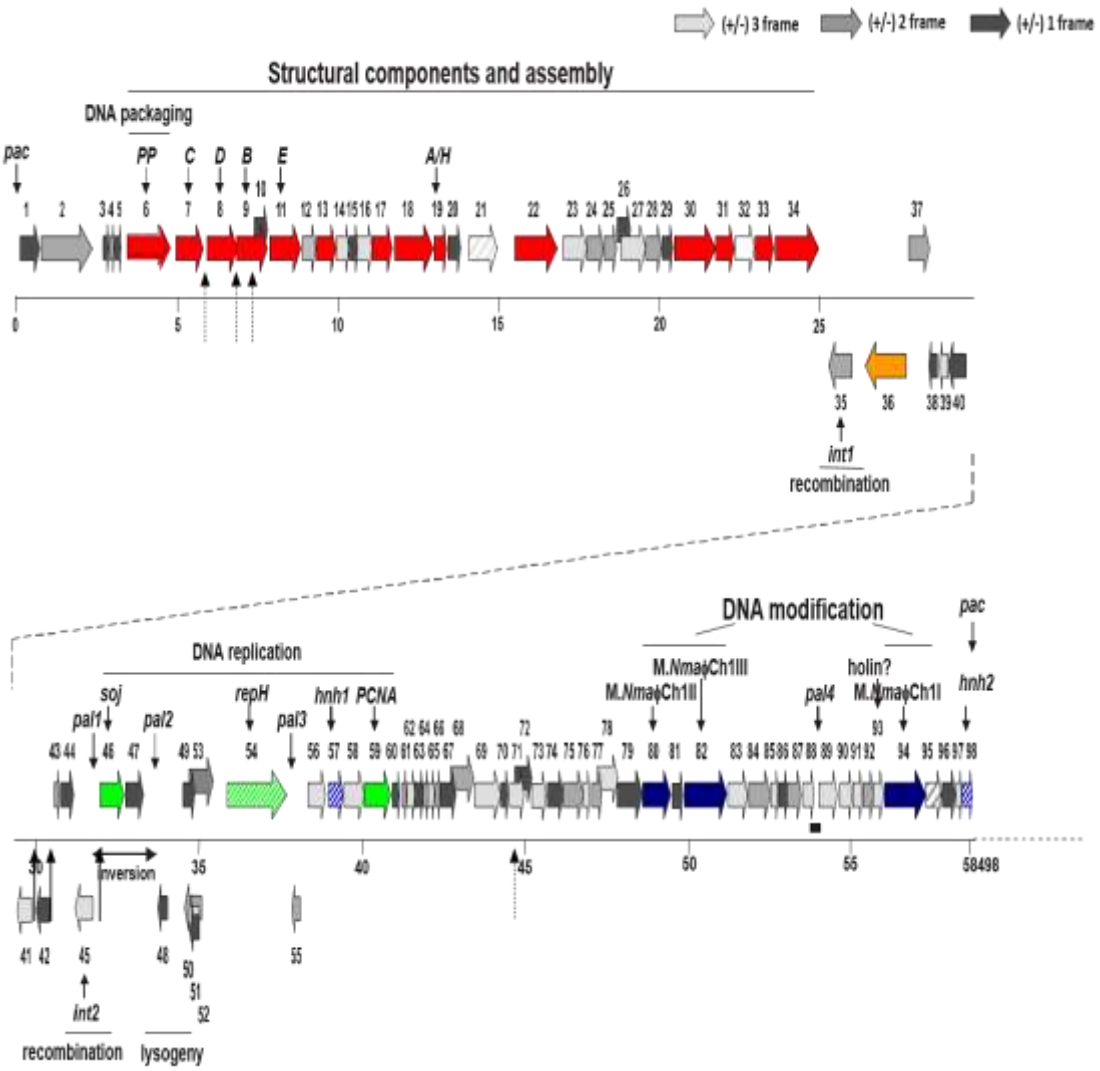

Figure 3. Schematic representation of the φCh1 genome. The viral genome contains 98 open reading frames, which are depicted as colored arrows. Light grey, grey and dark grey arrows represent the three different reading frames. The orientation of the ORFs and the putative or verified functions of the gene products are indicated by arrows. The genome consists of three functional modules: genes encoding structural proteins, regions mainly responsible for DNA replication and DNA modification respectively (Adapted from Klein *et al*., 2002).

1.3. Toxin Antitoxin (TA) systems

Almost all bacteria encode small toxins that can affect cell growth by binding to cellular targets which are involved in essential cellular processes, such as DNA replication, mRNA stability or ATP and protein synthesis (Pandey and Gerdes, 2005; Yamaguchi, Park and Inouye, 2011). These toxins form together the TA operon and are co-transcribed and co-translated with their matching antitoxins. In general, toxins are more stable than their conjugate antitoxin. Antitoxins are constantly produced in order to counterbalance the toxicity of toxins, but are proteolytically degraded under stress conditions, leading to the release of the toxins (Yamaguchi, Park and Inouye, 2011). On the other hand, toxins are immune to proteases and are free to fulfill their functions as nucleases or translational inhibitors upon proteolysis of the antitoxin (Bailey and Hayes, 2009).

There are three types of TA operons, based on the nature of the antitoxin and the composition of the TA systems. In the Type I TA system, the toxin gene expression is regulated by the antisense RNA antitoxin, which is transcribed from the same region as the toxin. Antitoxin and toxin form a double-stranded RNA molecule that initiates the degradation of the toxin mRNAs (Gerdes and Wagner, 2007). In the Type II TA system, both toxins and antitoxins consist of proteins that form a heteroduplex to neutralize the effects of the toxin (Yamaguchi and Inouye, 2009). In the Type III TA system, the sense RNA antitoxin interacts with the toxin protein, resulting in the formation of a RNA-protein complex, which inhibits therefore the function of the toxin (Fineran *et al.*, 2009). In normally growing cells, all three types of TA systems are constitutively transcribed, leading to the steady production of both toxins and antitoxins. Despite being trivial for normal cell growth, they are extensively widespread in bacteria and *archaea* (Pandey and Gerdes, 2005).

1.3.1. VapBC toxin-antitoxin system

VapBC (virulence associated protein) toxin-antitoxin systems represent the largest family of type II toxin-antitoxin system in prokaryotes (Robson *et al.*, 2009) and are quite abundant, especially in *archaea* (Gerdes, Christensen and Løbner-Olesen, 2005). The first characterized VapBC system was found in *Salmonella dublin*

(Pullinger and Lax, 1992). VapBC operon contains two genes: the *VapC* encodes a toxin PIN domain protein while *VapB* the conjugate antitoxin (Yamaguchi, Park and Inouye, 2011). In most Type II systems, the antitoxin genes are located upstream of their cognate toxin genes.

As depicted in Figure 4, *VapB* and *VapC* are under the control of the same promoter and have overlapping start and stop codons leading to their co-transcription and co-translation. Antitoxin forms a heterodimer with the stable toxin in order to neutralize the toxin toxicity and to autoregulate the TA module. This TA complex acts as transcriptional repressor of the TA operon by binding a palindromic sequence in the promoter region. Antitoxin itself is able to autoregulate the system, but more weakly than the TA complex. Under stress conditions, VapB protein is cleaved by proteases in an ATP-dependent manner, resulting in the release and activation of the toxin (Arcus *et al.*, 2011). This toxin activity leads to cell growth arrest and eventual cell death.

The cellular targets of toxins of Type II TA systems are highly diverse. CcdB and ParE toxins inhibit DNA gyrase and blocking therefore DNA replication (Couturier, Bahassi and Van Melderen, 1998; Yuan *et al.*, 2010). On the other hand, toxins like MazF in *E. coli* cleave cellular mRNAs, affecting mRNA stability (Yamaguchi and Inouye, 2009). A *MazF* homolog was recently identified in *Haloquadra walsbyi*, a halophilic archaeon isolated from a hypersaline pool on the Sinai Peninsula (Walsby, 1980). Unraveling the function of toxins is of fundamental importance for our understanding of the roles of the TA systems in prokaryotes. Toxins may benefit hosts adapting to environmental changes by slowing down or inhibiting cell growth or promoting cell apoptosis (Arcus *et al.*, 2011). To conclude, the constant presence of TA complexes may be advantageous for a cell and the survival in their natural habitats.

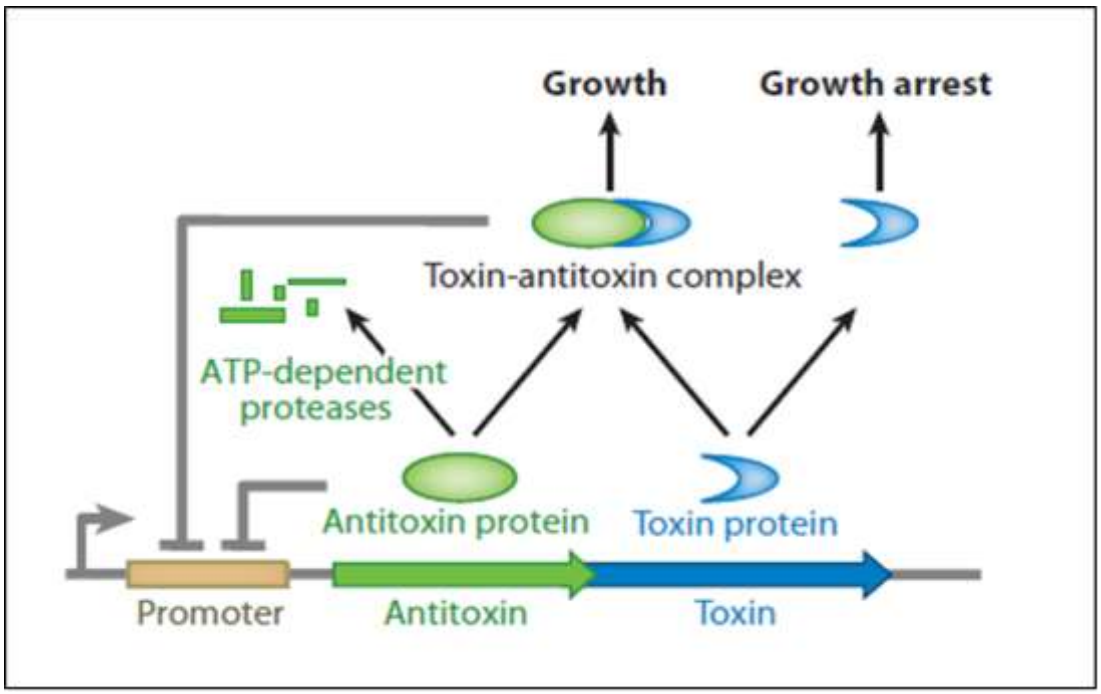

Figure 4. Schematic representation of the VapBC toxin-antitoxin system. *VapB* and *VapC* have overlapping start and stop codons and form an operon. The VapBC complex consists of the labile antitoxin VapB (green) that antagonizes the stable toxin VapC (blue). Antitoxin forms a heterodimeric polypeptide complex with toxin and inhibits toxicity of toxin leading to autoregulation of system. Degradation of the antitoxin results in the activation of the toxin (Yamaguchi *et al.*, 2011).

1.3.2. φCh1 ORF43/44 as a putative VapBC toxin-antitoxin system

The putative toxin ORF44 is upstream of the φCh1 replication domain and forms an operon together with ORF43. Both ORFs are under the control of the same promoter, namely p43, and overlap in one nucleotide (Iro *et al.*, 2007a), leading to their co-transcription and co-translation. Pfam analysis revealed the presence of a VapC-like PIN domain in gp44 (see Fig. 5). PIN domains are small protein domains identified by the presence of four conserved acidic residues (Matelska, Steczkiewicz and Ginalski, 2017) which form the active site that binds one or more divalent metal ions, like Mg^{2+} or Mn^{2+}. This domain consists of 130 amino acids and is present in all three domains of life. The PIN domains function as ribonucleases that cleave single stranded RNA in a sequence- or structure- dependent manner (Arcus *et al.*, 2011). In prokaryotes, the majority of these proteins comprise the toxic part of toxin-antitoxin systems (Matelska,

Steczkiewicz and Ginalski, 2017). The presence of the PIN domain in gp44 led to the hypothesis that gp44 is the putative toxin of the ORF43/44 TA system.

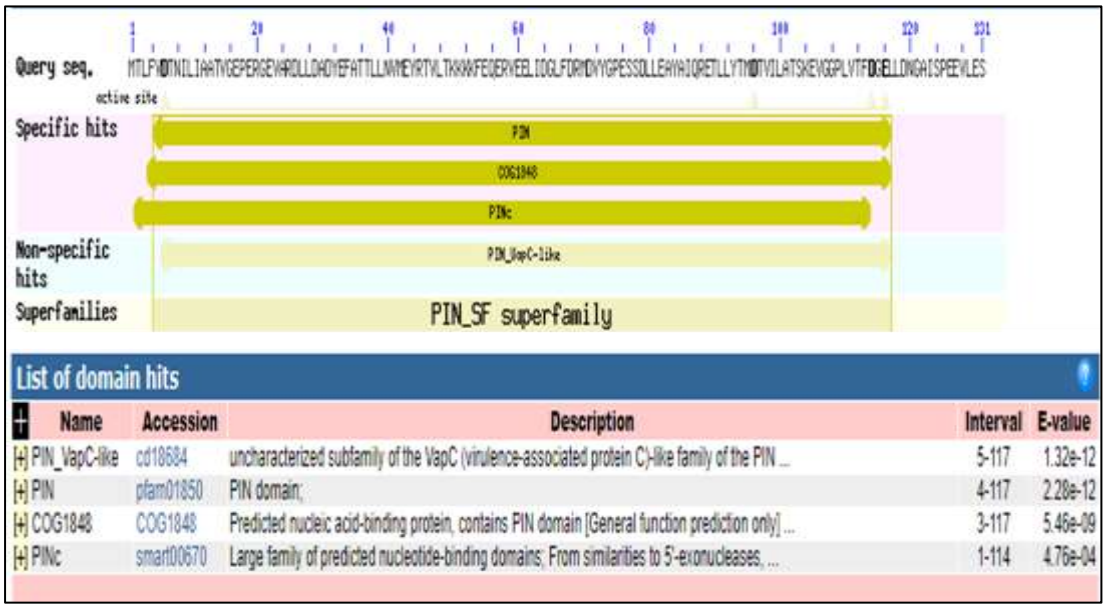

Figure 5. Analysis of the protein sequence of ORF44. Pfam analysis revealed a PIN-domain in the viral toxin gp44 and thus a homology to the VapBC toxin-antitoxin system.

Further studies in *H. volcanii* showed that ORF43 and ORF43/44 have an enhancing effect on the expression of genes under the control of the ORF49 promoter, whereas the presence of ORF44 had an antagonizing effect (Iro *et al.*, 2007a). Furthermore, experiments in the cured *N. magadii* L13 strain using transcriptional fusion of the promoter p43 with reporter gene $ORF34_{52}$ (encodes tail-fiber protein) demonstrated that, in the presence of ORF44, a truncated tail-fiber protein was produced, potentially suggesting the function of gp44 as an endoribonuclease (Hofbauer, 2015). Due to the high sequence similarity between $ORF34_{52}$ and the upstream region of ORF94, encoding a DNA methyltransferase (see Fig. 6), the experiment was repeated, but with ORF94 as the reporter gene instead of $ORF34_{52}$. Obtained results showed a 48-hour delay in reporter gene expression containing ORF44, but no truncation, indicating that gp44 may have cleaved the upstream region. (Hofbauer, 2015).

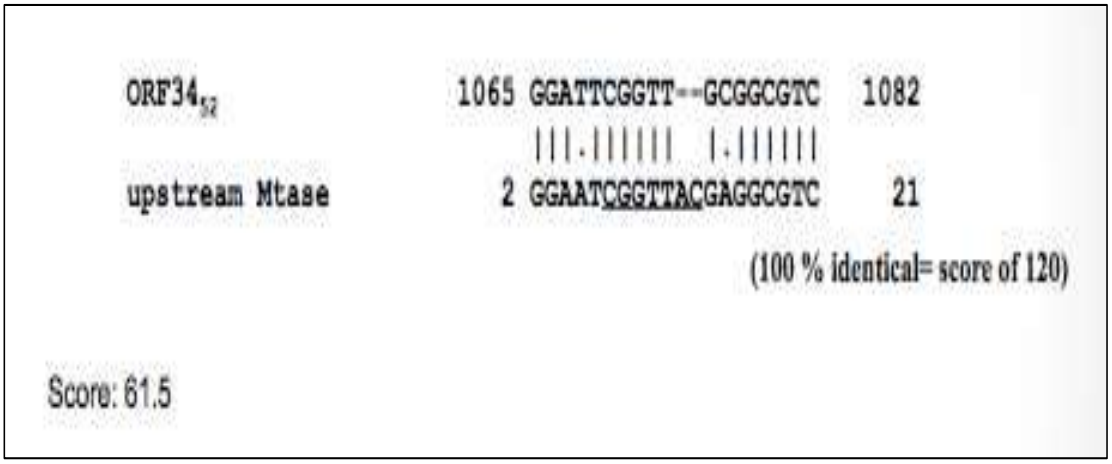

Figure 6. EMBOSS Water Pairwise Sequence Alignment. The coding sequence of tail fiber protein gp34$_{52}$ was aligned with the upstream region of the methyl transferase gene ORF94.

The aim of this thesis is to investigate the putative mRNA interferase activity of gp44. To further study the effect of ORF44, a ORF44 deletion mutant strain was constructed (Gillen, 2017). The stability of the mutant strain as well as the effect of salt on the lysis behavior and the production of viral particles were studied by continuous passaging of both wild type L11 and L11-Δ44. Phenotypic, complementation and overexpression analyses were additionally carried out. Furthermore, the influence of ORF43, the conjugate antitoxin of the putative φCh1 TA system, was examined by overexpressing the gene in a gene dosage-dependent manner. Finally, the isolation and purification of gp44 protein was attempted for *in vitro* functional studies.

2. Materials and Methods

2.1. Materials

2.1.1. Strains

Escherichia coli

Strain	Genotype	Source
Lemo21 (DE3)	*fhuA2, [lon], ompT, gal, (λDE3), [dcm], ΔhsdS/pLemo*(CamR), *λ DE3 = λ sBamHIo ΔEcoRIB, int::(lacI::PlacUV5::T7 gene1,) i21, Δnin5,* pLemo = pACYC184-*PrhaBADlysY*	Novagen
XL1-Blue	*endA1, gyrA96, hsdR17* ($r_{k-}m_{K+}$), *lac, recA1, relA1, supE44, thi,* (F′, $lacI^{q}$, *lacZ*ΔM15, $proAB^{+}$,, Tn10 (Tet^{R})]	Stratagene

Natrialba magadii

Strain	Genotype	Source
L11	Wild type strain - φCh1	Witte *et al.*, 1997
L11-ΔORF44	Deletion of ORF44	Gillen Yan, 2017
L13	φCh1 cured strain	Witte *et al.*, 1997

Haloferax volcanii

Strain	Genotype	Source
WD2	ΔpHV2	Charlebois *et al.*, 1987

2.1.2. Growth media

2.1.2.1. Lysogeny broth medium (LB) for *E. coli*

NaCl	5 g
Yeast extract	5 g

Peptone	10 g

pH 7

dH_2O ad 1 l

15 g/l agar for plates

2.1.2.2. *N. magadii* rich medium – NVM^+ / $NVM\text{-}CA^+$

NaCl	235 g
KCl	2.4 g
Yeast extract	11.7 g
Casein hydrolysate/ Casamino acids	8.8 g
Sodium citrate tribasic dihydrate	0.8 g

pH 9.5

dH_2O ad 935 ml

8 g/l agar for plates or 4 g/l agar for top agar

After autoclaving, media were complemented with:

0.57 M Na_2CO_3	62 ml
1 M $MgSO_4$	1 ml
20 mM $FeSO_4$	1 ml
Trace elements SL-6	1 ml

1000x Trace elements SL-6

$CoCl_2.6H_2O$	0.2 g
$CuCl_2.6H_2O$	10 mg

H_3BO_3	0.3 g
$MnCl_3.4H_2O$	30 mg
$Na_2MoO_4.H_2O$	30 mg
$NiCl_2.6H_2O$	20 mg
$ZnSO_4.7H_2O$	0.1 g

dH_2O ad 100 ml

Sterilized by filtration

2.1.2.3. Growth media for Haloarchaea – *H. volcanii*

2.1.2.3.1. Concentrated Salt Water (SW) solution - 30% (w/v)

NaCl	240 g
$MgCl_2.6H_2O$	30 g
$MgSO_4.7H_2O$	35 g
KCl	7 g
1 M $CaCl_2.2H_2O$ (sterile)	5 ml

pH 7.5 with 1 M Tris.Cl buffer (pH 7.5)

dH_2O ad 1 l

2.1.2.3.2. Modified growth medium – 18 % MGM^+

30 % Salt Water	600 ml
Peptone (Oxoid)	5 g
Yeast Extract	1 g

pH 7.4 with 1 M Tris base

dH_2O ad 1 l

15 g/l agar for plates

After autoclaving, media were complemented with 1 ml trace elements SL-6.

2.1.2.3.3. Hv – YPC complete medium

30 % Salt Water	600 ml
Yeast Extract	5 g
Peptone (Oxoid)	1 g
Casamino acids	1 g

pH 7.5 with 1 M KOH

dH_2O ad 1 l

After autoclaving, media were complemented with 1 ml trace elements SL-6 and 3 ml of 1 M $CaCl_2.2H_2O$ (sterile).

2.1.3. Antibiotics and further additives

Compound	Stock concentration	Final concentration	Preparation
Ampicillin	20 mg/ml	100 µg/ml	dissolved in dH_2O, sterile filtered, stored at 4°C
Chloramphenicol	40 mg/ml	20 µg/ml	dissolved in 96 % EtOH, stored at -20 °C
Tetracycline	10 mg/ml	10 µg/ml	dissolved in half of EtOH and half dH_2O, stored at -20 °C
Mevinolin	10 mg/ml	7.5 µg/ml *	120 mg of Lovastatin Hexal tablets dissolved in 12 ml 96 % EtOH, storage at -20 °C
Novobiocin	3 mg/ml	3 µg/ml **	dissolved in dH_2O, sterile filtered, storage at -20 °C
Bacitracin	7 mg/ml	70 µg/ml	dissolved in dH_2O, sterile filtered, storage at 4°C

IPTG	1 M	1 mM	dissolved in dH_2O, sterile filtered, storage at -20 °C
L-Rhamnose	1 M	1 mM	dissolved in dH_2O, sterile filtered, storage at -20 °C
PMSF	100 mM	1 mM	dissolved in 96 % EtOH, storage at -20 °C
L- tryptophan	0.6 M	2-4 mM	dissolved in 1M NaOH, storage at -20 °C
L- tryptophan for *H.volcanii*	30 mM	5 mM	dissolved in 18 % Salt water, sterile filtered, storage at 4°C

*: 5 µg/ml for *H. volcanii*

**: 0.3 µg/ml for *H. volcanii*

2.1.4. Plasmids

Plasmid	Features	Source
pMDS24	*bla*, ColE1, (mevR), DHFR, pHV2 ori	Jolley *et al.*, 1996
pRo-5-Mev	*bla*, ColE1 ori, *hmg* (mevR), φCh1-derived ori	Dina, 2019
pNB102	*bla*, ColE1 ori, *hmg* (mevR), φCh1 derived ori	Zhout *et al.*, 2004
pRV1-pTna	*bla*, *gyrB* (NovR), p*tna* promoted *bgaH*	Lund *et al.*, 2007
pRSETA	*bla*, pUC ori, T7 promoter, N-terminal 6x His-tag	Invitrogen
pRSETA-ORF44	pRSETA with φCh1 ORF44	Iro, 2006
pNB102-ORF43	pNB102 with ORF43 of φCh1 under the control of native promoter	This study
pNB102-ORF43/44	pNB102 with ORF43/44 of φCh1 under the control of native promoter	Till, 2010
pRo-5-Mev-ORF43	pRo5/mev with ORF43 of φCh1 under the control of native promoter	This study

pRo-5-Mev-ORF43/44	pRo5/mev with ORF43/44 of φCh1 under the control of native promoter	This study
pRV1-ptna-44	pRV1 with ORF44 of φCh1 under the control of tryptophan inducible promoter from *H. volcanii*	This study
pRo-5-Mev-tnaN-44	pRo5/mev with ORF44 of φCh1 under the control of tryptophan inducible promoter from *N. magadii*	This study
pMDS24-34_1	pMDS24 with ORF34 (+ orientation of *int1*) of φCh1 under the control of native promoter	This study
pMDS24-34_{52}	pMDS24 with ORF34 (- orientation of *int1*) of φCh1 under the control of native promoter	This study
pMDS24-34_{52}-ORF43	pMDS24 with ORF34 (- orientation of *int1*) and ORF43 of φCh1 under the control of native promoters	This study
pMDS24-34_{52}-tnaN-ORF44	pMDS24 with ORF34 (- orientation of *int1*) of φCh1 under the control of native promoter and with ORF44 under the control of tryptophan inducible promoter	This study
pMDS24-34_{52}-ORF43/44	pMDS24 with ORF34 (- orientation of *int1*) and ORF43/44 of φCh1 under the control of native promoters	This study
pMDS24-34_1-ORF43	pMDS24 with ORF34 (+ orientation of *int1*) and ORF43 of φCh1 under the control of native promoters	This study
pMDS24-34_1-tnaN-ORF44	pMDS24 with ORF34 (+ orientation of *int1*) of φCh1 under the control of native promoter and with ORF44 under the control of tryptophan inducible promoter	This study
pMDS24-34_1- ORF43/44	pMDS24 with ORF34 (+ orientation of *int1*) and ORF43/44 of φCh1 under the control of native promoters	This study

2.1.5. Primers

Primer name	Sequence (5' → 3')
43-Kpn-3	CAGCAGGGTACCCGTGTCGACGAACAGCG
43-5	CAGCAGTCTAGACGTTGTGCCAGCCGT
44-5-Nde-His	GATCCATATGCACCACCACCACCACCACACGCTGTTCGTCGACA
44-3-Bam	GTTAGGATCCACAGAACGGACGTACGAC
34-XbaI	CAGCAGTCTAGACGGCGTTCGAGGTCA
36-3	CAGCAGAAGCTTATTCAGGTTTCATGTCGCTG
Tna-Kpn-5	GAATGGTACCTGAGGAATCGACCGGTTTTG
43-Kpn-5	CAGCAGGTACCGTTGTGCCAGCCGT
44-Kpn-3	CAGCGGTACCGATTTAGGACTCGAGGACC
34-Hv-1	CCCCATGCCAAGCTTCTTCTAGACGGCGTTCGAGGTCACGTACAGTAG
34-Hv-2	GGCAGCCTCGACGGCTGGCACAACGTTATTCGAGTTTCATGTCGCTGAAC
43-Hv-1	GTTCAGCGACATGAAACTCGAATAACGTTGTGCCAGCCGTCGAGGCTGCC
43-Hv-2	CATGCCACTCTTCACACGCGGTACCTCATTCGCGCTCGCGCAGCTCGCGGA
43-Hv-3	CATGCCACTCTTCACACGCGGTACCTTAGGACTCGAGGACCTCCTCCGGGG
pro5-mev	CCTTATCAAACACGCACAC
34-Hv-3	GGCAGCCTCGACGGCTGGCACAACGTTGCATTGGTTCAGATCAGGTTTA
43-Hv-4	ATAAACCTGATCTGAACCAATGCAACGTTGTGCCAGCCGTCGAGGCTGCC
34-pTna-2	TAAACCTGATCTGAACCAATGCAACCTGAGGAATCGACCGGTTTT
34-pTna-3	GTTCAGCGACATGAAACTCGAATAACTGAGGAATCGACCGGTTTT
34-pTna-4	AAAACCGGTCGATTCCTCAGTTATTCGAGTTTCATGTCGCTGAAC
34-pTna-1	AAAACCGGTCGATTCCTCAGGTTGCATTGGTTCAGATCAGGTTTA
43-bam	CAGCGGATCCATGGCAATCGTCACC
43-hind	CAGCAAGCTTTCATTCGCGCTCG
56-RT5	GAACAGCGCCAGTCCA
56-RT3	GACCACCGGCTTCAGC
44-bam	CAGCGGATCCATGACGCTGTTCGTCG
44-hind	CAGCAAGCTTGATTTAGGACTCGAGGACC

2.1.6. DNA and protein ladders

DNA ladder	Size in bp	Company
GeneRuler 1kb DNA Ladder	250, 500, 750, 1000, 1500, 2000, 2500, 3000, 3500, 4000, 5000, 6000, 8000, 10000	Thermo Scientific
Quick-Load® Low Molecular Weight DNA Ladder	25, 50, 75, 100, 150, 200, 250, 300, 350, 500, 766	New England Biolabs

Protein ladder	Size in kDa	Company
PageRuler™ Prestained Protein Ladder	10, 15, 25, 35, 40, 55, 70, 100, 130, 180	Thermo Scientific
PageRuler™ Plus Prestained Protein Ladder	10, 15, 25, 35, 55, 70, 100, 130, 250	Thermo Scientific

2.1.7. Enzymes *

Enzyme	Product number	Company
Restriction enzymes	N/A	Thermo Scientific
T4 DNA ligase	M1801	Promega
Fast AP Alkaline Phosphatase	EF0652	Thermo Scientific
2x GoTag Green Master Mix	M7123	Promega
Phusion® Flash PCR Master Mix	F548S/F548L	Thermo Scientific
Lysozyme from chicken egg white	L6876	Sigma
Proteinase K	1019499	Qiagen

*: All enzymes and their respective buffers were used according to the instructions of the manufacturer.

2.1.8. Kits

Name	Usage	Company
Promega Wizard® SV Gel and PCR Clean-Up System	Purification of gel-eluted DNA fragments and PCR products	Promega
Wizard® Plus SV Minipreps DNA Purification System	Isolation of plasmid DNA	Promega
Gibson Assembly® HiFi 1-Step Kit	DNA cloning	Synthetic Genomics

2.1.9. Antibodies

2.1.9.1. Primary antibodies

Antibody	Target	Dilution	Source
α- Soj	Soj of φCh1	1:250	Hofbauer, 2015
α- Protein E	φCh1 gp11	1:2500	Klein *et al.*, 2000
α- Mtase	φCh1 gp94	1:500	Baranyi *et al.*, 2000
α- $gp34_{52}$ (rabbit 20)	φCh1 gp34	1:2500	Till, 2011

All antibodies were produced in rabbits and diluted in 1 x TBS, 0.3 % BSA, 0.02 % NaN_3.

2.1.9.2. Secondary antibodies

Antibody	Target	Dilution	Source
ECL™ Anti-Rabbit IgG, HRP linked whole antibody from donkey	Rabbit IgG	1:5000	GE Healthcare

All secondary antibodies were diluted in 1 x TBS.

2.1.10. Oligo RNAs

Oligoname	Sequence (5' → 3')	Source
34-mRNA-m	GCGUCUGACCAGACGGCGAUGACUCCGUGGCCGC GUCCAUCAUCGCAAGAAC	VBC-Biotech Service GmbH
34-mRNA-wt	GCGUCUGACCAGACGGCGAUGGAUUCGG UUGCGGCGUCCAUCAUCGCAAGAAC	VBC-Biotech Service GmbH

2.1.11. Buffers and solutions

2.1.11.1. Gel electrophoresis

2.1.11.1.1. DNA gels

5 x DNA loading dye		50 x TAE	
Tris.Cl pH 8.2	50 mM	Tris.Cl pH 8.2	2 M
SDS	0.1 % v/v	Acetic acid	1 M
Bromophenol blue	0.05 % w/v	EDTA	0.1 M
Xylene cyanol	0.05 % w/v		

0.8 – 1.3 % agarose		
Agarose	0.8 – 1.3 g	in 100 ml 1 x TAE

Ethidium bromide bath		
Ethidium bromide	10 µg/ml	in 100 ml 1 x TAE

2.1.11.1.2. RNA gels*

* All solutions were prepared in DEPC- treated ddH_2O

10 x TBE		2 x RNA loading dye	
Tris	108 g	Formamide	95 % v/v
Boric acid	55 g	Na_2EDTA	0.5 mM
Na_2EDTA	9.3 g	SDS	0.02 % v/v
pH 8		Xylene Cylene	0.01 % w/v
dH_2O ad 1 l		Bromphenol Blue	0.02 % w/v

12 % Urea-TBE PAA gel

Urea	9.61 g
10x TBE	2 ml
40 % PAA (19:1)	6 ml

dH_2O ad 20 ml and dissolve urea at 65 °C

After cooldown, add 160 µl 10 % APS and 16 µl TEMED

2.1.11.1.3. Protein gels

2 x Laemmli buffer		5 mM sodium phosphate buffer	
Tris.Cl pH 6.8	125 mM	Na_2HPO_4	1 M
SDS	4 % v/v	NaH_2PO_4	1 M
β-mercaptoethanol	10 % v/v	pH 6.8	
Glycerol	20 % v/v		
Bromphenol blue	0.04 % w/v		

30 % acrylamide solution (29:1)	
Acrylamide	73 g
N, N'-	2 g
methylene-bisacrylamide	
ddH_2O ad 250 ml and filter	

10 x SDS Running buffer	
Tris	250 mM
Glycine	1.92 M
SDS	1 % w/v

Stacking gel buffer	
Tris.Cl pH 6.8	0.5 M
SDS	0.4 % v/v

Separating gel buffer	
Tris.Cl pH 8.8	1.5 M
SDS	0.4 % v/v

Coomassie staining solution	
Methanol	25 % v/v
Acetic acid	10 % v/v
Coomassie Brillant Blue R250	0.25 % w/v

Destaining solution	
Acetic acid	10 % v/v

2.1.11.2. Gibson assembly

5 x ISO buffer	
Tric.Cl pH 7.5	500 mM
DL-Dithiothreitol	50 mM
dATP, dCTP, dGTP, dTTP	1 mM
NAD	5 mM
PEG-6000	25 % w/v

2 x Gibson Assembly Master Mix	
5 x ISO buffer	320 µl
Phusion polymerase	20 µl
T5 Exonuclease	1.5 µl
Taq DNA ligase	160 µl
ddH_2O ad 1 ml	

2.1.11.3. Western Blot

10 x TBS		1 x Towbin transfer buffer	
Tris.Cl pH 8.0	250 mM	Tris	25 mM
NaCl	1.37 M	Glycine	192 mM
		Methanol	20 % v/v

Ponceau-S staining solution		Blocking solution	
Ponceau-S	0.5 % w/v	Skim milk powder	5 % w/v
Trichloracetic acid	3 % v/v	in 1 x TBS	
Coumaric acid solution		Luminol solution	
Coumaric acid	0.148 g	Luminol	0.886 g
DMSO	10 ml	DMSO	20 ml

ECL buffer		Membrane stripping buffer	
1.5 M Tris.Cl pH 8.5	13.3 ml	1 M Tris.Cl pH 6.8	30 ml
Luminol	500 µl	β-mercaptoethanol	3.95 ml
Coumaric acid	250 µl	SDS	2 % v/v
dH_2O ad 200 ml		dH_2O ad 500 ml	

2.1.11.4. Preparation of competent cells and transformation

2.1.11.4.1. *E. coli*

MOPS I		MOPS II	
MOPS	100 mM	MOPS	100 mM

KCl	10 mM	KCl	10 mM
RbCl	10 mM	RbCl	10 mM
pH 7*		pH 6.5*	

MOPS IIa

MOPS	100 mM
KCl	10 mM
RbCl	10 mM
Glycerol	15 % v/v

pH 6.5*

*pH was adjusted with KOH

2.1.11.4.2. *N. magadii*

Buffered high salt spheroplasting solution

NaCl	2 M
KCl	27 mM
Tris.Cl pH 9.5	50 mM

After autoclaving: add 15 % v/v sucrose (sterilized by filtration)

Unbuffered high salt spheroplasting solution (UBSS-HS)

NaCl	2 M
KCl	27 mM

After autoclaving: add 15 % v/v sucrose (sterilized by filtration)

60 % PEG 600		0.5 M EDTA	
PEG 600	60 % v/v	EDTA	0.5 M
UBSS-HS	40 % v/v	pH 8 (adjusted with NaOH pellets)	

2.1.11.4.3. *H. volcanii*

Buffered low salt spheroplasting solution with glycerol

NaCl	1 M
KCl	27 mM
Tris.Cl pH 8.0	50 mM
Glycerol	15 % v/v

After autoclaving: add 15 % v/v sucrose (sterilized by filtration)

Unbuffered low salt spheroplasting solution (UBSS-LS)

NaCl	1 M
KCl	27 mM

After autoclaving: add 15 % v/v sucrose (sterilized by filtration)

60 % PEG 600

PEG 600	60 % v/v
UBSS-LS	40 % v/v

2.1.11.5. Protein isolation and purification

2.1.11.5.1. Purification from *E. coli* under denaturing conditions

Buffer B (Lysis buffer)

NaH_2PO_4	100 mM
Tris	10 mM
Urea	7 M
pH 8*	

Buffer C (Wash buffer)

NaH_2PO_4	100 mM
Tris	10 mM
Urea	8 M
pH 6.3**	

Buffer D (Elution buffer)

NaH_2PO_4	100 mM
Tris	10 mM
Urea	8 M
pH 5.9**	

Buffer E (Elution buffer)

NaH_2PO_4	100 mM
Tris	10 mM
Urea	8 M
pH 4.5**	

Renaturing Buffer 1

NaH_2PO_4	100 mM
Tris	10 mM
Urea	5 M
NaCl	1 M
pH 5.4**	

Renaturing Buffer 2

NaH_2PO_4	100 mM
Tris	10 mM
Urea	3 M
NaCl	2 M
pH 6.3**	

Renaturing Buffer 3

NaH_2PO_4	100 mM
Tris	10 mM
Urea	1 M
NaCl	3 M

Renaturing Buffer 4

NaH_2PO_4	100 mM
Tris	10 mM
NaCl	4 M
pH 8	

pH 7.2*

* pH was adjusted with NaOH before use.

** pH was adjusted with HCl before use.

2.1.11.5.2. Purification from *H. volcanii* under native conditions

Binding buffer		Wash buffer	
HEPES, pH 7.5	20 mM	HEPES, pH 7.5	20 mM
NaCl	2 M	NaCl	2 M
PMSF	1 mM	PMSF	1 mM
Imidazole	20 mM	Imidazole	50 mM

Elution buffer	
HEPES, pH 7.5	20 mM
NaCl	2 M
PMSF	1 mM
Imidazole	500 mM

2.2. Methods

2.2.1. DNA methods

2.2.1.1. Preparation of DNA templates and primers

N. magadii and *H. volcanii* templates were prepared by centrifuging 20 µl culture at 13.000 rpm for 3 min at RT followed by resuspension of the pellet in 100 µl dH_2O. 1 µl of cell suspension was used directly as template for PCR. For *E. coli*

overnight cultures, 1 µl of the culture was used as a DNA template. For preparative PCRs, φCh1 or vector DNA was used as a template with a final concentration of 50 – 100 ng/ µl.

Lyophilized primers were resuspended in dH_2O with a final concentration of 1 µg/µl, and further diluted 1:10 prior to PCR. Annealing temperatures of the primers were calculated using NEB Tm Calculator.

2.2.1.2. Preparative and analytical PCR

Phusion polymerase was used for preparative PCRs due to its 3'-5'-exonuclease activity. On the other hand, analytical PCRs were performed by using Taq polymerase. PCR reactions and programs were carried out according to the instructions of the manufacturer.

2.2.1.3. Quality control of PCR products and purification

The integrity of the amplified fragments was assessed by fractionation of DNA on an agarose gel. 5 µl of DNA mixed with 5 µl of 5 x DNA LD (loading dye) were applied onto the gel and visualized under UV light upon staining with ethidium bromide. Analytical PCR products (GoTaq Green Master Mix) were directly loaded onto the gel without addition of further DNA LD.

PCR products and plasmid DNA were purified using Wizard® SV Gel and PCR Clean-up System and Wizard®Plus SV Minipreps DNA Purification System respectively according to the manufacturer's information and eluted in 30 µl ddH_2O. The concentration of the purified DNA was measured by Nanodrop (ND-2000c, Thermo Scientific).

2.2.1.4. DNA restriction, dephosphorylation and ligation

All restrictions were performed using restriction enzymes and buffers from Thermo Scientific according to the manufacturer's instructions. Restriction was

performed at 37 °C overnight, followed by quality assessment on a 0.8% agarose gel using the unrestricted plasmid as a control. In case of partial digestion, 1 µl of enzyme was added and the reaction was further incubated at 37 °C.

In case of single digestion, plasmid DNA was additionally dephosphorylated in order to prevent re-circularization. Reaction was incubated 30 min at 37 °C, followed by inactivation of the alkaline phosphatase at 65 °C for 15 min. Prior to ligation, plasmid DNA was purified (see Section 2.2.1.3.).

Ligation was performed by using T4 DNA ligase according to the manufacturer's instructions. Molar ratios of vector to insert, 1:3 to 1:9, were used and the assay was incubated either for 3 hours at RT or overnight at 16 °C.

2.2.1.5. Gibson assembly

Gibson assembly was used instead of conventional cloning to ligate two fragments into pMDS24 vector. Plasmid DNA was linearized, gel purified and mixed together with equimolar amounts of the fragments (0.5 – 1 pmol per fragment) in 10 µl GA master mix. Reaction was performed at 50 °C for 15 min, followed by freezing at – 20 °C. 10 µl of the assembly was used to transform into *E.coli* XL1-Blue (see Section 2.2.2.1.2.).

2.2.2. Transformation procedures

2.2.2.1. Transformation in *E. coli*

2.2.2.1.1. Generation of *E. coli* competent cells

Overnight preculture was used as inoculum to grow XL1-Blue culture in 200 ml LB medium, supplemented with tetracycline, with a starting OD_{600} of 0.1. Bacterial culture was incubated at 37 °C with agitation until an OD_{600} of 0.6 to 1 was reached. Cells were then harvested by centrifugation at 10 krpm for 10 min at 4 °C and pellet was subsequently resuspended in 80 ml MOPS I. Upon incubation on ice for 10 minutes, a second centrifugation step was implemented, followed by the resuspension of the pellet in 80 ml MOPS II and incubation on ice for 30 min. Finally, a third

centrifugation was carried out and resulting pellet was resuspended in 4 ml MOPS IIa. 100 µl aliquots were stored at -80 °C.

2.2.2.1.2. Transformation of *E. coli* competent cells and screening

10 µl of the ligation reaction was added into 100 µl XL1-Blue competent thawed cells. The mixture was incubated on ice for 10 min, followed by a heat shock at 42 °C for 45 sec. Bacterial cells were cooled down briefly and 300 µl LB was added, followed by regeneration at 37 °C for 30 min with agitation. 100 µl (130 µl for Gibson assembly) of the transformation assay was plated on LB plates with antibiotics (amp/ tet) and incubated overnight at 37 °C.

Single colonies were inoculated in 5 ml LB (amp/ tet). Upon overnight growth, clones were tested by analytical PCR, followed by DNA isolation and sequencing (Microsynth). Positive clones were subsequently stored at -80 °C by adding 800 µl of 50 % glycerol into 1 ml of the fresh culture.

2.2.2.2. Transformation in *N. magadii*

2.2.2.2.1. Generation of *N. magadii* competent cells

N. magadii overnight culture was inoculated in 60 ml NVM^+ supplemented with bacitracin (70µg/ml) until OD_{600} of 0.6 to 1 was reached. Cells were harvested by centrifugation at 6 krpm for 15 min at RT, followed by resuspension in 30 ml buffered high-salt spheroblasting solution and addition of proteinase K to a final concentration of 0.1% v/v. Cell suspension was incubated for 2 days at 42 °C with agitation and formation of spheroblasts was observed under the microscope.

2.2.2.2.2. Transformation of *N. magadii* competent cells and screening

1.5 ml of the cell suspension was centrifuged at 10 krpm for 5 min at RT and the resulting pellet was resuspended in 150 µl buffered high-salt spheroblasting solution followed by the addition of 15 µl 0.5 M EDTA and incubation for 10 min at RT. 1-3 µg DNA (maximum 10 µl) was added and cell mixture was incubated for 5 min at RT. 150 µl of 60% PEG-600 was subsequently added to the transformation assay and incubated

for 30 min at RT. To completely remove PEG-600, cells were washed twice with 1 ml NVM^+ (10 krpm, 5 min, RT) and the resulting pellet was resuspended in 1 ml NVM^+, followed by incubation at 37 °C with agitation until cells reverted to original morphology. Upon regeneration, 100 µl of cell suspension was plated on NVM^+ agar plates with antibiotics and incubated at 42 °C until colonies were visible.

Single colonies were inoculated in 500 µl NVM^+ and incubated at 37 °C with agitation for 3 to 5 days. Template preparation and analytical PCR were performed as mentioned on sections 2.2.1.1. and 2.2.1.2.

2.2.2.3. Transformation in *H. volcanii*

2.2.2.3.1. Generation of *H. volcanii* competent cells

H. volcanii overnight culture was inoculated in 50 ml MGM^+ until OD_{700} of 0.8 to 1 was reached. Cells were harvested by centrifugation at 6 krpm for 15 min at RT, followed by resuspension in 10 ml buffered low-salt spheroblasting solution. Cell suspension was subsequently centrifuged at 6 krpm for 10 min at RT and the resulting pellet was resuspended in 5 ml buffered low-salt spheroblasting solution with 15 % glycerol. 150 µl aliquots were stored at -80 °C.

2.2.2.3.2. Transformation of *H. volcanii* competent cells and screening

The transformation procedure and screening of *H. volcanii* cells is identical to *N. magadii* protocol (see Section 2.2.2.2.2.). Only differences are the use of MGM^+ rich medium and buffered low-salt instead of high-salt spheroblasting solution. Furthermore, regeneration of *H. volcanii* cells is not mandatory.

2.2.2.3.3. Preparation of *H. volcanii* acetone powder

H. volcanii was inoculated in 1 L MGM^+ and grown until stationary phase. Cells were harvested by centrifugation at 6 krpm for 20 min at RT and the pellet was resuspended in 0.9 % NaCl (1 ml per 1 g of total cell mass), followed by incubation on ice for 5 min. 8 ml of acetone was added per 2 ml of cell suspension and further

incubated on ice for 30 min. A second centrifugation (10.000 g, 10 min, RT) was implemented and the pellet was resuspended in ice-cold acetone. Upon incubation on ice for 10 min, cell suspension was subjected to a third centrifugation (10.000 g, 10 min, RT). The resulting pellet was air dried overnight on a filter paper, subsequently pulverized, and stored at RT.

2.2.3. Protein methods

2.2.3.1. Preparation of crude protein extracts

1.5 ml of cell culture was centrifuged at 13.000 rpm for 3 minutes at room temperature. The supernatant was discarded and the pellet was resuspended in equal volumes of 5 mM sodium phosphate buffer pH 6.8 and 2 × Laemmli buffer. The amount of phosphate and Laemmli buffer was calculated based on the formula $OD_{600} \times 75$. *N. magadii* and *H. volcanii* protein extracts were incubated at 37 °C until complete dissolution of the pellet was achieved, followed by denaturation for 10 minutes at 95°C and storage at -20°C. *E. coli* protein extracts were immediately denatured and stored.

2.2.3.2. SDS-PAGE and Coomassie staining

A total volume of 10 µl/sample was loaded on a discontinuous 12 % SDS-polyacrylamide gel, containing a 4 % stacking and 12 % separating gel. Gels were prepared using BioRad Mini Protean apparatus and were placed in an electrophoretic chamber, covered with 1 × SDS running buffer. Bacterial proteins were fractioned at 40 V until the samples reached the stacking gel. Upon entry into the resolving gel, the voltage was increased to 60 V and separation of the proteins was continued until the bromphenol blue reached the bottom of the gel. The gel was stained with Coomassie brilliant blue solution for 10 min with agitation and was subsequently destained with destaining solution overnight.

On the other hand, a constant voltage of 30 V was applied for *N. magadii* and *H. volcanii* protein samples due to the high salt concentration.

2.2.3.3. Western Blot

Protein samples were separated by 12 % SDS-PAGE and electrophoretically transferred via semi-dry method onto a nitrocellulose membrane (9 × 6 cm; GE Healthcare AmershamTM ProtranTM 0.2 µm NC) at 25 mA for 30 min. The blotting device Trans-Blot® TurboTM Transfer System from BioRad was implemented; the blotting procedure is displayed in Fig. 7.

Figure 7. Front view of blotting sandwich. The applied electric current causes negatively charged proteins to migrate towards the anode.

Upon blotting, the membrane was stained with Ponceau S staining solution and destained with tap water. The nitrocellulose membrane was blocked with milk powder at 4 °C overnight. Afterwards, the membrane was washed with 1 × TBS for 10 minutes and 10 ml of primary antibody solution was added and incubated for one hour shaking at RT. The membrane was subsequently washed three times with 1 × TBS, followed by the addition of horseradish peroxidase-conjugated anti-rabbit Ig secondary antibody and incubation for one hour at RT. Upon washing, 3 ml ECL and 2 µl H_2O_2 were added and detection was achieved by ChemiDoc XRS+ imager and ImageLab software, with exposure time varying from five to 250 seconds.

Membranes were stripped by addition of 10 ml ROTI®Free Stripping Buffer (Roth), followed by incubation for 30 minutes at 37 °C. Stripping buffer was removed by extensive washing with 1 × TBS and membranes were re-blocked overnight.

2.2.4. Protein expression and purification

2.2.4.1. Gp44 purification from *E. coli* under denaturing conditions

The N-terminal hexahistidine-tagged viral protein gp44 (pRSETA-ORF44) was purified from *E. coli* strain BL21 (DE3). Cells were inoculated in 1 L LB medium containing ampicillin, chloramphenicol and L-Rhamnose at 37 °C with vigorous shaking until an optical density (600 nm) of 0.8 – 1 was reached. Gene expression was induced by the addition of 1 mM IPTG for 2 hours at 37 °C. Cells were harvested by centrifugation (6000 rpm) using a Sorvall F14 FIBER-LITE rotor at 4 °C for 20 min. The supernatant was discarded and the cell pellet was resuspended in 20 ml buffer B. The cell suspension was subsequently chemically lysed by the addition of egg white lysozyme for 50 min at RT shaking, followed by disruption via sonication (7 × 1.20 min, 80 % cycle). Cell lysate was centrifuged at 10.000 g for 20 min at 4°C to remove insoluble material and the supernatant was stirred overnight with 1 ml Ni-NTA slurry (QIAgen, equilibrated with buffer B) at 4 °C.

The slurry was applied to a column. The flow-through was collected and the column was subsequently washed twice with 6 ml Buffer C. Elution of the protein was carried out with 4 x 500 µl Buffer D followed by a second elution step with 4 x 500 µl Buffer E. Protein samples were mixed with equal volume of 2 × Laemmli buffer, heated at 95 °C for 10 min and loaded onto a 12 % SDS-PAGE gel.

2.2.4.2. Protein dialysis

Dialysis method was utilized for accomplishing both contaminant removal and buffer exchange. Protein samples were transferred into semi-permeable dialysis membranes and dialyzed stepwise against renaturing buffers 1 - 4 (see Section 2.1.10.2.5.1.) for an hour, followed by overnight dialysis in fresh buffer. Aliquots were taken on each dialysis step and the purified protein was analyzed by SDS-PAGE and mass spectrometry (MPL Proteomics department).

2.2.4.3. Gp44 purification from *H. volcanii* under native conditions

The N-terminal hexahistidine-tagged viral protein gp44 (pRV1-ptna-ORF44) was purified from *H. volcanii* under a tryptophan inducible promoter. pRV1-ptna utilizes the tryptophanase promoter of *H. volcanii*, which shows strong induction of expression upon addition of ≥ 1 mM tryptophan (Large *et al.*, 2007). A culture was grown overnight in 50 ml Hv-YPC broth containing novobiocin and used to inoculate 1 L Hv-YPC with novobiocin. The culture was incubated at 37 °C with shaking (200 rpm) until an OD_{650} of 0.3 was reached and was subsequently induced by adding 5 mM tryptophan (dissolved in 18 % salt water) for 48 hours to induce gene expression. The culture was then centrifuged at 3,300 g for 10 min at 4 °C, and the cells were resuspended in 20 ml ice-cold binding buffer and lysed by sonication on ice until the suspension was no longer turbid. The cell lysate was centrifuged at 16,000 g for 15 min at 4 °C and stirred overnight at 4 °C with 1 ml Ni-NTA slurry (QIAgen, equilibrated with binding buffer). The slurry was applied to a nickel - agarose column and the flow-through was collected and reloaded onto the column, followed by two washes with 5 ml of ice-cold binding buffer containing 50 mM imidazole and elution with 10 ml binding buffer containing 500 mM imidazole. Protein samples were analyzed on 12 % SDS-PAGE gel and gel was subsequently stained with Coomassie brilliant blue.

2.2.5. Cell culture passaging

2.2.5.1. Stability of *N. magadii* L11-ΔORF44 deletion mutant

Fresh plaques of both *N. magadii* L11 and *N. magadii* L11-ΔORF44 were inoculated in 10 ml NVM^+ rich medium. For the deletion mutant, novobiocin was added to the media due to the presence of the novobiocin cassette. The cultures were grown at 42 °C for 72 hours with agitation and were re-inoculated in 20 ml NVM^+ to an OD_{600} of 0.1, followed by incubation at 37 °C for 72 hours shaking. The pre-cultures were subsequently inoculated in 40 ml NVM^+ to an OD_{600} of 0.1 and incubated at 37 °C for 7 days with agitation (165 rpm). The optical density of the cultures were measured every 24 hours. Upon the onset of lysis, cultures were inoculated in 20 ml NVM^+ to an OD_{600} of 0.1 for 72 hours and further re-inoculated in 40 ml NVM^+ to an OD_{600} of 0.1. Furthermore, protein crude extracts were prepared (see Section 2.2.3.1.) and both cell-

rich and cell-free supernatants were collected for CFU measurements and virus titer analysis respectively. This procedure was repeated seven times for all seven passages. Two different compositions of NVM^+ were investigated; containing 4 M and 4.1 M NaCl respectively.

2.2.5.2. CFU meassurements and provirus detection

After onset of lysis, 1.5 ml culture was centrifuged at 13.000 rpm for 3 min at RT. Supernatant was discarded and the resulting pellet was resuspended in 1 ml fresh NVM^+ medium. Dilution series of the cell suspensions in NVM^+ were prepared (10^{-2} to 10^{-10}) and immediately plated on NVM^+ plates. Plates were sealed in plastic bags and incubated at 42 °C for 7 days, until colonies were visible.

To ensure that the archaeal cultures retained the provirus after passing, ten single colonies were inoculated in 500 µl NVM^+ (plus novobiocin for the mutant) and grown for 72 hours. Templates were prepared according to section 2.2.1.1. and analytical PCR was performed using ORF56 primers (56-RT5 and 56-RT3) .

2.2.5.3. Virus titer analysis

Upon onset of lysis, 1.5 ml culture was centrifuged at 13.000 rpm for 3 min at RT. 1 ml of supernatant was transferred to a fresh Eppendorf tube and 20 µl of chloroform was added. Dilution series of the cell lysate in NVM^+ were prepared (10^{-2} to 10^{-10}). 100 µl of each dilution was mixed with 300 µl fresh *N. magadii* L13 cells in 5 ml NVM^+ soft agar (prewarmed at 56 °C) and plated on NVM^+ plates. Plates were dried overnight at RT, sealed in plastic bags and incubated at 37 °C for 7 days until plaques were formed.

2.2.6. In vitro endoribonuclease assay

Oligo mRNAs (see Materials 2.1.10) were incubated with purified gp44 at 37 °C for 15, 30 and 60 min. Increasing amounts of NaCl were added to the standard reaction to an end volume of 20 µl. Aliquots were taken and mixed with 2 x RNA

loading dye, followed by heat shock at 70 °C for 10 min. Upon denaturation, the reaction was analyzed via denaturing urea PAGE.

Components	Volume in µl
34-mRNA (0.5 µg)	5
Dialyzed gp44	2
0.1 mM EDTA	1 (Stock: 0.5 M)
1 mM DTT	1 (Stock: 20 mM)
RNasin	0.5
20 mM Tris pH 8	0.8 (Stock: 500 mM)
NaCl *	x
DEPC dH_2O	Fill to 20 µl

* 0, 400, 1000 and 2000 mM

2.2.7. Cloning strategies

2.2.7.1. pRV1-ptna-ORF44

ORF44 was amplified with primers 44-5-Nde-His and 44-3-Bam from φCh1 DNA template, resulting in a fragment length of 430 bp. Both ORF44 and pRV1-ptna vector were restricted with *Nde*I and *Bam*HI.

2.2.7.2. pRo-5-Mev-p43-ORF43 and –p43-ORF43/44

ORF43 and ORF43/44 with native promoter were amplified with primers 43-Kpn-5 and 43-Kpn-3 and 43- Kpn-5 and 44- Kpn-3, respectively using φCh1 genome as a template. The amplified fragments had a length of 500 bp and 920 bp, respectively. Both fragments and pRo-5-Mev plasmid were restricted with *Kpn*I. Upon treatment with alkaline phosphatase, fragments were ligated into the digested vector.

2.2.7.3. pRo-5-Mev-tnaN-ORF44

ORF44 with *N.magadii* tryphtophan inducible promoter was amplified with primers 44-Kpn-3 and Tna-Kpn-5 using pBAD24-tnaN-44 as a template, giving a 920 bp long fragment. The amplicon was restricted with *Kpn*I. Upon treatment with alkaline phosphatase, tnaN-ORF44 was ligated into the digested vector.

2.2.7.4. pNB102-p43-ORF43

ORF43 and its upstream promoter region was PCR amplified with primers 43-5 and 43- Kpn-3 from φCh1 DNA, resulting in a 500 bp long fragment. The amplicon was restricted with *Kpn*I and *Xba*I enzymes, followed by ligation into pNB102 (*Kpn*I/ *Xba*I).

2.2.7.5. pMDS24-ORF34$_{52}$

ORF34 and its upstream promoter region was amplified with 34-XbaI and 36-3 primers using pBgb52 DNA as a template. Amplified product had a length of approximately 2000 bp and was digested with *Xba*I. pMDS24 plasmid was restricted with the same enzyme and treated with alkaline phosphatase. Upon dephosphorylation, ORF34$_{52}$ was ligated into pMDS24.

2.2.7.6. pMDS24-34$_1$ and -34$_{52}$ constructs via Gibson assembly

pMDS24 was restricted with *Xba*I and *Kpn*I. PCR fragments were amplified using specific Gibson primers according to table 1 and 2.

Fragment	Primer 1	Primer 2	Template	Fragment size
34$_1$ (promoter: p43)	34-Hv-1	34-Hv-3	pBgb1	1999 bp
p43-ORF43	43-Hv-4	43-Hv-2	φCH1	500 bp
p43-ORF43/44	43-Hv-4	43-Hv-3	φCH1	920 bp

34_1 (promoter: tnaN)	34-Hv-1	34-pTna-1	pBgb1	1999 bp
tnaN-ORF44	34-pTna-2	43-Hv-3	pBAD-tnaN-44	1000 bp

Table 1. Construction of pMDS24-34_1 via Gibson assembly.

Fragment	Primer 1	Primer 2	Template	Fragment size
34_{52} (promoter: p43)	34-Hv-1	34-Hv-2	pBgb52	2172 bp
p43-ORF43	43-Hv-1	43-Hv-2	φCH1	500 bp
p43-ORF43/44	43-Hv-1	43-Hv-3	φCH1	920 bp
34_{52} (promoter: tnaN)	34-Hv-1	34-pTna-4	pBgb52	2172 bp
tnaN-44	34-pTna-3	43-Hv-3	pBAD-tnaN-44	1000 bp

Table 2. Construction of pMDS24-34_{52} via Gibson assembly.

3. Results

3.1. Stability of the provirus in *N. magadii* L11-ΔORF44 deletion mutant

The viral gene ORF44 is located in the central part of the φCh1 genome and encodes a putative toxin, which is thought to be part of a potential toxin-antitoxin system of φCh1. In order to investigate the effect of ORF44, a deletion mutant strain was constructed via homologous recombination (Gillen, 2017). Previous studies have shown that the deletion of the regulatory gene ORF44 results in increased instability of the lysogenic strain (Edwards, 2018). To further characterize the deletion of ORF44 and the effects on the lysis behavior of the lysogenic strain, wild type *N. magadii L11* and *N. magadii* L11-ΔORF44 were passaged seven times in NVM^+ rich media containing 4 M and 4.1 M NaCl, respectively (see Section 2.2.5.1.).

As depicted in Figure 8B, *N. magadii* L11-ΔORF44 shows a 24-hour earlier onset of lysis during first passage compared to the wild type (Fig. 8A). The mutant strain continues to lyse after 48 hours during the first three passages, followed by a 24-hour delay on the lysis onset in the fourth passage. In the fifth passage however, an almost complete abolishment of the lysis rate is observed, whereas in the next two passages a slow rate of lysis can be witnessed again. On the other hand, wild type strain shows a weaker lysis rate at the start of the fourth passage until seventh passage, where lysis behavior is almost abolished (Fig. 8A).

In addition to growth kinetic analysis, PFU and CFU measurements were carried out as mentioned in the Methods section (2.2.5.2. and 2.2.5.3.). As shown in Figure 8C and D, CFU values vary throughout passages but no significant differences can be detected. On the contrary, consecutive passaging had an effect in the viral titer. Viral titer of wild type strain remains constant but shows a small decrease after fifth passage and reaches the lowest value in seventh passage. For the deletion mutant, viral titer decreases continuously throughout passages resulting in a reduction of two orders of magnitude compared to first passage (Fig. 8D).

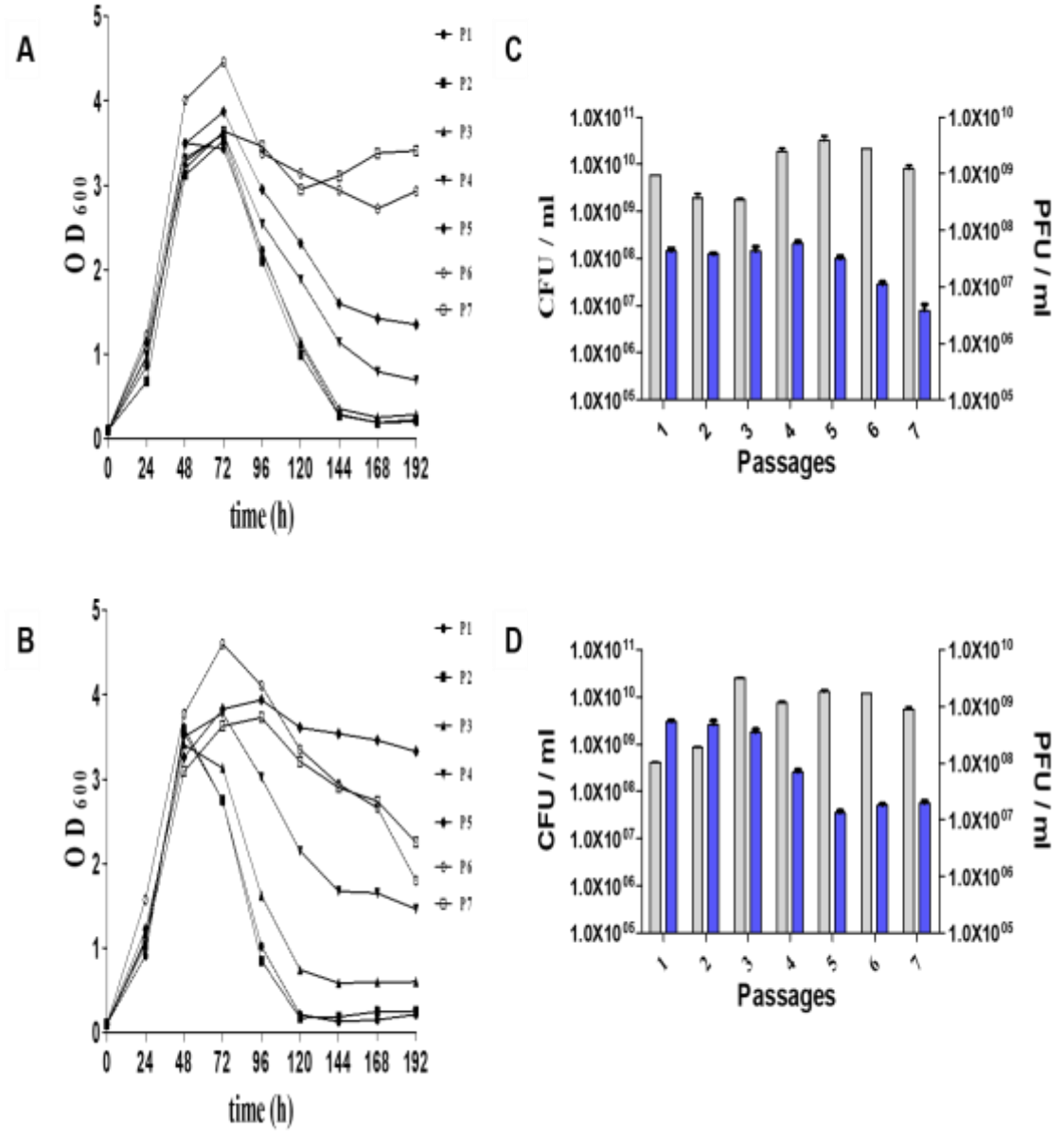

Figure 8. Effect of 4 M NaCl on the passaging of *N. magadii* L11 and L11-Δ44 deletion mutant. (A, B) Growth kinetics of wild type *N. magadii* L11 strain and L11-Δ44 respectively. Strains were inoculated in NVM^{+} rich medium, plus novobiocin for mutant, and grown at 37 °C with agitation until onset of lysis. Cell cultures were passaged by inoculation in fresh media to an OD_{600} of 0.1. Optical density at 600 nm was measured every 24 hours over the period of 8 days. P1-P7 indicate the number of passages. (C, D) Viral titer analysis and CFU measurements of *N. magadii* L11 and L11-ΔORF44 passages. Samples were taken every 24 hours as described under Methods. 1-7 indicate the number of passages; grey bars: CFU/ml, blue bars: PFU/ml. Error bars indicate SEM.

Upon increasing the salt concentration to 4.1 M NaCl, significant changes in the lysis behavior can be observed. As depicted in Figure 9A and B, both strains keep lysing normally, independent of the number of passages. Similarly, CFU values fluctuate throughout passages without any significant differences. However, the increase of the concentration of salt results in a completely different behavior of the viral titer. The release of viral particles is constantly increasing with prolonged passaging for *N. magadii* L11 in contrast to *N. magadii* L11-ΔORF44 that remains stable throughout seven passages (Fig. 9C and D). Comparing the viral titer of wild type in both media, less production of viral particles can be observed during the first three passages in media containing a higher salt concentration.

The presence of the viral DNA within *N. magadii* L11 and *N. magadii* L11-ΔORF44 passages was additionally analyzed via qualitative PCR. Upon onset of lysis throughout each passage, the provirus was detected by randomly screening ten single colonies for the presence of ORF56 with primers 56-RT5 and 56-RT3. As depicted in Figure 10, provirus can be observed in both wild type and mutant strains during fifth passage. Likewise, PCR was performed for all seven passages, leading to the same result (data not shown). Same clones were further screened for the presence of ORF44 using primers 44-bam and 44-hind (data not shown).

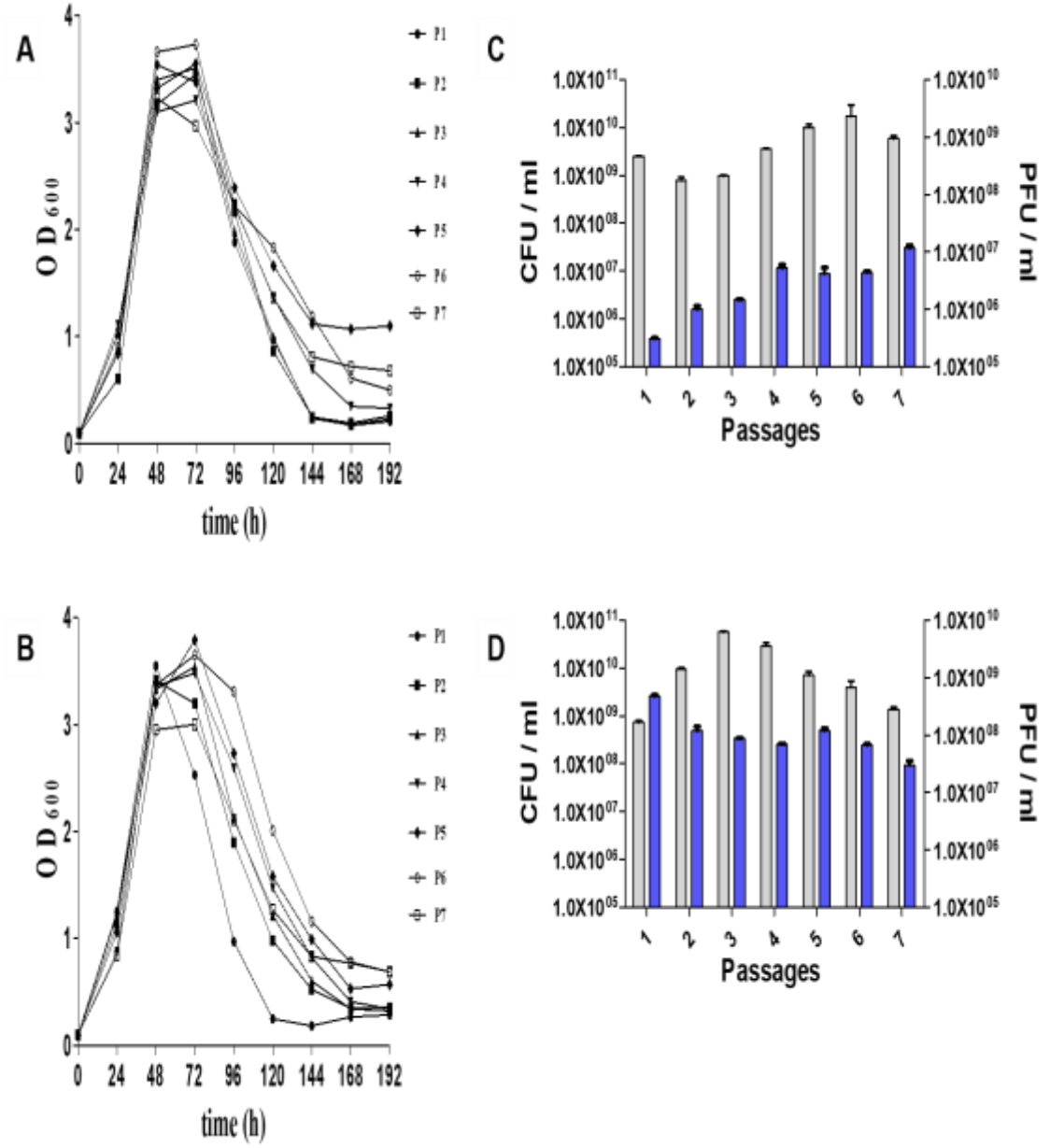

Figure 9. Effect of 4.1 M NaCl on the passaging of *N. magadii* L11 and L11-Δ44 deletion mutant. (A, B) Growth kinetics of wild type *N. magadii* L11 strain and L11-Δ44 respectively. Strains were inoculated in NVM^{+} rich medium, plus novobiocin for mutant, and grown at 37 °C with agitation until onset of lysis. Cell cultures were passaged by inoculation in fresh media to an OD_{600} of 0.1. Optical density at 600 nm was measured every 24 hours over the period of 8 days. P1-P7 indicate the number of passages. (C, D) Viral titer analysis and CFU measurements of *N. magadii* L11 and L11-ΔORF44 passages. Samples were taken every 24 hours as described under Methods. 1-7 indicate the number of passages; grey bars: CFU/ml, blue bars: PFU/ml. Error bars indicate SEM.

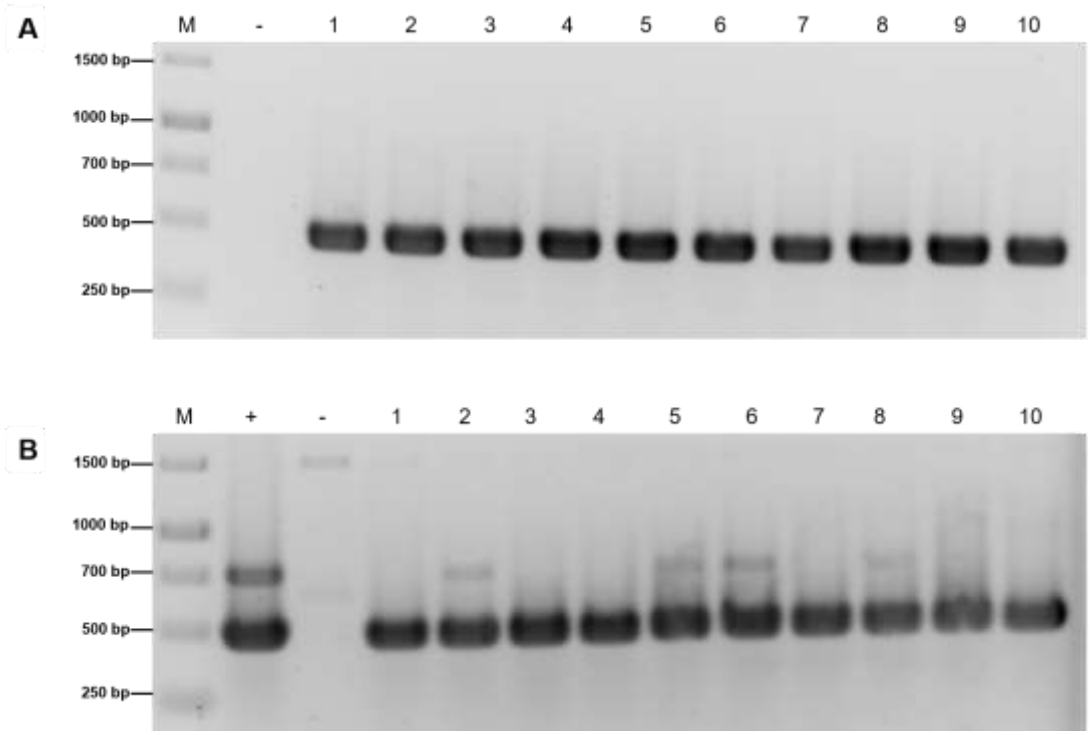

Figure 10. Verification of the presence of provirus in *N. magadii* L11 and L11-Δ44. Upon onset of lysis, cells were plated on NVM^{+} agar plates. Ten single colonies were tested for the presence of ORF56 via analytical PCR using primers 56-RT5 and 56-RT3, resulting in a 500 bp amplicon. M: 1 kb Generuler DNA ladder, +: *N. magadii* L11 positive control, -: *N. magadii* L13 negative control, lanes 1-7: passage 1-7. (A) wild type *N. magadii* L11 and (B) N. *magadii* L11-Δ44 deletion mutant.

Moreover, both lysogenic strains were subjected to western blot analysis in order to investigate the production of Soj and major capsid protein E. Polyclonal rabbit antibodies were prepared against these two proteins. As shown in Figure 11A, the production of protein E in *N. magadii* L11 is barely detectable after fifth passage, whereas in the ORF44-deficient strain a decrease can be observed after fourth passage. The production of the Soj protein remains constant for both strains. By increasing the salt concentration, the expression pattern of protein E in both *N. magadii* L11 and *N. magadii* L11-Δ44 strains is uniform (Fig. 11B).

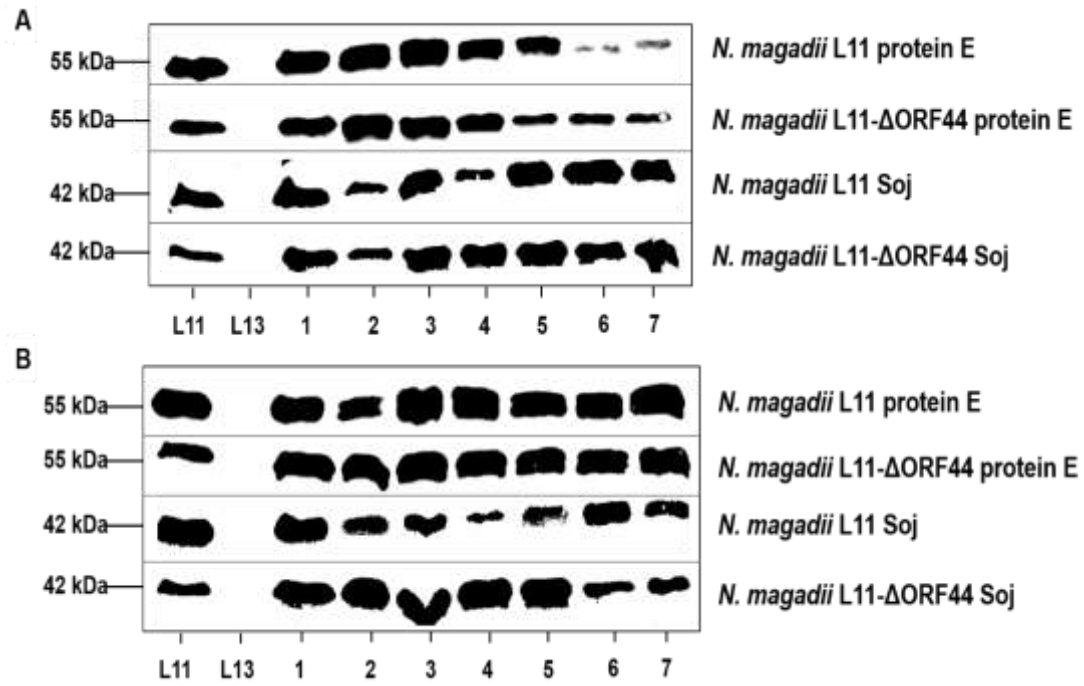

Figure 11. Western blot analysis of the protein production in *N. magadii* L11 and L11-Δ44 observed for seven passages. Crude protein extracts were obtained after onset of lysis as shown under Methods. Whole extracts were analyzed for the production of Soj and the major capsid protein E. Protein concentration was adjusted via Coomasie staining and equal amount of total protein was loaded on each well. Protein transfer was subsequently checked by Ponceau S staining. (A) NVM^+ with 4 M NaCl, (B) NVM^+ with 4.1 M NaCl. L11: positive control *N. magadii* L11, L13: negative control *N. magadii* L13, lanes 1-7: number of passages. Protein molecular weights are indicated on the left.

3.2. Further characterization of *N. magadii* L11-Δ44

To investigate the viral life cycle of the ORF44-deficient *N. magadii* L11 strain in more detail, *N. magadii* L11-Δ44 was inoculated in NVM-CA^+ supplemented with novobiocin. A 24-hour earlier onset of lysis is observed in the ORF44-disrupted strain than in the wild type (Fig. 12A). In addition, plaque assay shows an increased viral particle production in *N. magadii* L11-Δ44 after onset of lysis compared to wild type (Fig. 12B).

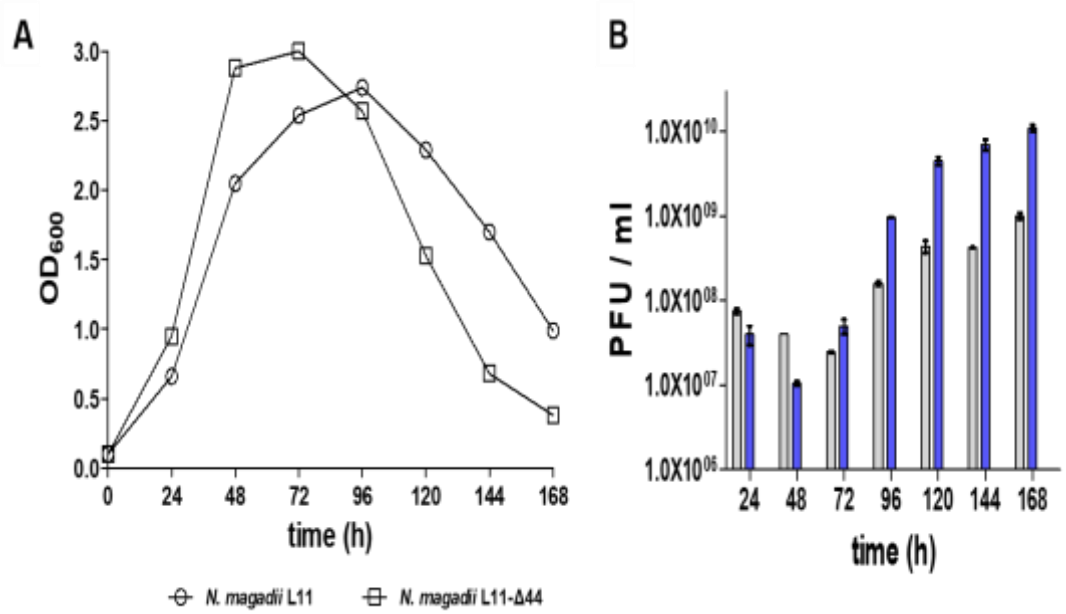

Figure 12. Lysis behavior of wild type *N. magadii* L11 and *N. magadii* L11-Δ44 in NVM-CA^{+} rich medium. Mutant strain was supplemented with novobiocin. (A) Growth kinetics of both strains. Optical density at 600 nm was measured every 24 hours over the period of 7 days. (B) Virus titer analysis. Cell free supernatants were collected from *N. magadii* L11 and *N. magadii* L11-ΔORF44 every 24 hours for 7 days. Grey bars: wild type *N. magadii* L11, blue bars: *N. magadii* L11-Δ44. Error bars indicate SEM.

The protein expression profiles of viral proteins in the wild type strain and the ORF44 disruption were analyzed via western blot using polyclonal antibodies. For this purpose, four different proteins were studied encoded by genes on different loci of the viral genome. As depicted in Figure 13, the deletion mutant strain (right panel) shows an earlier production of protein E, whereas the expression of gp34 is delayed for 24 hours compared to wild type (left panel). Regarding gp34, the protein seems to be truncated in *N. magadii* L11 resulting in a protein with a size difference of approximately 15 kDa. In addition, upregulation of the analyzed proteins is observed in the wild type during the first 24 hours.

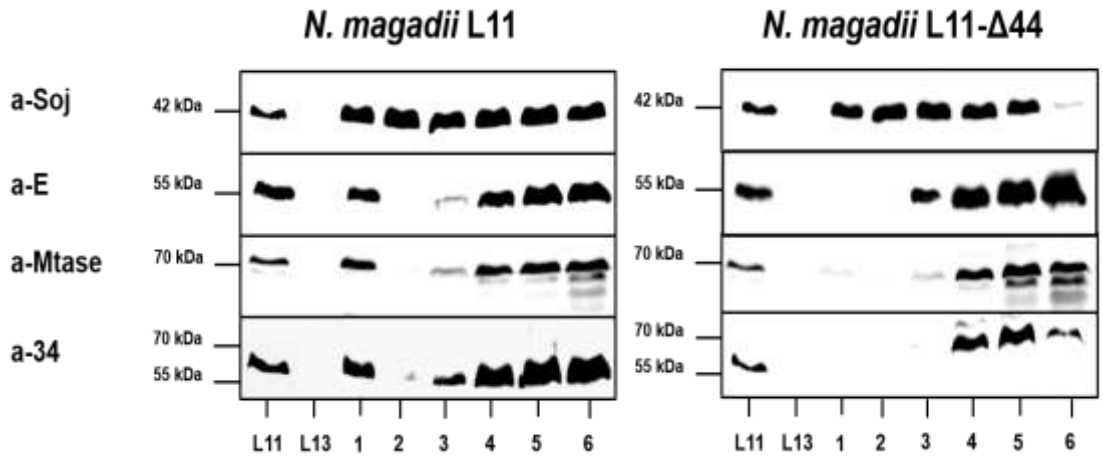

Figure 13. Western blot analysis of the protein production in *N. magadii* L11 and *N. magadii* L11-Δ44. Whole protein extracts were obtained every 24 hours for 6 days and analyzed for the production of four different proteins namely Soj, the major capsid protein E, DNA methyltransferase and the tail fiber protein gp34. L11: positive control *N. magadii* L11, L13: negative control *N. magadii* L13, lanes 1-6: crude protein extracts taken every 24 hours for 6 days**.** Protein sizes are indicated on the left.

3.3. Complementation of *N. magadii* L11-ΔORF44

In order to investigate whether the observed phenotype of the ORF44-deficient strain is directly or indirectly associated with the deletion of ORF44, *N. magadii* L11-Δ44 was transformed with the plasmid (pRo5Mev-tnaN-ORF44) under the control of the tryptophan inducible promoter, isolated from *N. magadii*. Gene expression was induced daily with 4 mM L-trp while the uninduced culture was used as a negative control. As shown in Figure 14A, the normal growth and lysis behavior is not restored by trans-complementation. The induction of *N. magadii* L11-Δ44 (pRo5Mev-tnaN-ORF44) leads to a 24 and 48 hours earlier lysis in comparison to *N. magadii* L11-Δ44 and *N. magadii* L11, respectively. Even the release of viral particles is significantly higher in the complementation strain compared to wild type containing empty plasmid (pRo5Mev) (Fig. 14B).

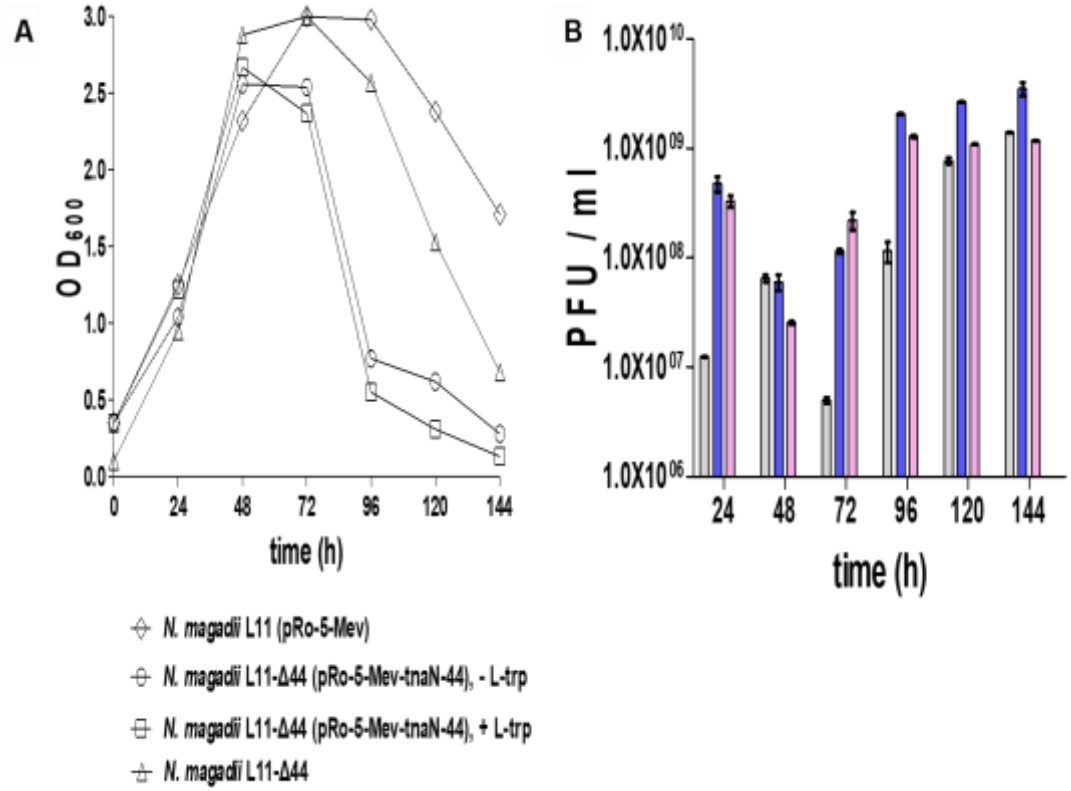

Figure 14. Phenotypic analysis of the complementation *N. magadii* L11-ΔORF44 (pRo5Mev-tnaN-ORF44) strain. (A) Growth kinetics of *N. magadii* L11-ΔORF44 strain transformed with the complementation plasmid (pRo5Mev-tnaN-ORF44). Strain was cultivated in 100 ml NVM-CA^{+}, supplemented with mevinolin, at 37 °C with aeration until an OD_{600} of 0.4 was reached. Culture was then split in half and induced with 4 mM L-trp. Optical density at 600 nm was measured every 24 hours over the period of 6 days. *N. magadii* L11 (pRo5Mev) was used as a positive control, while the uninduced *N. magadii* L11-ΔORF44 (pRo5Mev-tnaN-ORF44) as a negative control. (B) Virus titer analysis. Cell free supernatants were obtained every 24 hours for 6 days. Grey bars: *N. magadii* L11 (pRo5Mev), blue/pink bars: un-/induced *N. magadii* L11-ΔORF44 (pRo5Mev-tnaN-ORF44) respectively. Error bars indicate SEM.

In addition, protein expression profiles of viral proteins in the wild type strain, transformed with (pRo5Mev), and the complemented strain were assessed via western blot analysis. As shown in Figure 15, most analyzed proteins are detected in the cell lysate 24 hours earlier in the complementation strain excluding the non-structural *N. magadii* methyltransferase protein that is produced almost 48 hours earlier than in the wild type

strain (pRo5Mev). Furthermore, no significant changes can be observed between induced and uninduced state. Complementation of *N. magadii* L11-ΔORF44 lead to similar expression profiles of protein E and DNA methyltransferase as to *N. magadii* L11-ΔORF44 (Fig. 13), but no truncated $gp34_{52}$ is detected. The size of the tail fiber protein corresponds to wild type *N. magadii* L11.

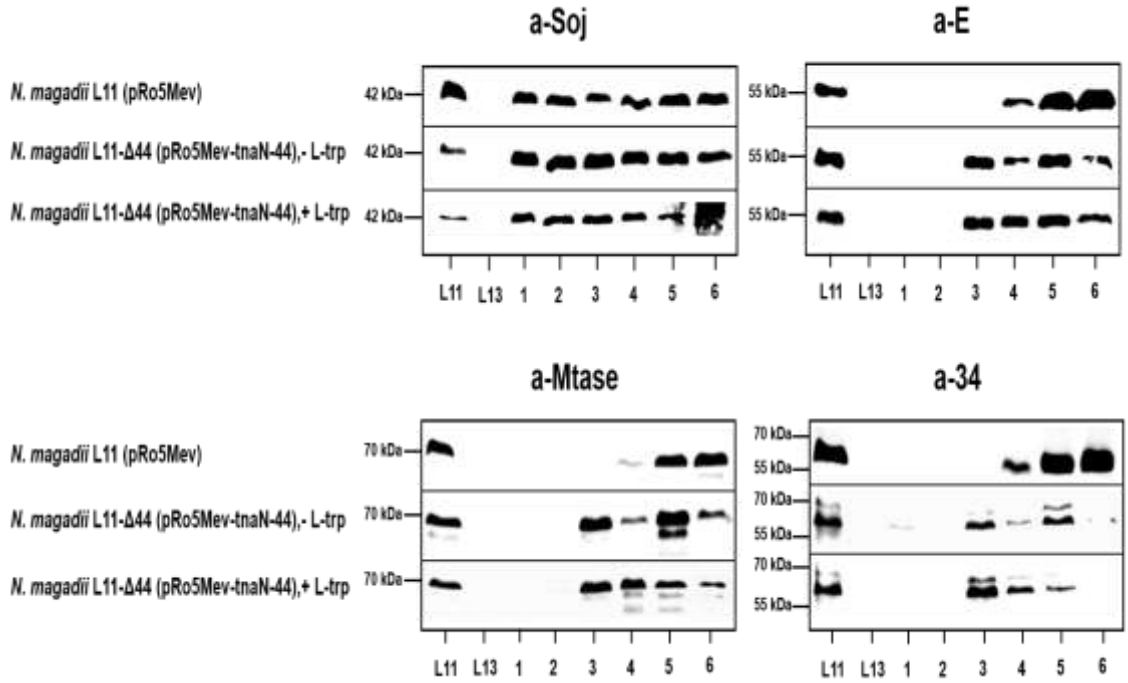

Figure 15. Western blot analysis of *N. magadii* L11-ΔORF44 strain containing the complementation plasmid pRo5Mev-tnaN-ORF44. Protein crude extracts were taken every 24 hours for 6 days and analyzed for the production of Soj, the major capsid protein E, DNA methyl-transferase and the tail fiber protein gp34. L11: positive control *N. magadii* L11, L13: negative control *N. magadii* L13, lanes 1-6: crude protein extracts taken every 24 hours for 6 days**.** Protein molecular weights are indicated on the left.

3.4. Overexpression of ORF43

To further elucidate the role of the putative viral toxin-antitoxin system 43/44, both the toxin ORF44 and the conjugate antitoxin ORF43 were transformed in the non-lysogenic *N. magadii* L13 strain. ORF43 and ORF43/44 were cloned into the multi-copy (pNB102) and low-copy (pRo5Mev) plasmids under the control of the native promoter

p43. On the other hand, transformation of ORF44 under native p43 promoter was unsuccessful due to the toxicity of the protein. Alternatively, ORF44 was cloned into (pRo5Mev) vector under the control of the tryptophan inducible promoter tnaN. The overexpression strains were grown in NVM-CA^{+} rich medium, supplemented with mevinolin. As shown in Figure 16A and C, the overexpression L13 strains exhibit similar growth behavior in contrast to the strain bearing tnaN-ORF44 that is barely propagating upon induction with 4 mM L-trp compared to the uninduced culture (Fig. 16B).

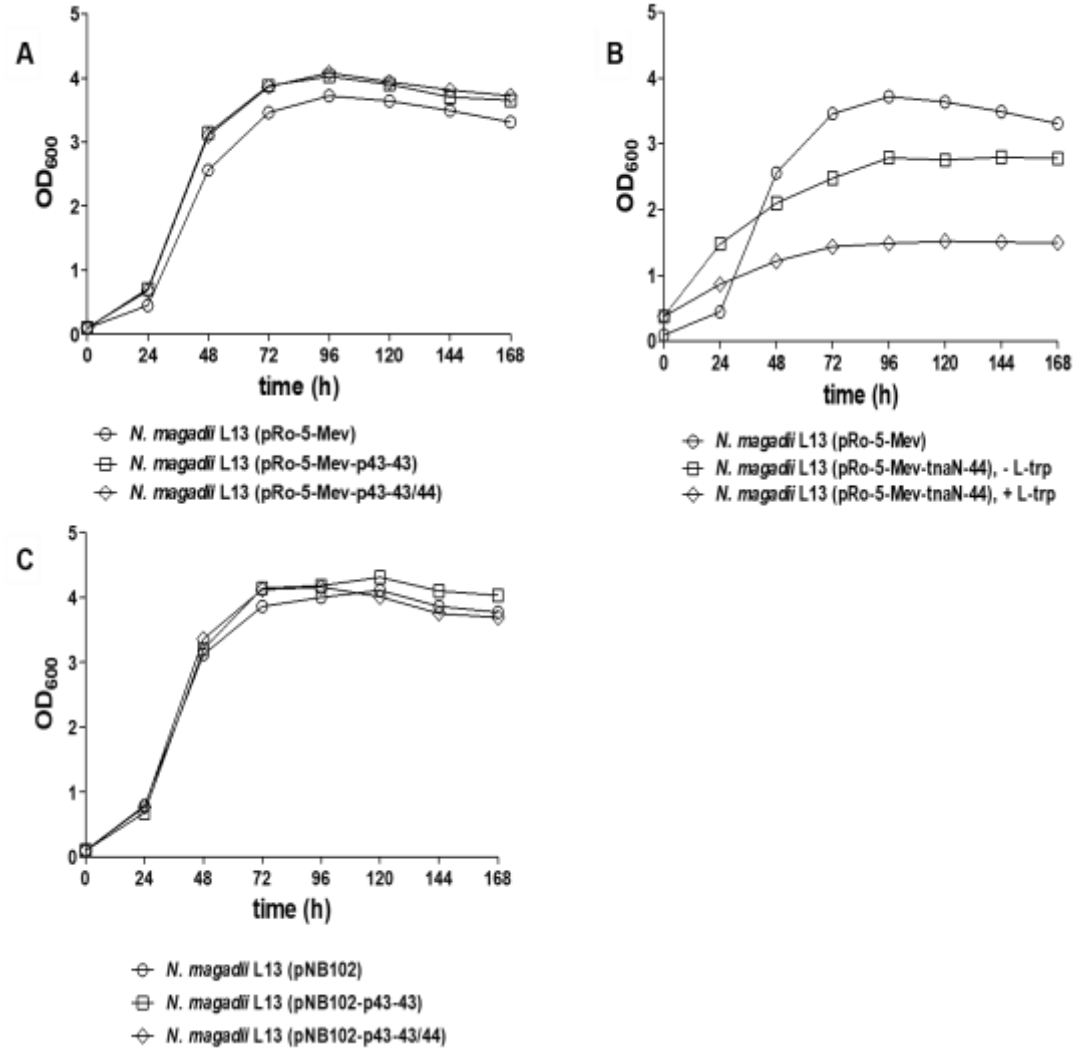

Figure 16. Growth kinetics of *N. magadii* L13 constructs. Strains were inoculated in 50 ml in NVM-CA^{+} rich medium, supplemented with mevinolin. Optical density at 600 nm was measured every 24 hours over the period of 7 days. *N. magadii* L13 (pRo5Mev) and L13 (pNB102) were used as controls. (A) Antitoxin ORF43 and

ORF43/44 under native promoter control in low-copy number plasmid (pRo5Mev), (B) Putative toxin ORF44 under the control of a tryptophan inducible promoter in (pRo5Mev). The growth of both un- and induced culture with 4 mM L-trp was monitored. (C) ORF43 and ORF43/44 under native promoter control in high copy number plasmid (pNB102).

Furthermore, *N. magadii* L13 transformants, namely *N. magadii* L13 (pNB102), (pNB102-ORF43), (pNB102-ORF43/44), (pRo5Mev), (pRo5Mev-ORF43), (pRo5Mev-ORF43/44) and (pRo5Mev-tnaN-ORF44) were infected with φCh1 (see Section 2.2.5.3.) and the effect on the plating efficiency of the φCh1 was determined. For comparison purposes, infection assay of ORF44 was carried out using both NVM^+ and $NVM\text{-}CA^+$ rich media. As shown in Figure 17B, the expression of ORF44 in both media does not have any meaningful effect on the plating efficiency of φCh1. Similarly, ORF43 expressed from the high copy number plasmid (pNB102) leads to similar results (Fig. 17C), whereas expression from (pRo5Mev) results in approximately one order of magnitude increase in the plating efficiency of the φCh1 (Fig. 17A).

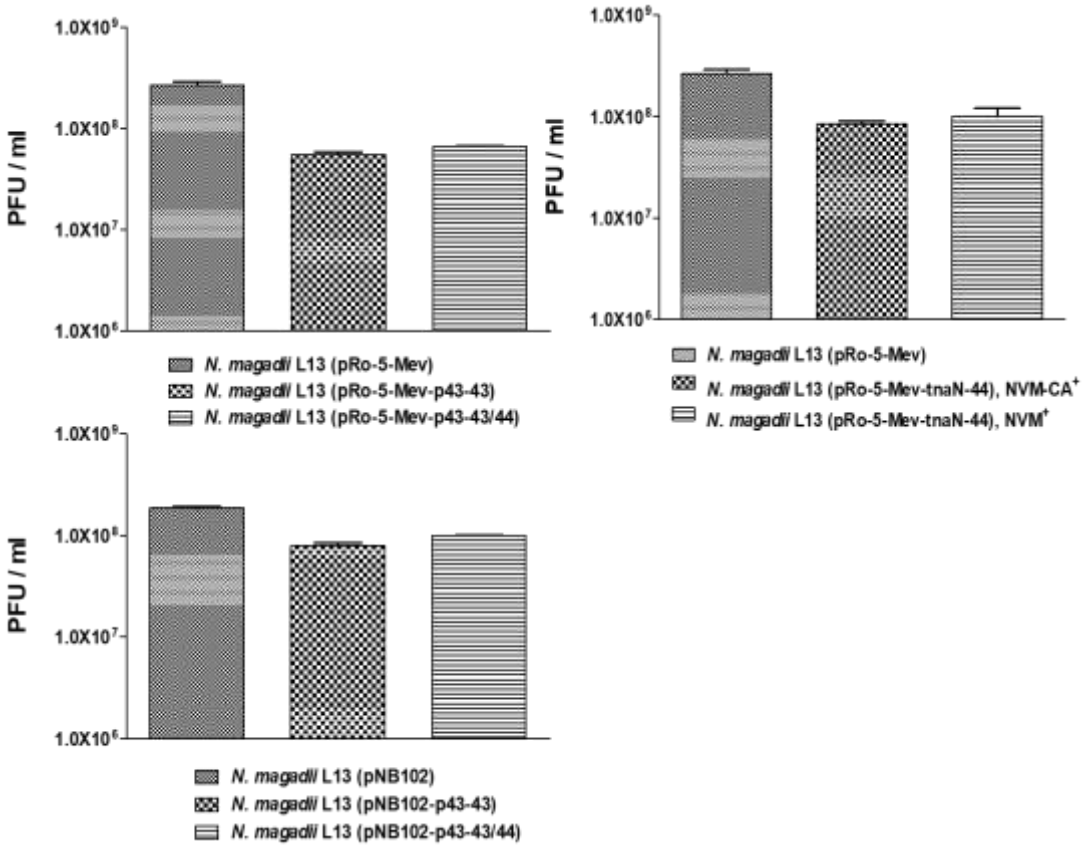

Figure 17. Effect of the ORF43 and ORF44 on the plating efficiency of φCh1. The L13 strains (as depicted in Figure 16) were subsequently infected with wild type φCH1 and plated on NVM^+ agar plates. In case of *N. magadii* L13 (pRo5Mev-tnaN-44) (B), both NVM^+ and $NVM\text{-}CA^+$ agar plates were used for comparison purposes. Upon incubation at 37 °C, the viral titer was calculated. *N. magadii* L13 (pRo5Mev) and L13 (pNB102) were used as controls. Error bars indicate SEM.

Upon the infection of the *N. magadii* L13 constructs with φCh1 viral particles, single plaques were inoculated in fresh $NVM\text{-}CA^+$ rich media and overexpression studies were carried out. As depicted in Figure 18, *N. magadii* L11 (pRo5Mev-ORF43) and ORF43/44 are growing slower that the wild type (pRo5Mev). On the contrary, ORF43 and ORF43/44 from the multi-copy plasmid show a similar phenotypic behavior to *N. magadii* L11 (pNB102) despite the 24-hour delay of onset of lysis.

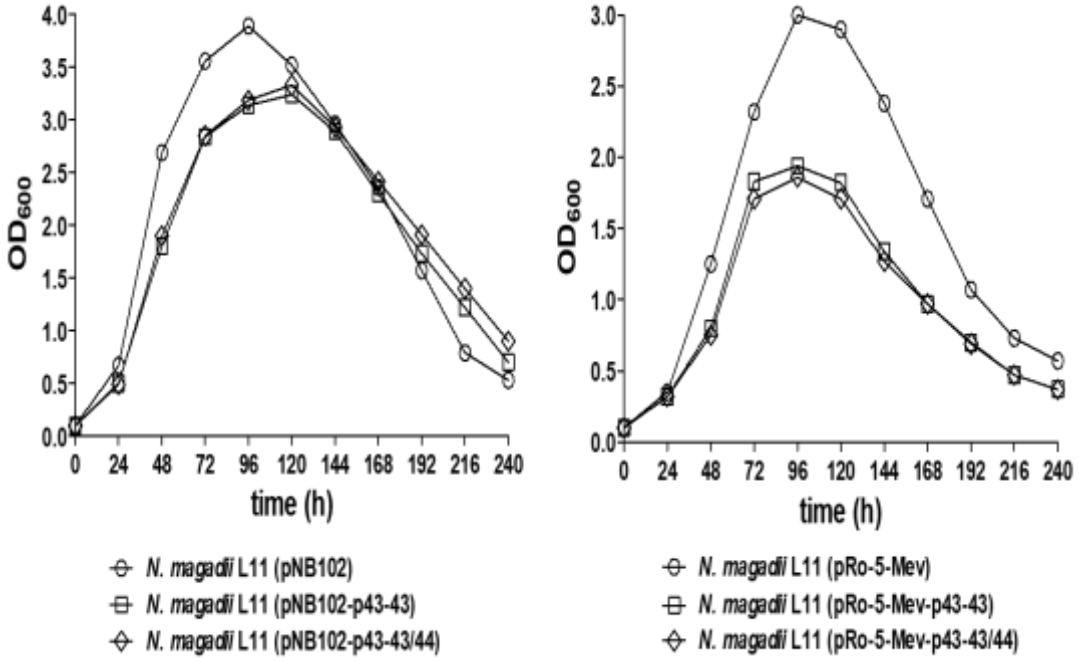

Figure 18. Growth kinetics analysis of overexpression N. magadii L11 strains. Episomal vectors pNB102 and pRo5Mev were used to overexpress ORF43 and ORF43/44 under the control of the native promoter p43. Strains were cultivated in 50 ml NVM-CA^{+} containing mevinolin with agitation at 37 °C. OD_{600} was measured every 24 hours for a duration of 10 days. (A), (B) Overexpression in high- and low-copy number plasmid, respectively.

In addition to the growth studies, the production of infectious viral particles in the overexpression strains was estimated via plaque assay. Obtained results are summarized in Figure 19. Viral titer in *N. magadii* L11 (pNB102-ORF43) and (ORF43/44) is almost two orders of magnitude higher after 24 hours than the control *N. magadii* L11 (pNB102), while *N. magadii* L11 (pRo5Mev-ORF43) and (ORF43/44) show 1 and 1,5 orders of magnitude increase in viral titer, respectively, during first 2 days compared to *N. magadii* L11 (pRo5Mev).

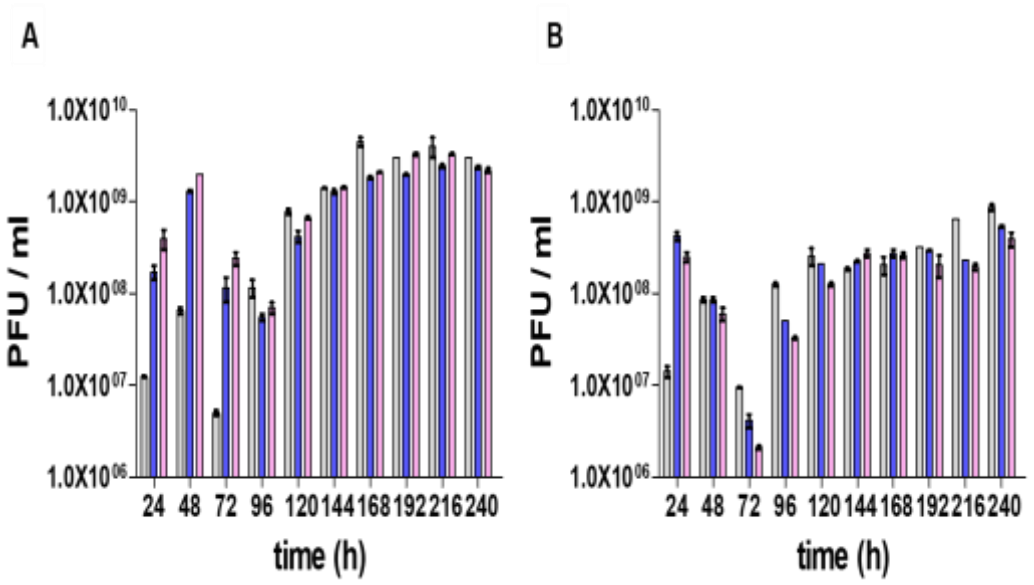

Figure 19. Analysis of viral titer of *N. magadii* overexpression strains. Cell-free supernatants were prepared every 24 hours for 10 days from the *N. magadii* overexpression strains (as shown in Figure 18). Plaque assay was utilized to estimate the viral titer. NVM-CA^{+} agar plates were incubated for 7 days at 37 °C followed by the counting of plaques. *N. magadii* L11 (pRo5Mev) and L11 (pNB102) were used as controls. (A) Overexpression in (pRo5Mev), (B) Overexpression in (pNB102), grey bars: *N. magadii* L11 (pRo5Mev) and L11 (pNB102) respectively, blue bars: *N. magadii* L11 strains overexpressing ORF43, pink bars: *N. magadii* L11 strains overexpressing ORF43/44. Error bars indicate SEM.

To investigate how overexpression of the ORF43 and ORF43/44 affects the production of viral proteins, the corresponding strains were subjected to western blot analysis. Polyclonal rabbit antibodies against Soj, the major capsid protein E, DNA methyltransferase protein and the tail fiber protein gp34 were used. According to Figure 20, overexpression strains transformed with low-copy (pRo5Mev) vector show upregulation of viral proteins throughout first 48 hours. No differences in the expression profiles of protein E and gp34 can be detected, whereas the viral methyltransferase protein is produced 24 hours earlier than the control *N. magadii* L11 (pRo5Mev) (down left panel). On the other hand, the overexpression of strains bearing the multi-copy plasmid (pNB102) leads to protein upregulation during the first 24 hours (Fig. 21). Furthermore, both the production of protein E and Mtase is delayed for 24 hours. Interestingly, the

proteins gp34 and Mtase show a higher production rate after 9th day compared to the control *N. magadii* L11 (pNB102).

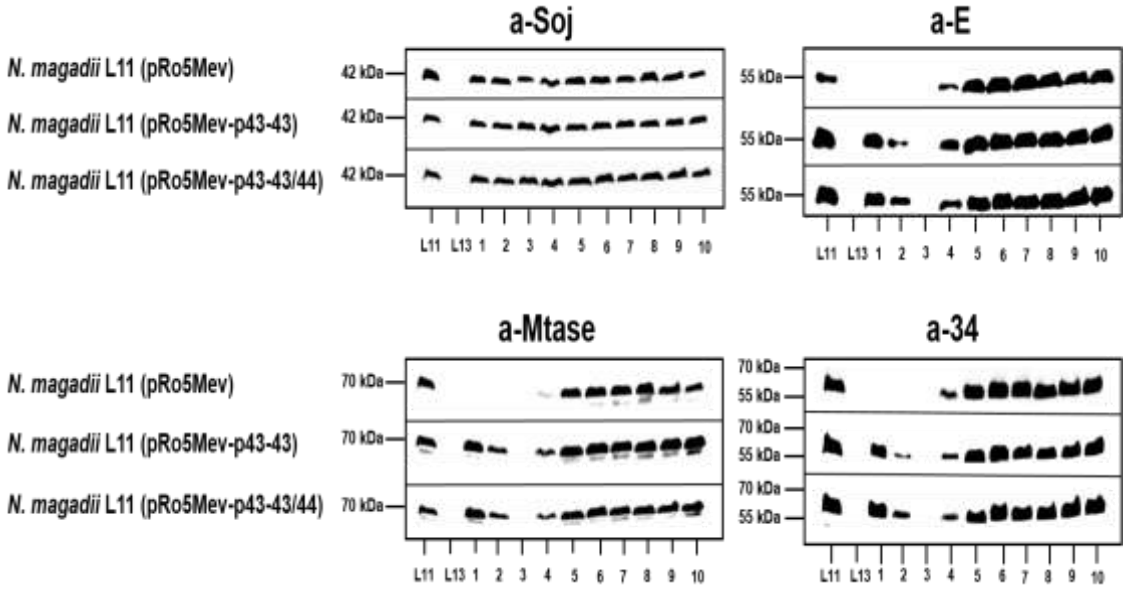

Figure 20. Western blot analysis of the protein production in the overexpression strains containing the low copy number vector pRo5Mev. Whole protein extracts were obtained every 24 hours for 10 days and subjected to western blot analysis for evaluation of the production of Soj, the major capsid protein E, DNA methyl-transferase and the tail fiber protein gp34. L11: positive control *N. magadii* L11, L13: negative control *N. magadii* L13, lanes 1-10: crude protein extracts collected every 24 hours for 10 days. The size of the different proteins is indicated on the left.

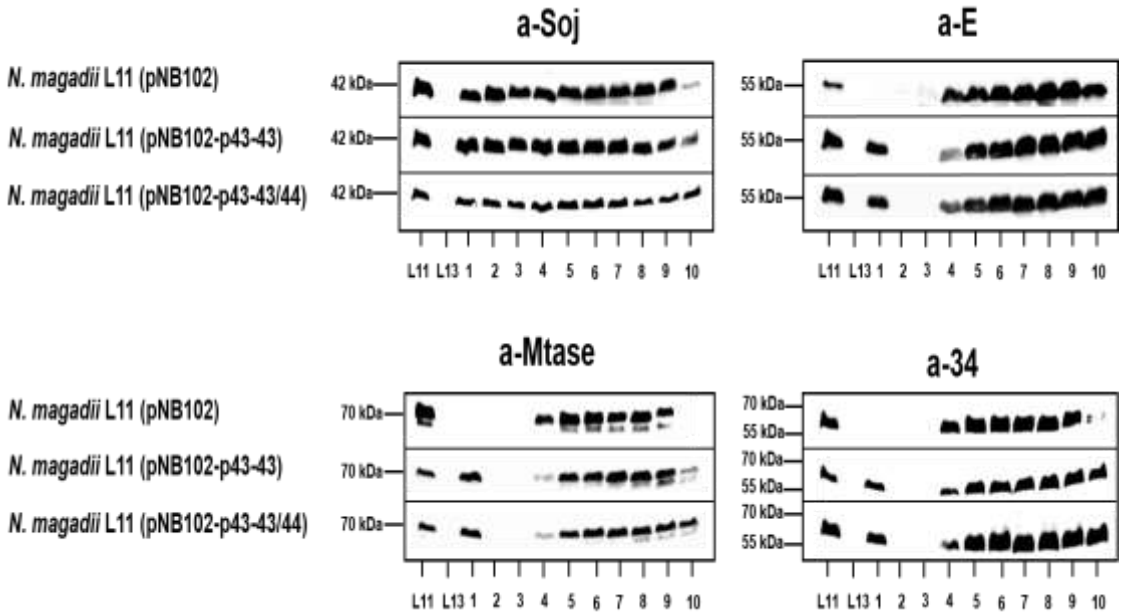

Figure 21. Western blot analysis of the protein production in the overexpression strains containing the high copy number vector pNB102. Whole protein extracts were obtained every 24 hours for 10 days and subjected to western blot analysis for evaluation of the production of Soj, the major capsid protein E, DNA methyl-transferase and the tail fiber protein gp34. L11: positive control *N. magadii* L11, L13: negative control *N. magadii* L13, lanes 1-10: crude protein extracts collected every 24 hours for 10 days. Protein molecular weights are indicated on the left.

3.5. Overexpression of ORF44

The overexpression of ORF44 was achieved by cloning of the gene under the control of the tnaN promoter. After transformation of *N. magadii* L13 with plasmid (pRo5Mev-tnaN-ORF44), the strain was infected with φCh1. Single plaques were incubated in fresh NVM-CA^{+} rich media. As shown in Figure 22A, *N. magadii* L11 (pRo5Mev-tnaN-44) exhibits similar growth pattern as the control (pRo5Mev). Viral titer analysis demonstrates 1.5 to 2 orders of magnitude increase in the production of viral particles during first and third day in the overexpression strain (Fig. 22B), whereas induction with 4 mM L-trp results in minor decrease in the release of infectious particles upon onset of lysis (see Fig. 22B, pink bars) compared to the uninduced state (blue bars).

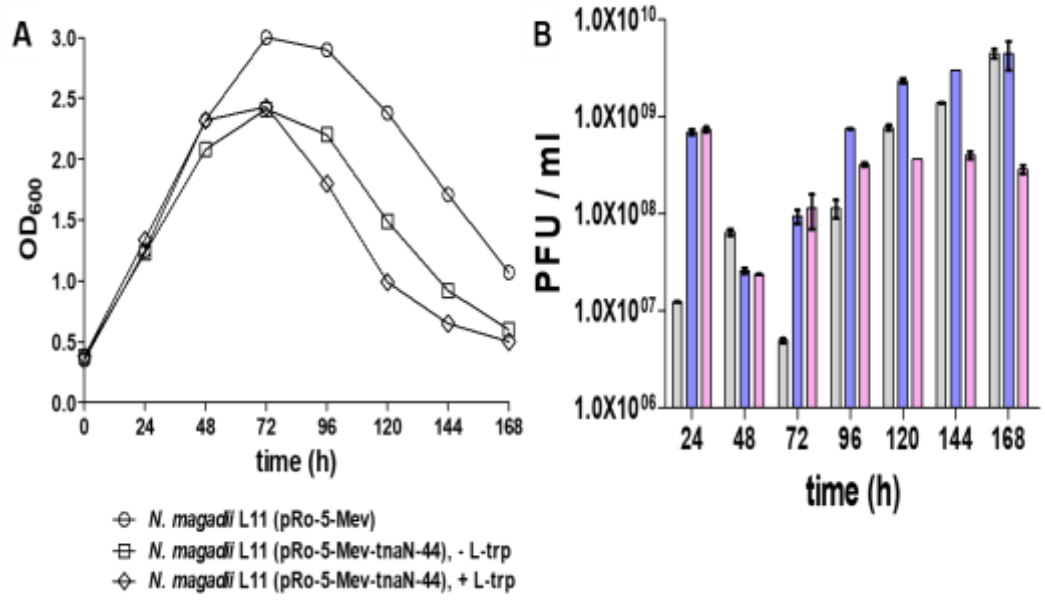

Figure 22. Phenotypic analysis of *N. magadii* L11 ORF44 overexpression strain. **(**pRo5Mev) plasmid was employed to overexpress ORF44 under the control of a tryptophan inducible promoter, isolated from *N. magadii.* (A) Overexpression strain was cultivated in 50 ml NVM-CA^{+}, supplemented with mevinolin, under aeration at 37 °C. Optical density at 600 nm was measured every 24 hours for 7 days. The growth of the culture was monitored with and without the addition of 4 mM L-trp. (B) Viral titer estimation. grey bars: *N. magadii* L11 (pRo5Mev), blue bars: uninduced culture, pink bars: induced culture. Error bars indicate SEM.

Furthermore, the expression patterns of viral proteins in the overexpression strain were analyzed via western blot. Daily induction of the promoter with 4 mM L-trp results in a 24- and 48- hour earlier production of protein E and the DNA methyltransferase, respectively, compared to the control *N. magadii* L11 (pRo5Mev). In addition, major downregulation of both proteins is observed on seventh day (see Fig. 23, top right and bottom left panel) while no effect in the production of gp34 can be seen (bottom right).

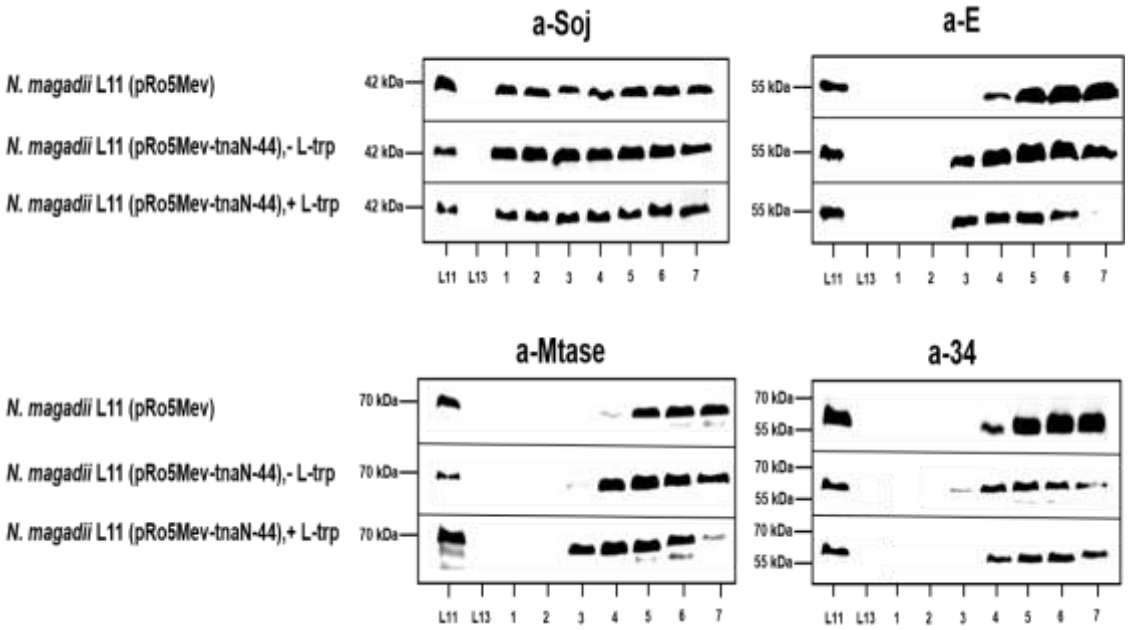

Figure 23. Western blot analysis of the protein production in the ORF44 overexpression. Protein crude extracts were obtained every 24 hours during 7 days and analyzed by western blot in order to assess the production of Soj, the major capsid protein E, DNA methyl-transferase and the tail fiber protein gp34. L11: positive control *N. magadii* L11, L13: negative control *N. magadii* L13, lanes 1-7: crude protein extracts collected every 24 hours for 10 days. Protein sizes are indicated on the left.

3.6. Effect of ORF43 and ORF44 on the tail fiber protein gp34 in *H.volcanii*

To determine the effect of ORF43 and ORF44 on the tail fiber protein gp34 of *N. magadii*, Gibson assembly method was employed to clone ORF43, ORF44 and ORF43/44 together with ORF34, under its native promoter, as a reporter gene. Two different orientations of the tail fiber protein gp34 were investigated. ORF44 was cloned under the control of tnaN promoter due to the high protein toxicity. All constructs were transformed into *H. volcanii*, a key model organism for archaeal biology.

To verify that only one orientation of gp34 is present in each construct, analytical PCRs were performed using the primer pairs 34-Hv-1/ 34-Hv-3 and 34-Hv-1/ 34-Hv-2 for 34_1 and 34_{52} respectively. The obtained amplicons have a length of 1999 bp and 2172 bp respectively (Fig. 24, lane 1 and 3). As negative control, PCRs were performed using

same templates but the 3’ primers were exchanged. As expected, no amplication can be observed (Fig. 24, lane 2 and 4).

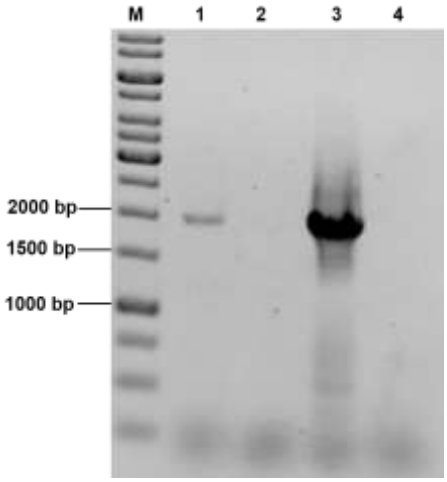

Figure 24. Agarose gel electrophoresis analysis of PCR amplification of extracted plasmid DNA from *H. volcanii*. Lane M: 1 kb Generuler DNA marker; Lanes 1 and 3 display the amplification of 34_1 and 34_{52} using the primer pairs 34-Hv-1/ 34-Hv-3 and 34-Hv-1/ 34-Hv-2 respectively, resulting in a 1999 bp and 2172 bp amplicon. Lanes 2 and 4 show no amplification. Same PCR was performed with same templates, but the 3’ primers were exchanged.

H. *volcanii* strains were inoculated in MGM^+ rich medium supplemented with mevinolin and growth kinetic analysis was carried out. As depicted in Figure 25A and B, daily induction with 2 mM L-trp results in growth deceleration in the strain bearing ORF44. Similar results are obtained when the gene expression was induced with 5 mM L-trp at the start of the growth (Fig. 25C).

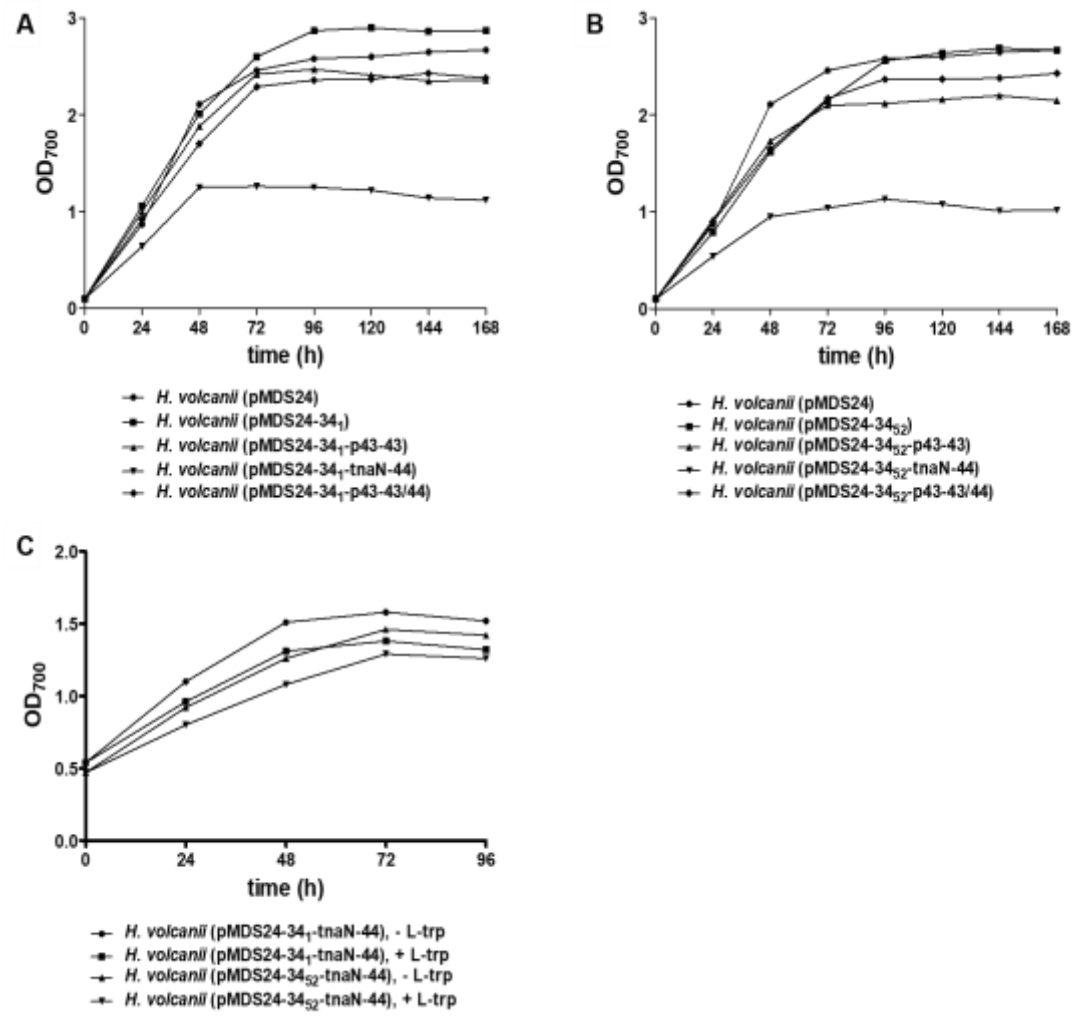

Figure 25. Growth kinetics analysis of *H. volcanii* strains expressing gp34 in two different orientations. Cultures were inoculated in 50 ml MGM^+ supplemented with mevinolin and grown at 37 °C with aeration. Optical density at 700 nm was measured every 24 hours. (A, B) Growth of strains expressing gp34 in + and – orientation respectively. For the induction of gp44, 2 mM L-trp was added daily to the media. (C) Effect of L-trp on the growth kinetics of *H. volcanii*. Cultures were split in two subcultures and one was induced with 5 mM L-trp at an OD_{700} of 0.5.

Western blot analyses were further achieved by using polyclonal a-gp34$_{52}$ antibodies. As shown in Figure 26, the presence of ORF44 leads almost to abolishment of gp34$_1$ protein synthesis (left panel), while a minor downregulation is observed for the minus orientation (right panel). On the other hand, ORF43 has an enhancing effect on the production of gp34 in both orientations compared to the controls *H. volcanii* (pMDS24-

ORF34). New whole protein extracts must be collected for the control (pMDS24-ORF34$_{52}$) and the western blot must be repeated. In addition, the experiment was repeated, but the gene expression was induced only once with 5 mM L-trp at the start of the growth. Similarly, both variants of the tail fiber protein gp34 are heavily downregulated, even before induction (see Fig. 27).

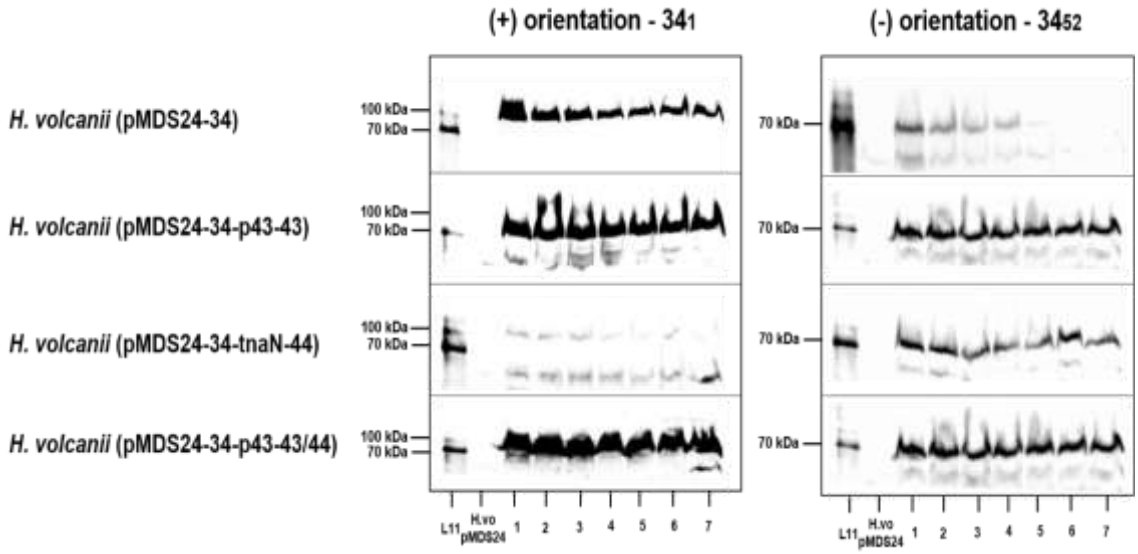

Figure 26. Western blot analysis of gp34 production in *H. volcanii*. Protein crude extracts were obtained every 24 hours for 7 days and analyzed by western blot in order to study the effect of gp43 and gp44 on the *N. magadii* tail fiber protein gp34. Two different orientations of gp34 were investigated and detected by a-34$_{52}$ rabbit antibodies. L11: positive control *N. magadii* L11, H.vo pMDS24: negative control *H. volcanii* (pMDS24), lanes 1-7: crude protein extracts collected every 24 hours for 7 days. Protein molecular weights are indicated on the left.

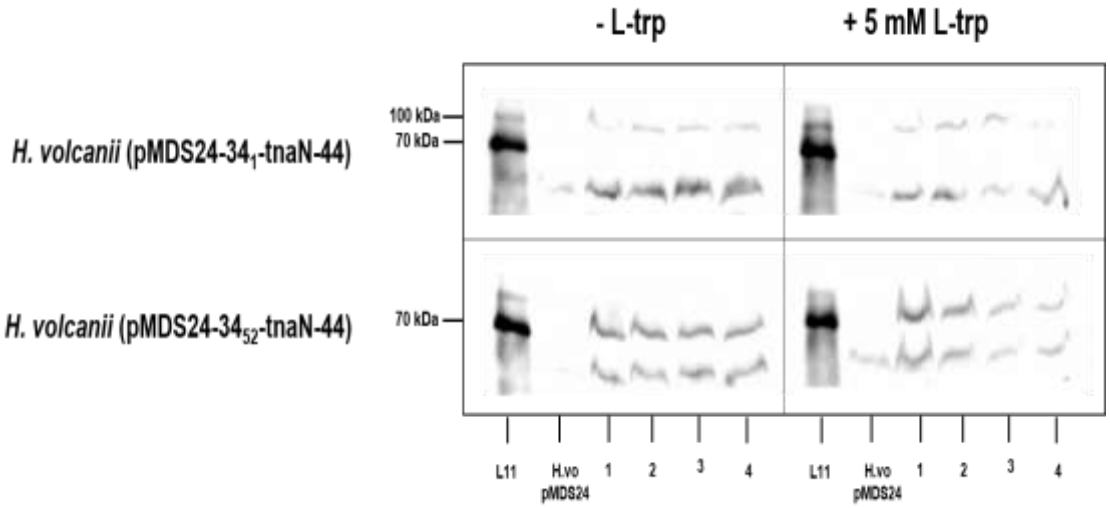

Figure 27. Western blot analysis of gp34 production in *H. volcanii*. Archaeal cultures were induced with 5 mM L-trp at the start of the growth and protein crude extracts were obtained every 24 until the lag phase was reached. Detection was achieved by a-34_{52} rabbit antibodies. L11: positive control *N. magadii* L11, H.vo pMDS24: negative control *H. volcanii* (pMDS24), lanes 1-4: crude protein extracts collected every 24 hours for 4 days. Protein molecular weights are indicated on the left.

3.7. Expression and purification of gp44 under denaturing conditions

In order to investigate the putative role of gp44 as an endoribonuclease, protein had to be isolated under native conditions. For this purpose, gp44 was isolated and purified from *E. coli* as mentioned in Methods section 2.2.4. In a first attempt to obtain gp44, ORF44 was cloned into pRSETA vector for expression of a N-terminal 6x His-tagged protein and transformed in *E. coli*. Gp44 was expressed as insoluble protein and the formation of inclusion bodies was detected from SDS-PAGE of crude lysates (data not shown). To overcome this problem, protein was purified under denaturing conditions (see Section 2.2.4.1). As depicted in Figure 28A, gp44 was successfully expressed and purified as soluble protein. For functional studies, protein must be in its native conformation. A stepwise dialysis plan was carried out, in order to remove urea while increasing pH and salt concentration (see Section 2.2.4.2). Protein aliquots were taken on each dialysis step and detected via SDS-PAGE (see Fig. 28B). Upon dialysis, the fraction was analyzed via mass spectrometry and gp44 was identified with an estimated size of

16.1 kDa (see Fig. 28C). As mentioned in Methods section (2.2.6), in vitro assays were performed, but no endoribonuclease activity could be detected (data not shown).

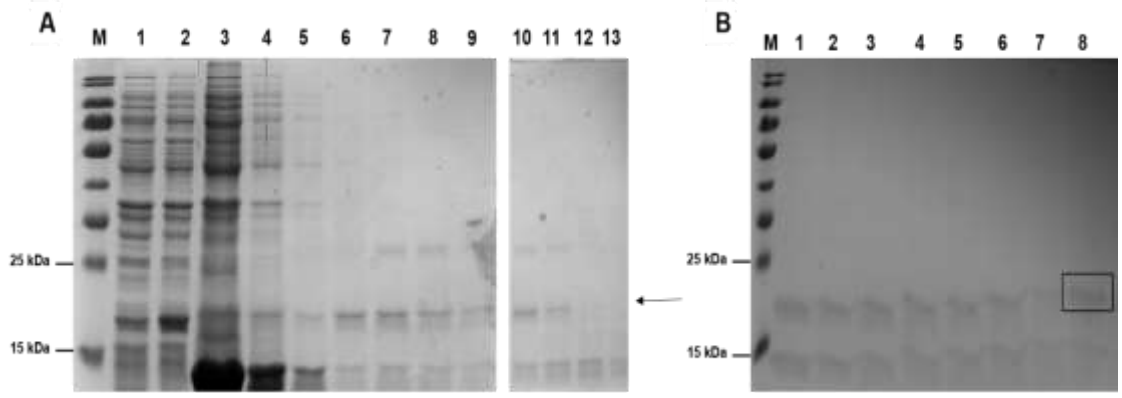

C

Protein IDs	Protein names	Gene names	Fasta headers	Number of proteins	Peptides	Sequence coverage [%]	Mol. weight [kDa]	Score	Intensity	iBAQ	MS/MS count	Only identified by site	Potential contaminant
Gp44			Gp44	1	9	69,9	16,1	180,5	3,75E+10	6,25E+09	557		

Figure 28. Purification of gp44 in *E.coli* under denaturing conditions. (A) Gp44 was his-tag purified and fractions were loaded on a 12 % SDS-PAGE. M: Prestained protein ladder; Lane 1, 2: before and after IPTG induction respectively; Lane 3: Flow through; Lane 4, 5: Wash steps; Lane 6 – 13: Elution fractions; Black arrow indicates the position of the eluted protein gp44. (B) Stepwise dialysis of gp44. M: Prestained protein ladder; Lane 1, 2: Renaturing buffer 1; Lane 3, 4: Renaturing buffer 2; Lane 5, 6: Renaturing buffer 3; Lane 7, 8: Renaturing buffer 4; Black box indicates the fraction which was analyzed via mass spectrometry. (C) Identification of gp44 protein via mass spectrometry.

Due to the inability to verify the proper folding of the protein during dialysis, an expression system more similar to *N. magadii* was implemented, i.e., *H. volcanii*, which has been well-established as a system for protein overexpression (Allers *et al.*, 2010). ORF44 was cloned into pRV1 vector, tagged with a N-terminal hexahistidine sequence, under the control of ptna, a tryptophan inducible promoter isolated from *H. volcanii*. Following protein purification under native conditions, obtained fractions were detected from SDS-PAGE but no protein could be observed upon Coomasie staining (data not shown).

4. Discussion

The focus of this study was to characterize the physiological roles of ORF43 and ORF44. Both ORFs have overlapping start and stop codons leading to their co-transcription and co-translation. The ORF43/44 system is a putative canonical TA system of φCh1, in which the toxin and antitoxin genes form an operon. DNA sequence analysis revealed a homology to the VapBC TA system, a locus that is quite abundant especially in *Archaea* (Gerdes, Christensen and Løbner-Olesen, 2005). Furthermore, a PIN domain in gp44 was determined by pfam analysis, which act as ribonucleases cleaving RNA molecules in a sequence-dependent manner (Arcus *et al.*, 2011).

ORF44 is a 395 bp open reading frame located upstream of the φCh1 DNA replication module (Klein *et al.*, 2002). In order to investigate the function of ORF44 *in vivo*, a deletion mutant strain, namely *N. magadii* L11-ΔORF44, was constructed by inserting the novobiocin resistance cassette in the reverse orientation and thereby, replacing ORF44 (Gillen, 2017). Growth curve analysis of the *N. magadii* L11-ΔORF44 deficient strain showed a 24-hour earlier onset of lysis compared to the wild-type *N. magadii* L11. In addition, virus titer experiments revealed no significant reduction or increase in the production of viral particles upon lysis compared to the wild type. Similar results were obtained by deletion of the regulatory genes ORF48 and ORF49 (Sabic, 2019), which are located downstream of ORF44. These findings suggest that ORF44 affects indirectly the viral lytic cycle and may have therefore an important regulatory role. Normally, if the plasmid containing the TA system is absent, the antitoxin is proteolytically cleaved leading to the activation of the stable toxic protein, which promotes cell death (Gerdes, Christensen and Løbner-Olesen, 2005). Previous studies showed that ORF43 alone and ORF43/44 have an enhancing effect on the intergenic region between ORF48 (rep) and ORF49. ORF43 binds to the 5' of ORF48 and enhances thus the transcription of ORF49, a regulatory gene involved in lytic life cycle of φCh1 (Iro *et al.*, 2007). By deleting ORF44, the antitoxin encoded by ORF43 accumulates in the cell leading to the premature transcription of ORF49 and therefore an earlier onset of lysis of *N. magadii* L11-ΔORF44.

Western blot analyses of whole protein extracts demonstrated a 24-hour earlier production of the major capsid protein E in *N. magadii* L11-ΔORF44, finding

consistent with the early onset of lysis and the increased amount of viral particles. Another interesting observation is the truncation of the tail fiber protein $gp34_{52}$ in the presence of ORF44 in *N. magadii* L11 compared to the deletion strain, where the protein signal appears to be 15 kDa higher. Experiments performed in *N. magadii* L13 strain with $ORF34_{52}$ as the reporter gene also revealed a truncation of gp34 in presence of ORF44, whereas the existence of ORF43 alone and ORF43/44 had no effect on the expression profile of the tail fiber protein (Hofbauer, 2015). These results prove potentially the putative function of gp44 as an endoribonuclease, which may cleave the coding sequence of ORF34 resulting in a truncated protein. Moreover, trans-complementation of the ORF44 deletion with the episomally expressed ORF44 under the control of the tryptophanase promoter tnaN from the low copy number plasmid pRo5-Mev did not restore neither the lysis behavior nor the expression profiles of protein E and DNA methyltransferase. On the other hand, the tail fiber protein gp34 appears to be truncated in the complementation strain compared to *N. magadii* L11-ΔORF44, indicating that gp44 has a direct effect on the tail fiber protein by potentially cleaving ORF34 mRNA in the coding region and acting therefore as an mRNA interferase. Further experiments must be performed in order to elucidate the mechanism of action of the gp44 protein. In addition, no significant differences in growth kinetics and protein profiles could be observed between the induced and un-induced cultures. This could indicate that the inducer concentration was too low or that the antibiotic resistance cassette exerted a *polar effect* on one of the surrounding genes, which is responsible for the resulting phenotype.

To further study the effect of ORF43 and ORF44 on the production of the viral tail fiber proteins, *H. volcanii* was employed. Both orientations of ORF34 were used as reporter genes and transformed together with ORF43 or ORF44 into *H. volcanii*. Due to the high toxicity of gp44, ORF44 was cloned under the control of the tryptophanase inducible promoter. Phenotypic analyses showed significant growth deceleration in the strain bearing ORF44 upon daily induction. On the other hand, western blot analysis revealed that ORF43 have an enhancing effect on the expression of gp34, while ORF44 had an antagonizing effect. No shortened variations of gp34 were observed in presence of ORF44, suggesting that this truncation is system dependent. In contrast to *H. volcanii*, *N. magadii* requires higher salt concentrations and alkaline pH, conditions that might be necessary for gp44 to exert its function as an mRNA interferase. Another key

difference is the use of the inducible instead of the native promoter, which leads to constitutive expression of the gene.

In parallel, overexpression studies were performed. The toxin ORF44 was cloned under the control of the tryptophanase inducible promoter into the low copy number plasmid pRo5Mev, whereas the conjugate antitoxin ORF43 with its native promoter p43 was cloned into both low and high copy number plasmids, namely pRo5Mev and pNB102, respectively. As expected, overexpression of ORF44 led to growth deceleration of *N. magadii*. Further analyses of the protein expression patterns revealed that episomal expression of the ORF44 results in the downregulation of viral genes· both major capsid protein E and DNA methyltransferase were detected 24-hours earlier compared to the *N. magadii* L11 (pRo5Mev). On the other hand, overexpression of ORF43 from multicopy plasmid pNB102 led to 24-hour delay in the lytic development compared to control *N. magadii* L11 (pNB102), phenotype coherent with the 24-hour late expression of protein E and DNA methyltransferase. This effect can be due to the additional metabolic burden for the cell, originating from the expression of a multicopy plasmid (Kristala). No significant differences were observed by the extrachromosomal expression of ORF43 from the low copy number plasmid pRo5mev, indicating that the regulatory role of the ORF43 is dosage dependent. These findings could indicate antagonistic roles of ORF43 and ORF44, further supporting the hypothesis of a putative TA system. Finally yet importantly, the plating efficiency of φCh1, in either NVM^+ or $NVM\text{-}CA^+$ media, was not affected by the episomal expression of the ORF43 and ORF44.

In addition, the stability of the *N. magadii* L11 ORF44-deficient mutant upon continuous subculturing was analyzed. Previous studies unveiled a constant reduction of the lysis rate upon passaging, leading to the earlier abolishment of lysis in the deletion mutant strain compared to wild type *N. magadii* L11 (Edwards, 2018). Both wild type and deletion stains were passaged seven times, upon onset of lysis, in NVM^+ media containing 4 M and 4.1 M salt, respectively. Under typical salt concentrations, the deletion mutant stopped lysing during fifth passage, resembling the growth behavior of the cured strain *N. magadii* L13. Partial abolishment of lysis was also observed for wt *N. magadii* L11 after six to seven passages. Despite the loss of lysis, the presence of the provirus was confirmed by analytical PCR. Furthermore, virus titer analysis revealed a continuous decrease in the production of viral particles from both strains

upon passaging. Additionally, the deletion mutant exhibited a significant decrease in the production of the major capsid protein E after fifth passage, two passages earlier than the wt strain, whereas the production of the Soj protein remained constant for both strains. Similar results were obtained by continuous passaging of the ORF48 (rep) – and ORF49 – deficient strains (Sabic, 2019), indicating that the deletion of ORF44 has an indirect effect on the lytic cycle of φCh1 by potentially affecting downstream genes. The aforementioned genes are located in the regulatory region of φCh1 and their disruption leads to increased genomic instability. Prolonged passaging can also lead to accumulation of mutations, which may affect the functionality of viral genes and thus its lytic life cycle.

On the other hand, slightly increasing the salt concentration to 4.1 M led to a completely different phenotype. Both strains continue to lyse normally upon passaging. The release of viral particles from the wt strain is constantly increasing instead of decreasing, while a minor decrease is observed for the *N. magadii* L11-ΔORF44 strain. Moreover, the major capsid protein E is significantly upregulated and constantly produced in both strains throughout the passages, whereas the production of Soj remains stable. Higher NaCl concentrations in the environment may lead to an increased intracellular accumulation of potassium ions, resulting in conformational changes in proteins and enzymes and possibly genome stability.

Last but not least, many fruitless attempts had been made to isolate and purify gp44 under native conditions. Haloalkalophilic enzymes function optimally at high salt concentrations and alkaline pH. However, heterologous expression in *E. coli* led to aggregation and formation of inclusion bodies due to the low ionic strength. The use of the haloarchaeon *H. volcanii* with the tryptophanase inducible promoter as a system for the overexpression and purification of halophilic proteins was also utilized, but deemed ineffective. However, gp44 was successfully purified in *E. coli* under denaturing conditions, but stepwise dialysis resulted in misfolding of the protein. Research into *Archaea* is limited compared to bacteria and eukaryotes. Nonetheless, future studies should focus on the characterization of ORF43/44 as a putative TA of φCh1. The production of functional antibodies against gp43 and gp44 is a necessity, in order to study the protein expression profiles *in vivo*. To analyze whether the truncation of $gp34_{52}$ in *N. magadii* L11 is media dependent, growth kinetics and western blot analysis must be re-performed in NVM^{+} rich medium. Finally, further development of

expression systems and strategies for isolation of toxic haloalkalophilic proteins will provide a better insight into the functions and structures of these proteins *in vitro*.

Abstract

Toxin-antitoxin systems consist of a stable expressed toxin and the conjugate antitoxin. DNA sequence analysis of ORF43/44 revealed a homology to the VapBC Type II TA system. ORF44 exists as operon with the cognate antitoxin ORF43, leading to transcriptional and translational coupling. Previous studies investigating the role of ORF44 have reported its function as a putative ribonuclease endonuclease that may cleave single stranded RNA in a sequence dependent manner. A PIN domain in gp44, identified via Pfam analysis, further strengthens this hypothesis. Additional findings suggest a repressor activity of gp44 and thus a potential role of ORF43/44 in regulating the transcription of viral genes and the progression of the lytic cycle of the myovirus φCh1, which infects the haloalkaliphilic archaeon *Natrialba magadii*.

Genetic analyses of haloviruses are rarely reported and the *in vivo* roles and functions of their proteins remain unknown. In this study, we aim to elucidate the potential roles of ORF43 and ORF44 and their effect on the infectivity of φCH1. For this purpose, phenotypic analyses, viral titer assays and protein analyses via Western blot were carried out.

ORF44 deletion mutant was constructed via homologous recombination by inserting the novobiocin resistance cassette. Passaging experiments showed complete abolishment of the lytic cycle and major decrease in the production of the major capsid protein E. Increasing the salt concentration in the medium lead to re-establishment of the normal lysis behavior and a uniform expression of protein E. Furthermore, *N. magadii* L11-ΔORF44 strain showed a 24-hour earlier lysis and increased production of viral particles compared to wild type strain. Presence of ORF44 resulted in the truncation of gp34 as proven by western blot analysis.

Constitutive expression of ORF43 and ORF44 in the cured *N. magadii* L13 strain had no significant influence on the plating efficiency of φCh1. In addition, overexpression of ORF44 under the control of the tryptophan inducible promoter tnaN affected the expression of protein E and the methyltransferase. Similar results were obtained by overexpressing ORF43 in a gene dosage dependent manner. In both cases, no effect on the tail fiber protein gp34 was observed.

To further explore the putative function of gp44 as a repressor or an endoribonuclease, ORF43 and ORF44 were transformed together with the tail fiber protein gp34 into *Haloferax volcanii*, a key model organism for enhancing the understanding of archaeal genomics. In presence of ORF44, a strong growth deceleration as well as a major downregulation of gp34 was observed, whereas ORF43 had an enhancing effect. Finally, we attempted to purify gp44 under native conditions for functional *in vitro* studies. Due to the lack of information and the extreme conditions, under which these proteins are expressed, isolation proved to be challenging and thereby unsuccessful.

KEYWORDS: φCh1, *Archaea*, *Natrialba magadii*, cured strain L13, lysogenic strain L11, Toxin-antitoxin system, *Haloferax volcanii*

Zusammenfassung

Toxin-Antitoxin-Systeme bestehen aus einem stabil exprimierten Toxin und dem konjugierten Antitoxin. Die DNA-Sequenzanalyse von ORF43/44 hat eine Homologie zum VapBC Typ II TA-System ergeben. ORF44 existiert als Operon mit dem Antitoxin kodierenden ORF43, was zu einer Transkriptions- und Translationskopplung führt. Frühere Studien haben die Funktion von ORF44 als eine scheinbare Ribonuklease-Endonuklease nahelegt, die einzelsträngige RNA sequenzabhängig spaltet. Dies wurde durch die Identifizierung einer PIN-Domäne in gp44 mittels einer Pfam Analyse verstärkt. Zusätzliche Befunde weisen auf eine Repressoraktivität von gp44 hin und somit eine mögliche Rolle von ORF43/44 bei der Regulierung der Transkription viraler Gene und des Fortschreitens des Lysezyklus des φCh1 Myovirus, das das haloalkaliphile Archäon *Natrialba magadii* infiziert.

Genetische Analysen von Haloviren werden selten berichtet und die in vivo Rollen und Funktionen ihrer Proteine bleiben unbekannt. In dieser Studie werden die möglichen Rollen von ORF43 und ORF44 sowie ihre Auswirkungen auf die Infektiosität von φCh1 untersucht. Zu diesem Zweck wurden phänotypische Analysen, Virustiter-Ansätze und Proteinanalysen mittels Western Blot durchgeführt.

Die ORF44-Deletionsmutante wurde mittels homologer Rekombination durch das Einsetzen der Novobiozin-Resistenzkassette konstruiert. Passagierungs-Experimente haben eine vollständige Aufhebung des Lysezyklus und eine starke Abnahme der Produktion des Hauptkapsidproteins E gezeigt. Eine Erhöhung der Salzkonzentration im Medium hat zur Wiederherstellung des normalen Lyseverhaltens und zu einer gleichmäßigen Expression von Protein E geführt. Im Vergleich zum Wildtyp-Stamm hat der L11-Δ44 Stamm weiterhin eine 24 Stunden-frühere Lyse und eine erhöhte Produktion von Viruspartikeln angezeigt. Die Western-Blot-Analyse hat eine Verkürzung von gp34 beim Vorhandensein von ORF44 nachgewiesen.

Die konstitutive Expression von ORF43 und ORF44 im Virus-freien Stamm *N. magadii* L13 Stamm hatte keinen signifikanten Einfluss auf die Plattierungseffizienz von φCh1. Die induzierte Überexpression von ORF44 unter der Kontrolle des Tryptophan Promotors tnaN hat die Expression von Protein E und der Methyltransferase beeinflusst. Die Überexpression von ORF43 auf einer Gendosis-

abhängigen Weise hat ähnliche Ergebnisse geliefert. In beiden Fällen wurde kein Effekt auf das Schwanzfaserprotein gp34 beobachtet.

ORF43 und ORF44 wurden zusammen mit dem Schwanzfaserprotein gp34 in den Schlüsselmodellorganismus *Haloferax volcanii* transformiert, der zur Verbesserung des Verständnisses der archaealen Genomik dient, um die mutmaßliche Funktion von gp44 als Repressor oder Endoribonuklease weiter zu untersuchen. In Gegenwart von ORF44 wurde eine starke Wachstumsverzögerung sowie eine starke Unterregulierung von gp34 beobachtet, während ORF43 einen verstärkenden Effekt aufgewiesen hat. Schließlich wurde versucht, das gp44 Protein unter nativen Bedingungen zu reinigen. Die Isolierung hat aufgrund des Mangels an Informationen und der extremen Bedingungen, unter denen diese Proteine exprimiert werden, als schwierig erwiesen und war somit erfolglos.

Schlüsselwörter: φCh1, *Archaea*, *Natrialba magadii*, ausgehärter Stamm L13, lysogenischer Stamm L11, Toxin-Antitoxin System, *Haloferax volcanii*

REFERENCES

Albers, S. V. and Meyer, B. H. (2011) 'The archaeal cell envelope', *Nature Reviews Microbiology*, pp. 414–426. doi: 10.1038/nrmicro2576.

Allers, T. *et al.* (2010) 'Improved strains and plasmid vectors for conditional overexpression of His-tagged proteins in Haloferax volcanii', *Applied and Environmental Microbiology*, 76(6), pp. 1759–1769. doi: 10.1128/AEM.02670-09.

Allers, T. (2010) 'Overexpression and purification of halophilic proteins in Haloferax volcanii', *Bioengineered Bugs*. Landes Bioscience, 1(4), pp. 290–292. doi: 10.4161/bbug.1.4.11794.

Allers, T. and Ngo, H. P. (2003) 'Genetic analysis of homologous recombination in Archaea: Haloferax volcanii as a model organism', in *Biochemical Society Transactions*, pp. 706–709. doi: 10.1042/BST0310706.

Andrei, A. Ş., Banciu, H. L. and Oren, A. (2012) 'Living with salt: Metabolic and phylogenetic diversity of archaea inhabiting saline ecosystems', *FEMS Microbiology Letters*, pp. 1–9. doi: 10.1111/j.1574-6968.2012.02526.x.

Arcus, V. L. *et al.* (2011) 'The PIN-domain ribonucleases and the prokaryotic VapBC toxin-antitoxin array', *Protein Engineering, Design and Selection*. Oxford Academic, 24(1–2), pp. 33–40. doi: 10.1093/protein/gzq081.

Arnold, H. P. *et al.* (2000) 'A novel lipothrixvirus, SIFV, of the extremely thermophilic crenarchaeon Sulfolobus', *Virology*. Academic Press Inc., 267(2), pp. 252–266. doi: 10.1006/viro.1999.0105.

Bailey, S. E. S. and Hayes, F. (2009) 'Influence of operator site geometry on transcriptional control by the YefM-YoeB toxin-antitoxin complex', *Journal of Bacteriology*. American Society for Microbiology Journals, 191(3), pp. 762–772. doi: 10.1128/JB.01331-08.

Baranyi, U. *et al.* (2000) 'The archaeal halophilic virus-encoded Dam-like methyltransferase M.φCh1-I methylates adenine residues and complements dam mutants in the low salt environment of Escherichia coli', *Molecular Microbiology*. John Wiley & Sons, Ltd, 35(5), pp. 1168–1179. doi: 10.1046/j.1365-2958.2000.01786.x.

Bernander, R. (2000) ‘Chromosome replication, nucleoid segregation and cell division in Archaea’, *Trends in Microbiology*, pp. 278–283. doi: 10.1016/S0966-842X(00)01760-1.

Bitan-Banin, G., Ortenberg, R. and Mevarech, M. (2003) ‘Development of a gene knockout system for the halophilic archaeon Haloferax volcanii by use of the pyrE gene’, *Journal of Bacteriology*, 185(3), pp. 772–778. doi: 10.1128/JB.185.3.772-778.2003.

Breuert, S. *et al.* (2006) ‘Regulated polyploidy in halophilic archaea’, *PLoS ONE*, 1(1). doi: 10.1371/journal.pone.0000092.

Brochier-Armanet, C. *et al.* (2008) ‘Mesophilic crenarchaeota: Proposal for a third archaeal phylum, the Thaumarchaeota’, *Nature Reviews Microbiology*. Nature Publishing Group, 6(3), pp. 245–252. doi: 10.1038/nrmicro1852.

Brown, J. R. and Doolittle, W. F. (1997) ‘Archaea and the prokaryote-to-eukaryote transition.’, *Microbiology and molecular biology reviews : MMBR*, 61(4), pp. 456–502. doi: 10.1128/.61.4.456-502.1997.

Bryant, D. A. and Frigaard, N. U. (2006) ‘Prokaryotic photosynthesis and phototrophy illuminated’, *Trends in Microbiology*, pp. 488–496. doi: 10.1016/j.tim.2006.09.001.

Charlebois, R. L. *et al.* (1987) ‘Characterization of pHV2 from Halobacterium volcanii and its use in demonstrating transformation of an archaebacterium.’, *Proceedings of the National Academy of Sciences of the United States of America*, 84(23), pp. 8530–8534. doi: 10.1073/pnas.84.23.8530.

Christian, J. H. B. and Waltho, J. A. (1962) ‘Solute concentrations within cells of halophilic and non-halophilic bacteria’, *BBA - Biochimica et Biophysica Acta*, 65(3), pp. 506–508. doi: 10.1016/0006-3002(62)90453-5.

Cline, S. W. and Ford Doolittle, W. (1987) ‘Efficient transfection of the archaebacterium Halobacterium halobium’, *Journal of Bacteriology*. American Society for Microbiology Journals, 169(3), pp. 1341–1344. doi: 10.1128/jb.169.3.1341-1344.1987.

Couturier, M., Bahassi, E. M. and Van Melderen, L. (1998) ‘Bacterial death by DNA gyrase poisoning’, *Trends in Microbiology*. Elsevier Ltd, pp. 269–275. doi:

10.1016/S0966-842X(98)01311-0.

Dellas, N. *et al.* (2014) 'Archaeal Viruses: Diversity, Replication, and Structure', *Annual Review of Virology*. Annual Reviews, 1(1), pp. 399–426. doi: 10.1146/annurev-virology-031413-085357.

DeLong, E. F. (1992) 'Archaea in coastal marine environments', *Proceedings of the National Academy of Sciences of the United States of America*. National Academy of Sciences, 89(12), pp. 5685–5689. doi: 10.1073/pnas.89.12.5685.

Drlica, K. and Franco, R. J. (1988) 'Inhibitors of DNA Topoisomerases', *Biochemistry*. American Chemical Society, 27(7), pp. 2253–2259. doi: 10.1021/bi00407a001.

Dyall-Smith, M., Tang, S. L. and Bath, C. (2003) 'Haloarchaeal viruses: How diverse are they?', *Research in Microbiology*. Elsevier Masson SAS, pp. 309–313. doi: 10.1016/S0923-2508(03)00076-7.

Edwards, M. A. (2018) *Stability of the ΦCh1 ORF44 deletion mutant and characterization of the function of gp44 - E-Theses*. University of Vienna. Available at: https://othes.univie.ac.at/51335/ (Accessed: 9 April 2020).

Fendrihan, S. *et al.* (2007) 'Extremely halophilic archaea and the issue of long-term microbial survival', in *Life in Extreme Environments*. Springer Netherlands, pp. 125–140. doi: 10.1007/978-1-4020-6285-8_8.

Fineran, P. C. *et al.* (2009) 'The phage abortive infection system, ToxIN, functions as a protein-RNA toxin-antitoxin pair', *Proceedings of the National Academy of Sciences of the United States of America*. National Academy of Sciences, 106(3), pp. 894–899. doi: 10.1073/pnas.0808832106.

Gerdes, K., Christensen, S. K. and Løbner-Olesen, A. (2005) 'Prokaryotic toxin-antitoxin stress response loci', *Nature Reviews Microbiology*, 3(5), pp. 371–382. doi: 10.1038/nrmicro1147.

Gerdes, K. and Wagner, E. G. H. (2007) 'RNA antitoxins', *Current Opinion in Microbiology*. Elsevier Current Trends, pp. 117–124. doi: 10.1016/j.mib.2007.03.003.

Gillen, Y. C. J. (2017) *Construction of mutant ΦCh1-ΔORF44, its characterization and first steps in the generation of mutant ΦCh1-ΔORF56 - E-Theses*. University of Vienna. Available at: http://othes.univie.ac.at/45952/ (Accessed: 11 March 2020).

Grant, W. D. and Larsen, H. (1989) 'Extremely halophilic archaerobacteria', *Manual of Systematic Bacteriology*, 3, pp. 2219–2233.

Gupta, R. S. *et al.* (2016) 'A phylogenomic reappraisal of family-level divisions within the class Halobacteria: proposal to divide the order Halobacteriales into the families Halobacteriaceae, Haloarculaceae fam. nov., and Halococcaceae fam. nov., and the order Haloferacales into the families, Haloferacaceae and Halorubraceae fam nov.', *Antonie van Leeuwenhoek, International Journal of General and Molecular Microbiology*. Springer Netherlands, 109(4), pp. 565–587. doi: 10.1007/s10482-016-0660-2.

Gupta, R. S., Naushad, S. and Baker, S. (2015) 'Phylogenomic analyses and molecular signatures for the class Halobacteria and its two major clades: A proposal for division of the class Halobacteria into an emended order Halobacteriales and two new orders, Haloferacales ord. nov. and Natrialbales ord. nov., containing the novel families Haloferacaceae fam. nov. and Natrialbaceae fam. nov', *International Journal of Systematic and Evolutionary Microbiology*. Society for General Microbiology, 65(3), pp. 1050–1069. doi: 10.1099/ijs.0.070136-0.

Haldenby, S., White, M. F. and Allers, T. (2009) 'RecA family proteins in archaea: RadA and its cousins', *Biochemical Society Transactions*. Portland Press, 37(1), pp. 102–107. doi: 10.1042/BST0370102.

Haring, M. *et al.* (2005) 'Viral Diversity in Hot Springs of Pozzuoli, Italy, and Characterization of a Unique Archaeal Virus, Acidianus Bottle-Shaped Virus, from a New Family, the Ampullaviridae', *Journal of Virology*. American Society for Microbiology, 79(15), pp. 9904–9911. doi: 10.1128/jvi.79.15.9904-9911.2005.

Hartman, A. L. *et al.* (2010) 'The complete genome sequence of Haloferax volcanii DS2, a model archaeon', *PLoS ONE*. Public Library of Science, 5(3). doi: 10.1371/journal.pone.0009605.

Hofbauer, C. (2015) *The function of gp34 and its regulation by ORF79 of φCh1 as well as the influence of other regulation elements.* University of Vienna. Available at: http://othes.univie.ac.at/35424/ (Accessed: 6 March 2020).

Howland, J. (2000) 'The surprising archaea: discovering another domain of life'. Available at:

https://books.google.com/books?hl=el&lr=&id=cWae0vGkX4QC&oi=fnd&pg=PP2&dq=Howland,+John+L.+(2000).+The+Surprising+Archaea:+Discovering+Another+Domain+of+Life.+Oxford:+Oxford+University+Press.+p.+32.+ISBN+978-0-19-511183-5.&ots=jZVle7FL2e&sig=QcVqSkSLF8nEMju8x9quAkcyDdE (Accessed: 11 March 2020).

Iranzo, J., Krupovic, M. and Koonin, E. V. (2016) 'The double-stranded DNA virosphere as a modular hierarchical network of gene sharing', *mBio*. American Society for Microbiology, 7(4). doi: 10.1128/mBio.00978-16.

Iro, M. *et al.* (2007a) 'The lysogenic region of virus φCh1: Identification of a repressor-operator system and determination of its activity in halophilic Archaea', *Extremophiles*. Springer, 11(2), pp. 383–396. doi: 10.1007/s00792-006-0040-3.

Iro, M. *et al.* (2007b) 'The lysogenic region of virus φCh1: Identification of a repressor-operator system and determination of its activity in halophilic Archaea', *Extremophiles*, 11(2), pp. 383–396. doi: 10.1007/s00792-006-0040-3.

Janekovic, D. *et al.* (1983) 'TTV1, TTV2 and TTV3, a family of viruses of the extremely thermophilic, anaerobic, sulfur reducing archaebacterium Thermoproteus tenax', *MGG Molecular & General Genetics*. Springer-Verlag, 192(1–2), pp. 39–45. doi: 10.1007/BF00327644.

Jarrell, K. F., Jones, G. M. and Nair, D. B. (2010) 'Biosynthesis and role of N-linked glycosylation in cell surface structures of Archaea with a focus on flagella and S layers', *International Journal of Microbiology*, p. 470138. doi: 10.1155/2010/470138.

Kamekura, M. *et al.* (1997) 'Diversity of Alkaliphilic Halobacteria : Proposals for Transfer of Na trono bacterium vacuola tum , Na trono ba cterium magadii , and Natronobacterium pharaonis to Halorubrum , Natrialba , and Natronomonas gen . nov ., Respectively , as Halorubrum', *Int. J. Sys. bacteriol.*, 47(July), pp. 853–857.

Klein, R. *et al.* (2002) 'Natrialba magadii virus φCh1: First complete nucleotide sequence and functional organization of a virus infecting a haloalkaliphilic archaeon', *Molecular Microbiology*, 45(3), pp. 851–863. doi: 10.1046/j.1365-2958.2002.03064.x.

Klein, R. *et al.* (2012) 'Haloarchaeal myovirus φCh1 harbours a phase variation system for the production of protein variants with distinct cell surface adhesion specificities',

Molecular Microbiology, 83(1), pp. 137–150. doi: 10.1111/j.1365-2958.2011.07921.x.

König, H., Rachel, R. and Claus, H. (2014) 'Proteinaceous Surface Layers of Archaea: Ultrastructure and Biochemistry', in *Archaea*. American Society of Microbiology, pp. 315–340. doi: 10.1128/9781555815516.ch14.

Krupovic, M. *et al.* (2014) 'Unification of the Globally Distributed Spindle-Shaped Viruses of the Archaea', *Journal of Virology*. American Society for Microbiology, 88(4), pp. 2354–2358. doi: 10.1128/jvi.02941-13.

Krupovic, M. *et al.* (2018) 'Viruses of archaea: Structural, functional, environmental and evolutionary genomics', *Virus Research*. Elsevier B.V., pp. 181–193. doi: 10.1016/j.virusres.2017.11.025.

Lai, M. C. *et al.* (1991) 'Distribution of compatible solutes in the halophilic methanogenic archaebacteria', *Journal of Bacteriology*. American Society for Microbiology Journals, 173(17), pp. 5352–5358. doi: 10.1128/jb.173.17.5352-5358.1991.

Lai, M. C. and Gunsalus, R. P. (1992) 'Glycine betaine and potassium ion are the major compatible solutes in the extremely halophilic methanogen Methanohalophilus strain Z7302', *Journal of Bacteriology*, pp. 7474–7477. doi: 10.1128/jb.174.22.7474-7477.1992.

Lam, W. L. and Doolittle, W. F. (1992) 'Mevinolin-resistant mutations identify a promoter and the gene for a eukaryote-like 3-hydroxy-3-methylglutaryl-coenzyme A reductase in the archaebacterium Haloferax volcanii', *Journal of Biological Chemistry*, 267(9), pp. 5829–5834. Available at: http://www.jbc.org/content/267/9/5829.short (Accessed: 5 March 2020).

Lanyi, J. K. (1974) 'Salt dependent properties of proteins from extremely halophilic bacteria', *Bacteriological Reviews*. American Society for Microbiology (ASM), 38(3), pp. 272–290. doi: 10.1128/mmbr.38.3.272-290.1974.

Large, A. *et al.* (2007) 'Characterization of a tightly controlled promoter of the halophilic archaeon Haloferax volcanii and its use in the analysis of the essential cct1 gene', *Molecular Microbiology*. John Wiley & Sons, Ltd, 66(5), pp. 1092–1106. doi: 10.1111/j.1365-2958.2007.05980.x.

Ma, Y. *et al.* (2010) 'Halophiles 2010: Life in saline environments', *Applied and Environmental Microbiology*. American Society for Microbiology, pp. 6971–6981. doi: 10.1128/AEM.01868-10.

Martin, A. *et al.* (1984) ' SAV 1, a temperate u.v.-inducible DNA virus-like particle from the archaebacterium Sulfolobus acidocaldarius isolate B12 ', *The EMBO Journal*. Wiley, 3(9), pp. 2165–2168. doi: 10.1002/j.1460-2075.1984.tb02107.x.

Matelska, D., Steczkiewicz, K. and Ginalski, K. (2017) 'Comprehensive classification of the PIN domain-like superfamily', *Nucleic Acids Research*, 45(12), pp. 6995–7020. doi: 10.1093/nar/gkx494.

Mayrhofer-Iro, M. *et al.* (2013a) 'Utilization of virus φCh1 elements to establish a shuttle vector system for halo(alkali)philic Archaea via transformation of Natrialba magadii', *Applied and Environmental Microbiology*, 79(8), pp. 2741–2748. doi: 10.1128/AEM.03287-12.

Mayrhofer-Iro, M. *et al.* (2013b) 'Utilization of virus φCh1 elements to establish a shuttle vector system for halo(alkali)philic Archaea via transformation of Natrialba magadii', *Applied and Environmental Microbiology*. American Society for Microbiology, 79(8), pp. 2741–2748. doi: 10.1128/AEM.03287-12.

Mengele, R. and Sumper, M. (1992) 'Drastic differences in glycosylation of related S-layer glycoproteins from moderate and extreme halophiles', *Journal of Biological Chemistry*, 267(12), pp. 8182–8185. Available at: http://www.jbc.org/ (Accessed: 5 March 2020).

Ng, W. L. and DasSarma, S. (1993) 'Minimal replication origin of the 200-kilobase Halobacterium plasmid pNRC100', *Journal of Bacteriology*. American Society for Microbiology Journals, 175(15), pp. 4584–4596. doi: 10.1128/jb.175.15.4584-4596.1993.

Olsen, G. J. and Woese, C. R. (1997) 'Archaeal genomics: An overview', *Cell*, pp. 991–994. doi: 10.1016/S0092-8674(00)80284-6.

Oren, A. (1999) 'Bioenergetic Aspects of Halophilism', *Microbiology and Molecular Biology Reviews*, 63(2), pp. 334–348. doi: 10.1128/mmbr.63.2.334-348.1999.

Oren, A. (2002) 'Diversity of halophilic microorganisms: Environments, phylogeny,

physiology, and applications', *Journal of Industrial Microbiology & Biotechnology*, 28(1), pp. 56–63. doi: 10.1038/sj.jim.7000176.

Oren, A. (2006) 'The Order Halobacteriales', in *The Prokaryotes*, pp. 113–164. doi: 10.1007/0-387-30743-5_8.

Ortega, G. *et al.* (2011) 'Halophilic enzyme activation induced by salts', *Scientific Reports*. Nature Publishing Group, 1(1), pp. 1–6. doi: 10.1038/srep00006.

Pandey, D. P. and Gerdes, K. (2005) 'Toxin-antitoxin loci are highly abundant in free-living but lost from host-associated prokaryotes', *Nucleic Acids Research*, 33(3), pp. 966–976. doi: 10.1093/nar/gki201.

Pikuta, E. V., Hoover, R. B. and Tang, J. (2007) 'Microbial extremophiles at the limits of life', *Critical Reviews in Microbiology*, pp. 183–209. doi: 10.1080/10408410701451948.

Porter, K., Russ, B. E. and Dyall-Smith, M. L. (2007) 'Virus-host interactions in salt lakes', *Current Opinion in Microbiology*. Elsevier Current Trends, pp. 418–424. doi: 10.1016/j.mib.2007.05.017.

Pullinger, G. D. and Lax, A. J. (1992) 'A Salmonella dublin virulence plasmid locus that affects bacterial growth under nutrient-limited conditions', *Molecular Microbiology*. John Wiley & Sons, Ltd, 6(12), pp. 1631–1643. doi: 10.1111/j.1365-2958.1992.tb00888.x.

Robb, F., DasSarma, S. and Fleischmann, E. (1995) 'Archaea: a laboratory manual. Halophiles'. Available at: https://www.socgenmicrobiol.org.uk/pubs/micro_today/book_reviews/QRFEB96/QRF96_16.cfm (Accessed: 5 March 2020).

Robson, J. *et al.* (2009) 'The vapBC Operon from Mycobacterium smegmatis Is An Autoregulated Toxin-Antitoxin Module That Controls Growth via Inhibition of Translation', *Journal of Molecular Biology*. Academic Press, 390(3), pp. 353–367. doi: 10.1016/j.jmb.2009.05.006.

Rodrigues-Oliveira, T. *et al.* (2017) 'Archaeal S-layers: Overview and current state of the art', *Frontiers in Microbiology*. Frontiers Media S.A. doi: 10.3389/fmicb.2017.02597.

Ronnekleiv, M. (1995) ‘Bacterial carotenoids 53* C50-carotenoids 23; carotenoids of Haloferax volcanii versus other halophilic bacteria’, *Biochemical Systematics and Ecology*. Pergamon, 23(6), pp. 627–634. doi: 10.1016/0305-1978(95)00047-X.

Sabic, D. (2019) The regulation of gene expression in haloalkaliphilic virus φCh1: further characterization of the role of rep and ORF49. University of Vienna.

Schnabel, H. *et al.* (1984) ‘ Sequence analysis of the insertion element ISH1.8 and of associated structural changes in the genome of phage ΦH of the archaebacterium Halobacterium halobium ’, *The EMBO Journal*. Wiley, 3(8), pp. 1717–1722. doi: 10.1002/j.1460-2075.1984.tb02037.x.

Senčilo, A. and Roine, E. (2014) ‘A Glimpse of the genomic diversity of haloarchaeal tailed viruses’, *Frontiers in Microbiology*. Frontiers Research Foundation, 5(MAR), p. 84. doi: 10.3389/fmicb.2014.00084.

Sleytr, U. B. and Beveridge, T. J. (1999) ‘Bacterial S-layers’, *Trends in Microbiology*, pp. 253–260. doi: 10.1016/S0966-842X(99)01513-9.

Soliman, G. S. H. and Trueper, H. G. (1982) ‘Halobacterium pharaonis sp.nov., a new, extremely haloalkaliphilic archaebacterium with low magnesium requirement’, *Zentralblatt fur Bakteriologie.Allgemeine Angewandte und Okologische Microbiologie Abt.1 Orig.C Hyg.*, 3(2), pp. 318–329. doi: 10.1016/S0721-9571(82)80045-8.

Sorokin, D. Y. *et al.* (2018) ‘Methanonatronarchaeum thermophilum gen. Nov., sp. nov. and ’Candidatus methanohalarchaeum thermophilum’, extremely halo(natrono)philic methyl-reducing methanogens from hypersaline lakes comprising a new euryarchaeal class Methanonatronarchaeia classis nov’, *International Journal of Systematic and Evolutionary Microbiology*. Microbiology Society, 68(7), pp. 2199–2208. doi: 10.1099/ijsem.0.002810.

Tindall, B. J., Ross, H. N. M. and Grant, W. D. (1984) ‘Natronobacterium gen. nov. and Natronococcus gen. nov., Two New Genera of Haloalkaliphilic Archaebacteria’, *Systematic and Applied Microbiology*. Urban & Fischer, 5(1), pp. 41–57. doi: 10.1016/S0723-2020(84)80050-8.

Torsvik, T. and Dundas, I. D. (1974) ‘Bacteriophage of Halobacterium salinarium’, *Nature*. Nature Publishing Group, 248(5450), pp. 680–681. doi: 10.1038/248680a0.

Torsvik, T. and Dundas, I. D. (1980) 'Persisting phage infection in Halobacterium salinarium str. 1', *Journal of General Virology*. Microbiology Society, 47(1), pp. 29–36. doi: 10.1099/0022-1317-47-1-29.

Valentine, D. L. (2007) 'Adaptations to energy stress dictate the ecology and evolution of the Archaea', *Nature Reviews Microbiology*, 5(4), pp. 316–323. doi: 10.1038/nrmicro1619.

Ventosa, A. and Ventosa, A. (2004) 'Halophilic microorganisms'. Available at: https://link.springer.com/content/pdf/10.1007/978-3-662-07656-9.pdf (Accessed: 11 March 2020).

Van De Vossenberg, J. L. C. M. *et al.* (1999) 'Homeostasis of the membrane proton permeability in Bacillus subtilis grown at different temperatures', *Biochimica et Biophysica Acta - Biomembranes*, 1419(1), pp. 97–104. doi: 10.1016/S0005-2736(99)00063-2.

Wais, A. C. *et al.* (1975) 'Salt-dependent bacteriophage infecting Halobacterium cutirubrum and H. Halobium', *Nature*, 256(5515), pp. 314–315. doi: 10.1038/256314a0.

Walsby, A. E. (1980) 'A square bacterium [16]', *Nature*. Nature Publishing Group, pp. 69–71. doi: 10.1038/283069a0.

Witte, A. *et al.* (1997) 'Characterization of Natronobacterium magadii phage ΦGh1, a unique archaeal phage containing DNA and RNA', *Molecular Microbiology*, 23(3), pp. 603–616. doi: 10.1046/j.1365-2958.1997.d01-1879.x.

Woese, C. R. (1994) 'There must be a prokaryote somewhere: Microbiology's search for itself', *Microbiological Reviews*, 58(1), pp. 1–9. doi: 10.1128/mmbr.58.1.1-9.1994.

Woese, C. R. and Fox, G. E. (1977) 'Phylogenetic structure of the prokaryotic domain: The primary kingdoms', *Proceedings of the National Academy of Sciences of the United States of America*, 74(11), pp. 5088–5090. doi: 10.1073/pnas.74.11.5088.

Woese, C. R., Kandler, O. and Wheelis, M. L. (1990) 'Towards a natural system of organisms: Proposal for the domains Archaea, Bacteria, and Eucarya', *Proceedings of the National Academy of Sciences of the United States of America*. National Academy of Sciences, 87(12), pp. 4576–4579. doi: 10.1073/pnas.87.12.4576.

Xue, Y. *et al.* (2005) 'Halalkalicoccus tibetensis gen. nov., sp. nov., representing a novel genus of haloalkaliphilic archaea', *International Journal of Systematic and Evolutionary Microbiology*. Microbiology Society, 55(6), pp. 2501–2505. doi: 10.1099/ijs.0.63916-0.

Yadav, A. N. *et al.* (2015) 'Haloarchaea Endowed with Phosphorus Solubilization Attribute Implicated in Phosphorus Cycle', *Scientific Reports*. Nature Publishing Group, 5(1), pp. 1–10. doi: 10.1038/srep12293.

Yamaguchi, Y. and Inouye, M. (2009) 'Chapter 12 mRNA Interferases, Sequence-Specific Endoribonucleases from the Toxin-Antitoxin Systems', *Progress in Molecular Biology and Translational Science*. Academic Press, pp. 467–500. doi: 10.1016/S0079-6603(08)00812-X.

Yamaguchi, Y., Park, J.-H. and Inouye, M. (2011) 'Toxin-Antitoxin Systems in Bacteria and Archaea', *Annual Review of Genetics*, 45(1), pp. 61–79. doi: 10.1146/annurev-genet-110410-132412.

Yuan, J. *et al.* (2010) 'Vibrio cholerae ParE2 poisons DNA gyrase via a mechanism distinct from other gyrase inhibitors', *Journal of Biological Chemistry*. American Society for Biochemistry and Molecular Biology, 285(51), pp. 40397–40408. doi: 10.1074/jbc.M110.138776.

Yurist-Doutsch, S. *et al.* (2008) 'Sweet to the extreme: Protein glycosylation in Archaea', *Molecular Microbiology*, pp. 1079–1084. doi: 10.1111/j.1365-2958.2008.06224.x.

Zhou, M., Xiang, H., Sun, C., Li, Y., *et al.* (2004) 'Complete sequence and molecular characterization of pNB101, a rolling-circle replicating plasmid from the haloalkaliphilic archaeon Natronobacterium sp. strain AS7091', *Extremophiles*. Springer, 8(2), pp. 91–98. doi: 10.1007/s00792-003-0366-z.

Zhou, M., Xiang, H., Sun, C. and Tan, H. (2004) 'Construction of a novel shuttle vector based on an RCR-plasmid from a haloalkaliphilic archaeon and transformation into other haloarchaea', *Biotechnology Letters*. Springer, 26(14), pp. 1107–1113. doi: 10.1023/B:BILE.0000035493.21986.20.